ISSN : 0972-642X

ISG NEWSLETTER

Vol. 19 No. 3 December 2013

Special Issue on

Marine and Coastal Dynamics

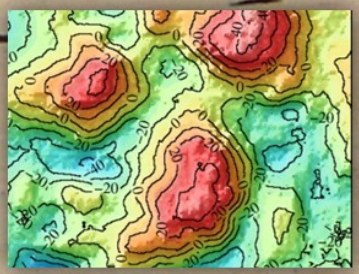
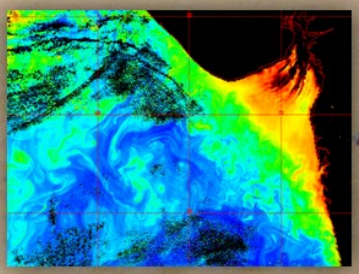
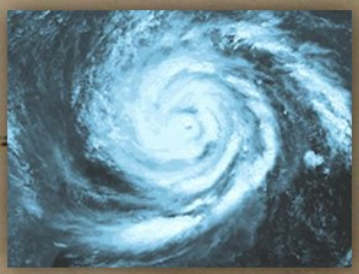
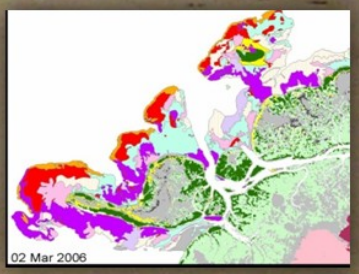




INDIAN SOCIETY OF GEOMATICS

www.isgindia.org
secretary@isgindia.org

ISG Executive Council 2011-2014

Address for correspondence:
C/o. Secretary, Indian Society of Geomatics (ISG), Room No. 4022, Space Applications Centre (ISRO), Ahmedabad-380015, Gujarat.

Web : www.isgindia.org *Phone: +91-79-26914022*

Editorial Board – ISG Newsletter

Send your contributions/comments to the Editor at the above e-mail.

ISG NEWSLETTER

Volume 19, No. 3

Special issue on
Marine and Coastal Dynamics

December, 2013

In this Issue

Editorial

Editorial

This issue of Newsletter is based on the theme of "Marine and Coastal Dynamics" on which ISG along with ISRS is organising a National Symposium during Dec 4-6, 2013 at Andhra University, Visakhapatnam. This issue is special for the theme as well as for its print publications for distribution amongst the participants.

Oceans dominate the earth and form long boundaries with land. The man is lured to this confluence since time immemorial and for many reasons. Unique landscapes, marine fisheries, beaches and coastal tourism, water transport, moderated habitat and many such things have made coasts as the most populated regions of the world. The importance of studying coasts and marine environment is obvious.

While Symposium will address more weighty issues and latest findings, this newsletter puts key issues and their current stage of research in simple articles written by persons of eminence in their fields. It is hoped that this format is quick and thorough for education and awareness on one hand and sums up research fronts and status information on the other.

This issue features key articles on coastal dynamics by Prof Ramasamy, sea level rise by Dr C J Kumanan, marine and coastal ecosystems by Dr Anjali Bahuguna, Ms. Nandini Ray Chaudhary, Shri Mohit Kumar, Ocean colour and fisheries by Dr Prakash Chauhan and Dr. Beena Kumari, Physical and Geological Oceanography by Dr Rajkumar and Dr. Sreejith, cyclone prediction by Dr. Neeru Jaiswal. We wished to cover many more aspects of ocean and coasts but were constrained to glimpses of key dimensions.

You are welcome to read these articles and share with your colleagues. You can have email dialogue with authors. The softcopy can be downloaded from ISG website (www.isgindia.org). Your feedback is important for our work - so please write a few lines.

Before closing let me thank the Authors who have shown exemplary turnaround - from overnight to few minutes. Shri Gaurav Jain joins us from this issue onwards. He is a young scientist with lot of writing credentials.

R. P. Dubey
Editor

Remote Sensing of Ocean Colour from Space

Prakash Chauhan

Space Applications Centre, ISRO, Ahmedabad, India
Email: prakash@sac.isro.gov.in

The Earth's climate is maintained by a balance between the energy that reaches the Earth from the Sun and that which goes from the Earth back out to space. The lithosphere, biosphere, hydrosphere, cryosphere and atmosphere all work interactively in regulating this balance, and together form part of the Earth's climate system. Among the different agents of the climate system, Oceans play an important role. The world ocean absorbs about 97% of the solar radiation incident on it and provides 85% of the water vapour in the atmosphere. It exchanges, absorbs and emits a host of radiatively important gases. Ocean biota, in particular phytoplankton plays a fundamental role in regulating the Earth's energy balance. Three general climatic impacts of phytoplankton are distinguished. Firstly, photosynthetic carbon fixation by these organisms and the subsequent downward transport of organic carbon facilitate oceanic storage of Carbon dioxide (CO2), one of the major greenhouse gases. Secondly, some of these microscopic algae form extensive blooms in coastal areas, temperate and Polar Regions of the global ocean. The absorption and scattering properties of these biogenic particles in surface waters affect the ocean surface reflectance and heating of surface waters. Thirdly, phytoplankton contributes to the global atmospheric sulphate aerosol burden, cloud condensation nuclei and cloud albedo through the indirect production of the cloud-aerosol precursor dimethylsulphide gas (DMS).

Remote sensing instruments exploit electromagnetic radiation to study surface processes on earth. Passive sensors use reflected sunlight or heat being emitted by objects along the earth's surface, while active sensors transmit laser or microwaves that are then reflected back to and recorded by the sensor. Many orbiting satellites currently map ocean properties such as colour, surface temperature, height, wind velocities, roughness of the ocean surface, and wave height. There are several advantages to using remote sensing techniques, such as accessing otherwise difficult locations and rapidly mapping large swaths of the earth's surface. For example, sensors that are aboard polar-orbiting satellites can map the entire surface of the earth each day. Each two-minute scene recorded by such a satellite sensor, which has a 1-km spatial resolution, would take 11 years to sample for a ship travelling at about 20 km per hour. The satellite based remote sensing data set provides the basis for temporal and spatial variability studies with time periods from days to decades and with spatial sizes from mesoscale to global. The spatial scale requires the use of satellite-based observations, and the temporal scale requires the use of measurements from more than a single satellite instrument. The patterns of ocean phytoplankton concentrations

estimated from satellites provide a fundamental input to physical-biogeochemical process studies of oceans and are used to study ocean primary production, the first step in the sequestering of excess atmospheric carbon dioxide and living marine resources such as Fisheries.

MAPPING THE OCEANS USING OCEAN COLOUR

The colour of the ocean is determined by sea water itself and by the constituent types and their amounts dissolved and suspended in it which comprehensively vary based on the type and location of the water body. Figure 1 shows typical examples of varying shades of colours exhibited by sea at different places around the Indian waters. Ocean Colour remote sensing uses the spectral reflectance of water to infer what it contains. For example, many of us consider the deep blue colour of oceans or other large bodies of water to mean that they are clean, whereas the brown colour of rivers and streams mean they are carrying suspended mud or other materials. Changes in ocean-colour in open-ocean are largely governed by the presence of phytoplankton, and therefore, their concentration is derivable from inversion of the reflectance spectrum; in particular, when this spectrum is recorded from space.

The physical basis of detecting the micro-organism such as Phytoplankton from space lies with the fact that the Sunlight that enters the ocean can either be absorbed or scattered back (Figure 2). Pure water absorbs most red light but strongly scatters most blue light. Thus, open ocean waters with very little material in them appear deep blue, while waters carrying dissolved organic materials that absorb blue light strongly appear brown. Chlorophyll-containing microalgae assemblages—phytoplankton—absorb both blue and red light, making phytoplankton- containing waters look green. In addition, chlorophyll emits a small fraction of the absorbed light at a longer wavelength as red fluorescence, providing another signal for remote sensing. Scientists use these variations in the colour of water to estimate the amount of phytoplankton, suspended sediment, and dissolved organic material. Satellite based ocean-colour remote sensing has emerged as one of the most important tool for the monitoring the oceanic phytoplankton over last four decades. The methods of detecting and mapping

***Figure 1**: Different colour of sea waters observed around Arabian Sea*

phytoplankton concentration from space-borne platform was successfully developed using the first proof of concept mission called Coastal Zone Colour Scanner (CZCS), launched by NASA in November 1978. The CZCS legacy is far beyond what was initially expected from this "proof-of-concept" mission, and the global picture that emerged from the CZCS data set has deeply renewed oceanographers' vision of oceanic biota, and conclusively demonstrated the benefit of ocean-colour remote sensing to oceanography. As a consequence, a series of new sensors e.g. IRS-P3 MOS of DLR Germany, SeaWiFS & MODIS of NASA USA, OCTS and GLI of NASDA, Japan, MERIS of ESA and OCEANSAT-1 & 2 OCM of ISRO India were launched in the last 15 years.

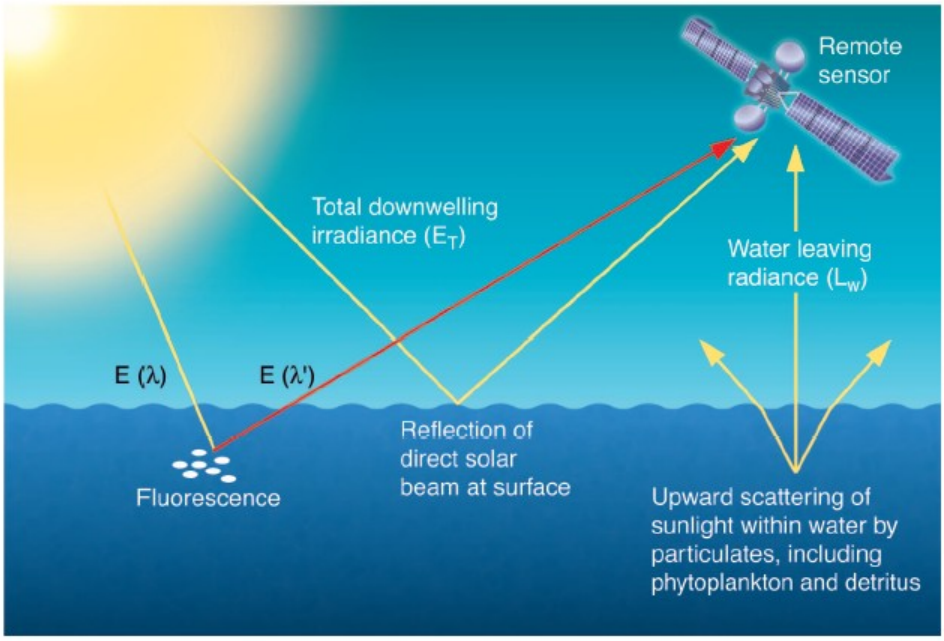

***Figure 2**: The colour of the ocean is recorded by a satellite sensor by measuring the "remote sensing reflectance (Rrs)" at specific wavelengths. Rrs is the ratio of light leaving the water (Lw) to the light incident on it (ET) and is determined by the absorption (a) and backscattering (bb) of light in the water column.*

Quantitatively relating the variations in the "ocean-colour" as seen from a satellite to the varying concentrations of chlorophyll-containing unicellular algae (the phytoplankton cells) was a challenge addressed by different ocean-colour satellite missions. All phytoplankton species (about 30,000 species within 12 phyla) contain the ubiquitous photosynthetic pigment, chlorophyll-a, which is responsible for in-water radiation absorption in the "blue part" of the spectrum, explaining the shift in ocean-colour, from "deep blue"(violet), "blue," "blue-green," "green," and even "brown" ambiences, for waters with progressively higher phytoplankton concentrations. A highly varying trail of pigments is actually associated with chlorophyll-a, as well as a varying amount of dissolved substances and particles The amount of phytoplankton and their optical properties (absorption and scattering) affect the spectral diffuse reflectance of the ocean, defined as the ratio of upwelling to downwelling irradiance at a given depth. Since phytoplankton pigments generally absorb more in blue than in green, the greener the water, the more phytoplankton. Thus by measuring ocean-colour, the spectral reflectance at zero depth, one can obtain estimates of phytoplankton pigment concentration. A variety

of algorithms such as empirical, semi-empirical and analytical, have been developed, relating spectral radiance coming out of ocean and phytoplankton pigment/suspended sediment concentration, also known as bio-optical algorithms. During the last decade number of ocean-colour sensor have been flown into space. Most of the ocean-colour sensors have spectral bands in blue/green region of electromagnetic spectrum along with at-least two spectral bands in near-infrared (NIR) region for the characterization of marine aerosols. Table 1 shows the spectral band-width of some of the important ocean-colour sensors.

The satellite based estimation of phytoplankton pigment concentration involves two major steps, the first is known as atmospheric correction of visible channels to obtain normalised water leaving radiances and the second is application of bio-optical algorithm for phytoplankton estimation. Before interpreting the ocean-colour as measured by satellite, the contribution of the atmosphere (about 90% of the recorded signal) must be estimated, a step which is referred to as the atmospheric correction. The atmospheric component consists of molecular (Rayleigh) and aerosols scattered light. The Rayleigh component can be calculated and removed, however the main difficulty is introduced by the highly varying optical properties of atmospheric aerosols. These properties result from local processes, from the large-scale atmosphere circulation, and from the remote sources of the particles, all of which are not known a priori when performing the correction. Several techniques exist for the new-generation sensors, based on their ability to gain information about the spectral dependency of aerosol scattering through measurements in near-infrared bands (where the open ocean is essentially "black") for extrapolating the atmosphere radiance into the visible. The water leaving radiance is related to the ratio of backscatter to absorption summed for all the constituents of the upper part of the water column. After the atmospheric correction has been done, chlorophyll-*a* is inferred from the ratio of water-leaving radiances at two or more

Table 1: Ocean–Colour spectral bands of some of the recent sensors

SeaWiFS		OCEANSAT -1 OCM		OCEANSAT -2 OCM		MODIS	
Band No	Spectral range(nm)	Band No	Spectral range(nm)	Band No	Spectral range(nm)	Band No	Spectral range(nm)
1.	402-422	1.	402-422	1.	402-422	8.	405-420
2.	433-453	2.	433-453	2.	433-453	9.	438-448
3.	480-500	3.	480-500	3.	480-500	10.	483-493
4.	500-520	4.	500-520	4.	500-520	11.	526-536
5.	545-565	5.	545-565	5.	545-565	12.	546-556
6.	660-680	6.	660-680	6.	610-630	13.	662-672
7.	745-785	7.	745-785	7.	725-755	14.	673-683
8.	845-885	8.	845-885	8.	845-885	15.	743-753
						16.	862-877
Spatial Resolution 1 Km		Spatial Resolution ~ 360 m		Spatial Resolution ~360 m		Spatial Resolution 1 Km	

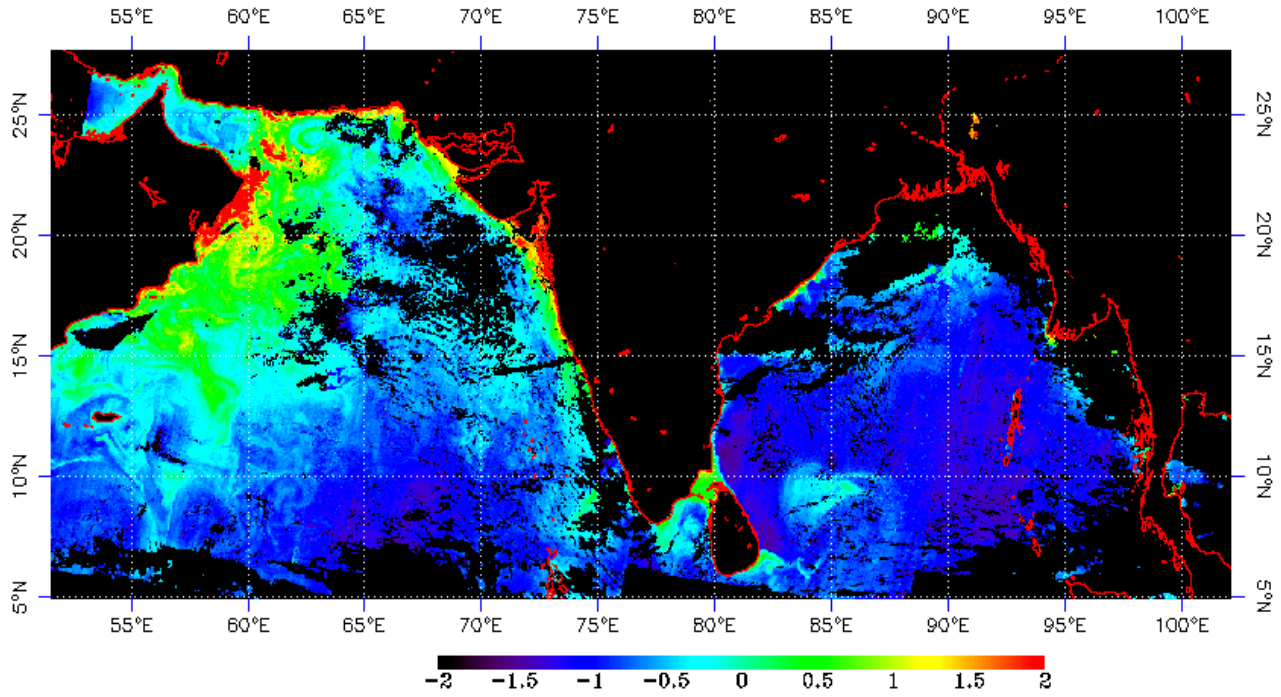

***Figure 3**: Phytoplankton distribution image derived from OCEANSAT OCM images during the month of July for the Arabian Sea and Bay of Bengal.*

wavelengths, using empirical relationships established from a series of simultaneous *in-situ* measurements of radiances and chlorophyll.

A number of bio-optical algorithms for chlorophyll-*a*, retrieval have been developed to relate measurements of ocean radiance to the *in-situ* concentrations of phytoplankton pigments. Most of these equations are derived from statistical regression of radiance versus chlorophyll. Advances in various theoretical studies and new parameterization of some optical properties have yielded better knowledge of the marine light field and have provided new tools for modelling ocean-colour. Figure 3 & 4 shows the distribution of phytoplankton in the Bay of Bengal and Arabian Sea during the month of July as captured by OCEANSAT OCM instrument. The red to green colour shows increased phytoplankton in the western Arabian Sea associated with wind driven upwelling along the Arabian coast. Contrary to Arabian Sea, Bay

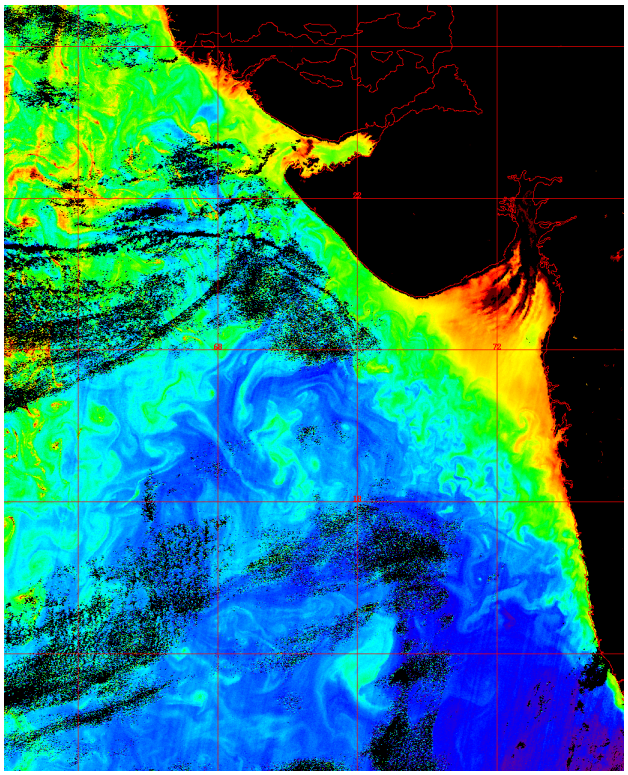

***Figure 4**: High Resolution Chlorophyll-a image from OCM-2 sensor off the coast of Gujarat showing distribution of Phytoplankton patches.*

of Bengal shows relatively less phytoplankton (represented by blue colour).

APPLICATIONS OF OCEAN COLOUR DATA

The availability of remotely sensed measurements of phytoplankton distribution has been found outstandingly rewarding for biological oceanographers, showing organized structure against a background of heterogeneous oceanographic measurements from ships. The operational ocean colour data and derived geophysical products are now days being used for host of applications to understand ocean biology and physical oceanography processes. Some of the key applications are, i) identification of potential fishing zones with improved reliability, ii) Modelling primary production for fish stock assessment and assessment of the role of ocean removing CO_2 from atmosphere, iii) Study of toxic and non-toxic algal blooms, iv) study of coastal processes by using sediment movement in coastal waters and v) water quality mapping for pollution studies, oil spill detection etc. In many areas, including the oceans around India a phenomenon referred to as upwelling brings nutrient-rich waters from deep in the ocean to the surface. This phenomenon is being studied by a suite of sensors, including those that map sea surface temperatures (SST), surface wind velocities, and sea surface height (SSH). These nutrient enrichments result in high densities of planktons and other microalgae in surface waters. Figure 5 shows an example of Noctiluca Miliaris phytoplankton bloom detected by OCEANSAT OCM sensor during the winter months in the western Arabian Sea. These blooms have special biogeochemical significance in the role of oceanic biology in climate control. Application of the satellite images includes diverse oceanic biogeochemical problems including carbon fluxes related to bloom conditions and sea-air fluxes due to nitrogen fixing Trichodesmium blooms.

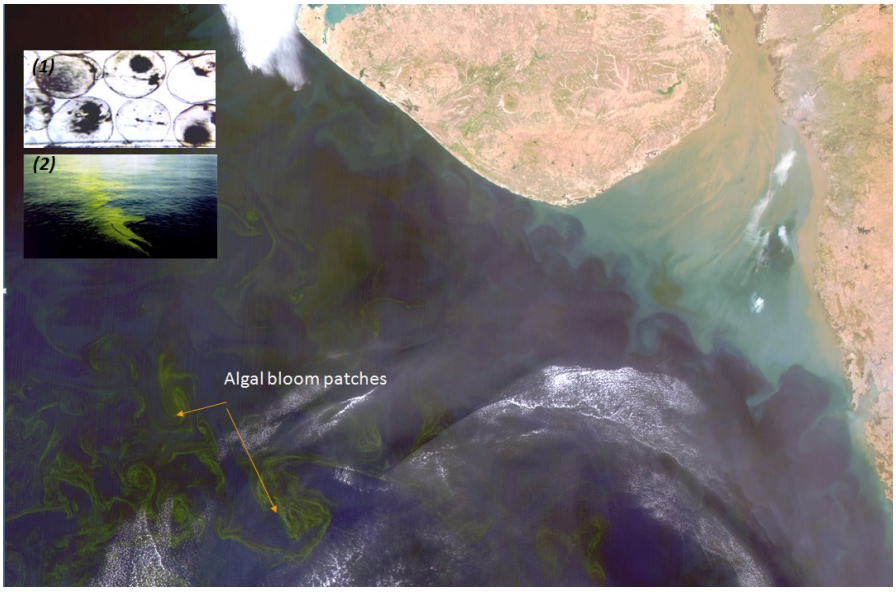

***Figure 5**: OCM true colour image off the coast of Gujarat. Green coloured patches of Notiluca Miliaris (type of phytoplankton) are seen in bottom left corner of the image. (Inset image shows, 1) cells of Notiluca Miliars and 2) field image of the Arabian Sea, parrot green colour of Notiluca dominated waters).*

Today, satellites are also being used to detect a range of specific phytoplankton. For instance, they are used to map the planktonic marine cyanobacterium Trichodesmium that occurs throughout the marine tropical regions. In addition to its role in fixing carbon through photosynthesis, this organism also fixes nitrogen

gas to produce organic nitrogen, making this otherwise scarce nutrient available in waters where it resides. Although Trichodesmium lacks specialized heterocyst cells that some nitrogen-fixing cyanobacteria depend on, it contains proteinaceous vacuoles, or gas vesicles, providing cells with buoyancy and keeping such populations near the surface where light is plentiful. Trichodesmium occurs as individual trichomes as well as multifilament aggregates, often referred to as colonies (Figure 6 a & b). Several optical properties make Trichodesmium an excellent microbe for study by remote sensing. For instance, its gas vesicles are very highly reflective. The absorption and fluorescence spectra of this pigment are readily distinguished from chlorophyll-a. Finally, its near-surface habitat (staying in a zone within about 50mfrom the ocean surface) makes it relatively easy to observe. Algorithms that are based on the six colour bands detected by the OCM sensor can be used to identify Trichodesmium blooms. Figure 6 shows one such example, where OCM data has been used to detect Trichodesmium blooms on the west coast of India in the month of April 2006.

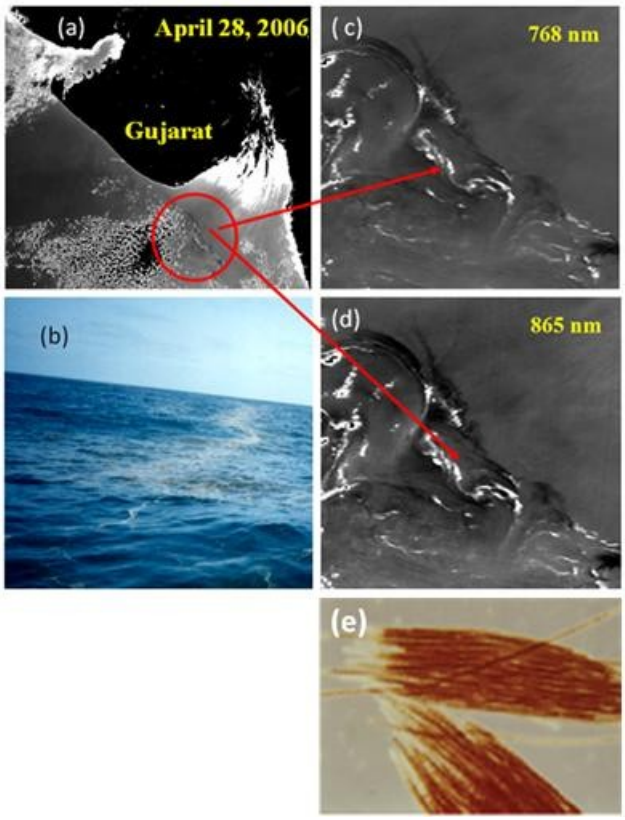

***Figure 6**: Detection of Trichodesmium blooms on the (a) west coast of India, (b) field picture of the bloom dominated brown colored waters, (c & d) OCM bands of 768 and 865 nm are useful of the detection of gaseous vesicles which makes them are very highly reflective, (e) Trichodesmium colony.*

Apart from detecting types of phytoplankton from space, Ocean chlorophyll images have also been used in conjunction with SST data to find potential fishing zone (PFZ) grounds in the sea. Bio-physical features and processes acts as a catalyst for the accumulation of fish in a given area in the ocean. Ocean colour is indicator of the first level productivity in the ocean, which in turn triggers the fish accumulation. And also colour gradient provides column information and reveals subsurface picture of water circulation and water productivity. An integrated approach using OCM derived chlorophyll and AVHRR derived SST has been used for PFZ generation. Figrue 7 shows the OCM image along with SST contours to find PFZ regions.

It is clear from the above that the satellite based ocean-colour data set provides the basis for temporal and spatial variability studies with time periods from days to decades and with spatial sizes from mesoscale to global apart from applications related to marine resources assesment. A large number of advance ocean-colour instrument are presently operating (e.g OCEANSAT-2 OCM, MODIS, MERIS etc.) and are also being planned for the continued long term ocean observations (e.g. OCEANSAT-3 OCM, NPOSS etc.). One of the key future thrust area of ocean-colour monitoring using

satellites will be to provide well calibrated long term climate data records (CDRs) of ocean productivity for identification and quantification of trends in the biomass of oceanic algae in response to global environmental changes. Keeping in-view of these observations and role of ocean biology in climate regulation, there is strong need to build the ocean-colour time series using the multiple ocean-colour sensors. These long-term, internally consistent ocean-colour time series will be useful to validate the global change scenarios that are produced by global ocean models.

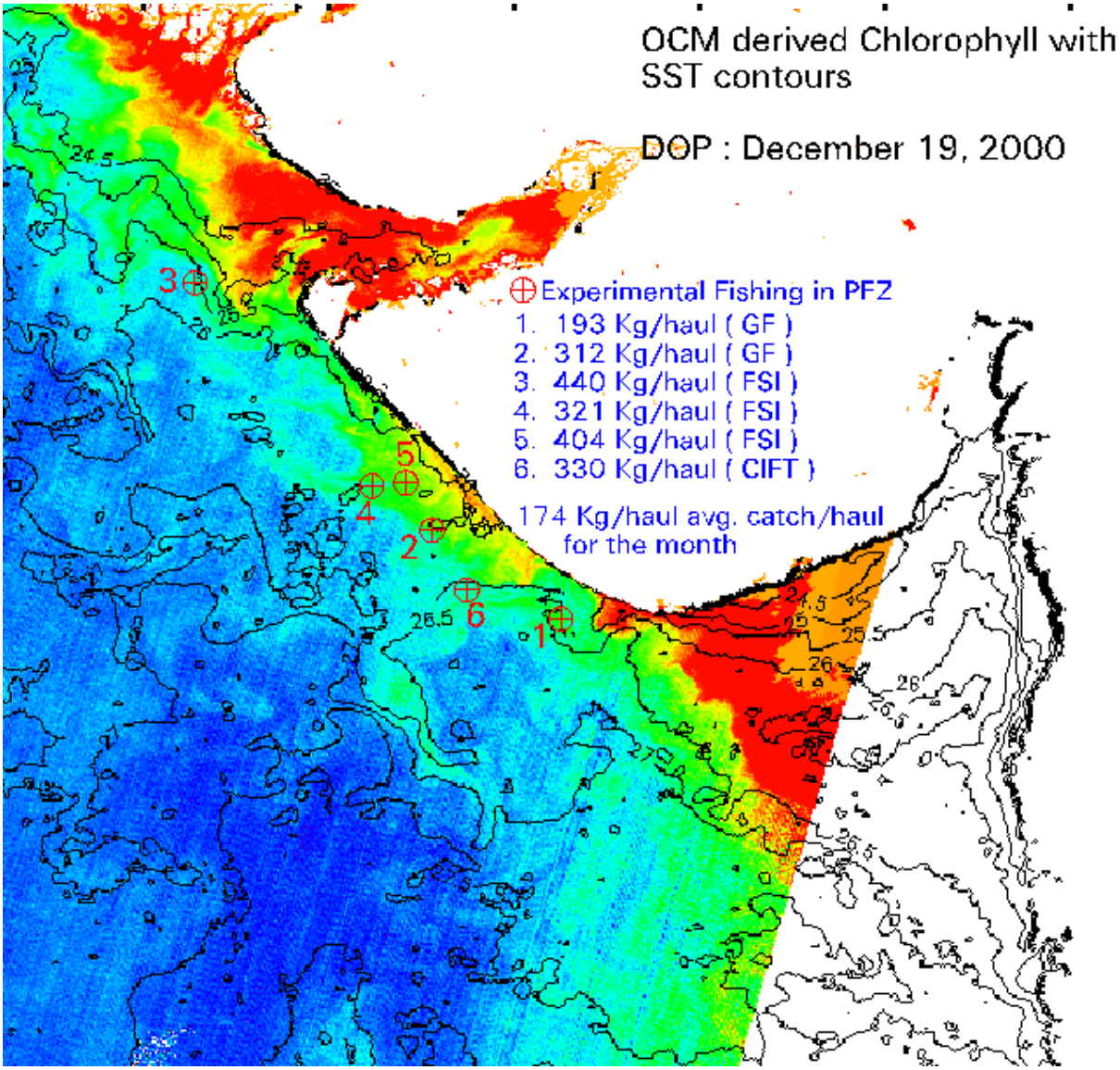

***Figure** 7: SST contours overlaid on the chlorophyll image. Such products are used for PFZ forecast.*

Physical Oceanography using Satellite Data

Raj Kumar and Rashmi Sharma

Space Applications Centre, ISRO, Ahmedabad, India
Email: rksharma@sac.isro.gov.in

INTRODUCTION

Oceanography, a multi-disciplinary science includes Physical oceanography, Marine geology, Marine chemistry, Marine biology, Marine technology and others. The oceans are central to the continued existence of life on our planet covering approximately seventy percent of the Earth's surface. Most of the livelihood of coastal population depends upon the ocean living resources. In addition to the fishing skills of these fishermen, they also consider the physical state of the ocean as part of their daily routine. In addition to these we depend on the ocean for water transportation, recreation, minerals and energy. Oceans are also store house of huge energy. Ocean surface currents cause changes in global weather patterns and whereas deeper ocean currents, commonly known as thermohaline circulation have a large impact on climate change and global warming. These changes in the oceans occur at various scales, ranging from diurnal to decadal. Due to all the above reasons, it is essential to monitor and predict oceans behaviour.

Due to the turbulent nature of the oceans, it requires continuous and simultaneous observations at all points of the globe for all times or at least as frequently as possible. The observations would have to cover a complete specification of thermodynamic and turbulent state of ocean, earth's surface and upper atmosphere referred as atmospheric system. The sparse surface, deeper oceanic and lower atmospheric observations obtained using ships, buoys and floats are not adequate to provide sufficient information about the global state of ocean needed by theoretical models. Therefore, the gaps in the observational frequencies and the spatial coverage is sought to be filled by space-borne observations.

Satellite Oceanography encompasses oceanographic research and technological development resulting from space borne sensors in Earth's orbit. These sensors make observations of oceanographic parameters such as sea surface winds, sea surface temperature (SST), ocean waves, sea surface salinity (SSS), sea surface height (SSH) and ocean colour. These observations are assimilated in the numerical ocean models to provide ocean state prediction a few days in advance. Additionally, in situ observations are required to study the processes at deeper levels in the oceans, as satellites cannot provide sub-surface information directly. In situ data are also required to assess the accuracy of satellite derived parameters. Therefore in order to model the ocean state to provide accurate ocean state predictions (waves and circulation) for various applications, one

needs to follow an integrated approach wherein space-based information in situ measurements and numerical models are all part of the system.

In physical oceanography, like in any observational science, the length and time scales of the observations must match those of the phenomena under investigation. Therefore, it is necessary to consider whether the length and time scales of ocean phenomena are capable of being sampled adequately by the techniques of remote sensing from space. In-situ observation onboard ships and buoys generally find it easier to resolve in time rather than space. Satellite observations, on the other hand, can give reasonable spatial resolution (a few meters upwards) and broad area coverage. Time resolution may not be that good (no better than four passes a day). If there is known or expected frequency/wavelength relationship as for surface waves, it may not matter for many applications that the time domain is not adequately resolved, since occasional synoptic views of the wave-field can give much valuable information. Space observations provide synoptic and repetitive coverage of the ocean in contrast to the sparse and isolated in-situ ship observations. Space-borne sensors provide observations of regions of the ocean, which are inaccessible to ships. Certain measurements specific to orbital platforms such as sea surface height have been available only through satellite oceanography. The measurements provided by the space-borne sensors pertaining to the sea surface have manifestation of the subsurface oceanic processes. Sensors on-board space platforms use electromagnetic radiation in visible, near infrared, thermal infrared and microwave regions to measure diverse physical, biological and geological parameters of the ocean. History of Satellite Oceanography began with the launch of first artificial satellite by the USSR in 1957. Since then spectacular advances have been made in this field.

ELECTROMAGNETIC SPECTRUM

Remote sensing technology makes use of electromagnetic (EM) radiations of certain wavelength in EM spectrum to distinguish different objects, as different objects radiate differently. The light which our eyes “our remote sensors" detect is the visible part of EM spectrum. There is a lot of radiation around us which is "invisible" to our eyes, but can be detected by other remote sensing instruments and used. The visible wavelengths cover a range from approximately 0.4 µm to 0.7 µm. The next portion of the spectrum of interest is the infrared (IR) region, which covers the wavelength range from approximately 0.7 µm to 100 µm - more than 100 times as wide as the visible portion and can be divided into two categories based on their radiation properties - the reflected IR (0.7 – 3.0 µm), and the emitted or thermal IR (3.0 µm to 100 µm). Radiation in the reflected IR region is used for remote sensing purposes in ways very similar to radiation in the visible portion. The energy in thermal IR region is essentially the radiation that is emitted from the Earth's surface in the form of heat. The next portion of the spectrum to remote sensing is the microwave region from about 1 mm to 1 m. This covers the longest wavelengths used for remote sensing.

Satellite observations are based on measurements of radiation either emitted from earth or radiation returned as back-scatter from earth-atmosphere system when a satellite-based pulse source illuminates (active sensing) the target. The absorption by atmospheric gases and reflection / emission from earth’s surface is the backbone of these remote sensing methods. As far as the Ocean is concerned, one can either use

solar radiation reflected/scattered from it (mainly used for Ocean colour monitoring, which is related to biological productivity, sediments etc.), or thermal infrared emitted from it (relates to SST), or microwave radiation emitted from it (relates to temperature, roughness of the sea and salinity), or active microwave sensor (which give more details of the sea roughness, leading to Sea Surface Wind Vector, SSH, Wave Height, Wave Spectra etc.).

SPACE-BORNE SENSORS FOR SATELLITE OCEANOGRAPHY

All space-borne sensors use portion of the electromagnetic energy; either naturally emitted from sun or artificially radiated using a LIDAR or radar. The sensors which depend on solar radiation or natural self-emissions are grouped under passive sensors, while those using electromagnetic energy sources of their own are called active sensors. Atmosphere is an all-pervading medium through which observation of any oceanic process from a space platform needs to be carried out. Regions of electromagnetic spectrum for which atmosphere is transparent are treated as atmospheric windows for operation of space-borne sensors. One of the major limitations on the use of visible, infrared and thermal infrared spectrum for operational estimation of oceanographic parameters is their inability to observe the sea surface through cloud cover. The microwave region of the electromagnetic spectrum is transparent to the presence of clouds. Synergistic use of optical and microwave remote sensing data has provided a unique opportunity in addressing several outstanding oceanographic applications, particularly in the tropics.

The remote sensing sensors can be divided into following categories:

- Visible wavelength "ocean colour" sensors
- Infrared radiometers for sea surface temperature
- Passive microwave radiometers
- Active microwave sensors – Radars

The fundamental variables measurable from space and the main oceanographic quantities that can be inferred are given in Table 1.

Table 1: Ocean variables measurable from Space

Basic Quantity	Sensor type	Derived information
Radiance	IR, passive microwave, visible	SST, chlorophyll, sediments, Salinity
Distance	Radar Altimeter	Sea level, currents
Backscatter	Radars	Winds, waves, eddies, internal waves, slicks, currents

Radiometers: Radiometers are passive sensors operating in the visible, infrared and microwave regions of electromagnetic spectrum to detect naturally emitted or reflected radiation from the earth's surface. Radiometers can be both imaging and non-imaging type. Reflected solar radiation dominates in the visible and near infrared region, while natural thermal emission is the major contributor of the electromagnetic energy in the thermal IR and microwave region. While the spectral bands chosen in the visible region are sensitive to reflectance/absorption properties of water constituents, the spectral bands in the infrared/ microwave region are sensitive to atmospheric components.

Reflectance of seawater depends on sea surface

roughness as well as presence of water constituents such as salinity, chlorophyll, turbidity, coastal bathymetry, etc. Measuring the absorption characteristics of ocean surface in the visible region, one can get the information on water constituents. Light interacts with the water constituents and this interaction is wavelength dependent. Hence upwelled light in different bands are then related to above constituents empirically to derive these parameters.

In passive radiometer, the basic principle underlying the remote sensing methods is the natural thermal emission from a target, dependent on its temperature and emissivity. For an ideal black body whose emissivity is unity, the natural thermal emission is governed by Planck's law. The quantity of electromagnetic energy emitted from the earth surface peaks at ~10. The relationship between peak, wavelength λ_{max} i.e. the wavelength at which maximum radiation is emitted, and the physical temperature of blackbody, T, are given by the Wein's displacement law. At microwave frequency (1-40 GHz), the Planck's relation between emitted radiation and the physical temperature of blackbody is replaced by Raleigh-Jean's approximation stating that the emitted radiation is directly proportional to the temperature of the emitting surface. The above relation is much simpler than the one for IR radiometry where the full Planck's function must be used.

We will briefly outline the retrieval technique for SST in both IR and microwave regions:

Infrared Techniques: From Wien's displacement law, terrestrial emissions peak at around 10 µm because of its temperature (~300 K). SST measurement using IR radiometers make use of this by measuring the radiation emitted in the 10-12 µm band as an indicator of the SST. This region being more transparent (least absorption by the gases in the atmosphere), except for highly variable atmospheric water vapour, is called 'Atmospheric window'. To correct for the water vapour absorption, the split window channel (i.e. 10.3-11.3 µm, T_{11} and 11.5-12.5 µm, T_{12}) observations are utilised. Absorption in the second split window channel is more than the first channel; therefore, the difference of brightness temperature observations in these two channels gives quantitative estimate of atmospheric water vapour that is required for correction in the SST computation. Simple dual channel algorithm has following form:

$$SST = A_0.T_{11} + A_1.(T_{11} - T_{12}) + A_2.(T_{11} - T_{12}).(\sec(\theta) - 1) + A_3 \sec(\theta) + A_4$$

Where A_0, A_1, and A_2 are coefficients derived using regression analysis between actual SST and collocated satellite observations. And θ is observation zenith angle needed to correct for the zenith angle variation. In infrared 3.7 µm wavelength is highly sensitive for surface temperature variations. However, during daytime this channel cannot be used due to contamination from reflected solar radiation in this wavelength and is used during night-time to provide accurate SST. Due to strong absorption of infrared radiation by clouds, Infrared techniques cannot be used in presence of clouds. In cloudy conditions microwave techniques are used to infer SST from satellites.

Microwave Techniques: Systems normally operating in the microwave part of the spectrum, 1-200 GHz, observe the thermal radiation emitted by the sea surface, radiation emitted by the atmosphere and that reflected by the sea surface. At these comparatively long wavelengths, there is no scattering by the

atmosphere or aerosols, haze, dust or small water particles in the clouds, so that microwave sensors have effectively all-weather sensing capability, although liquid water in the form of precipitation does scatter the radiation and can render the atmosphere opaque at microwave frequencies. On the other hand, the major disadvantage in this frequency range is weak thermal emission and low signal at the sensor. To overcome noise levels a large field of view is received, with relatively coarse spatial resolution. The emissivity of the sea at microwave frequencies is also very small and varies with the dielectric properties of seawater, and the surface roughness. Since the dielectric constant varies with temperature, salinity and frequency, the observations of a multi-channel microwave radiometer must contain information not only about the seas surface temperature, but also about the ocean salinity and the sea state. Operationally, 6 GHz and 10 GHz Channels have been used from satellite sensors to retrieve SST, e.g., Nimbus SMMR, Oceansat-1 MSMR, TRMM TMI, DMSP SSMI, Aqua AMSR etc. A typical algorithm for retrieval of SST from Microwave radiometer observations make use of multi-channel observations to correct for sea surface roughness, atmospheric water vapor, cloud liquid water etc, and has the following form:

$$SST = A_1.T_{6H} + A_2.T_{6V} + A_3.T_{10H} + A_4.T_{10V} + A_5.T_{18H} + A_6.T_{18V} + A_7.T_{21H} + A_8.T_{21V} + A_9$$

Where, $A_{1\text{-}9}$ are coefficients derived empirically, and T_{nH} and T_{nV} are H and V-polarization brightness temperatures at different frequencies Accuracy of SST retrievals from microwave radiometers is poorer than infrared observations, but they have advantage due to all weather capability.

Radar Altimeter: Altimeter uses a nadir-viewing radar to transmit short pulses, typically of a few nano seconds duration, and detects the return pulse along with the two-way travel time. As the name signifies, the primary goal of an altimeter mission is the measurement of the altitude of the sea surface from a reference ellipsoid. This is done by bouncing a radar beam at a particular microwave frequency and by measuring the two-way travel time of the radar pulse. Knowing the speed of the electromagnetic wave, and the precomputed height of the satellite above a reference ellipsoid, one can then easily compute the sea surface height (SSH). However, due to the interaction of the radar pulse during its passage through ionosphere, atmosphere, ocean surface, several corrections have to be applied in order to achieve highly accurate SSH. Apart from SSH, one can also compute another important characteristic of the sea surface, which is the significant wave height (SWH), related to the slope of the leading edge of the reflected pulse. Obtaining SWH of course requires

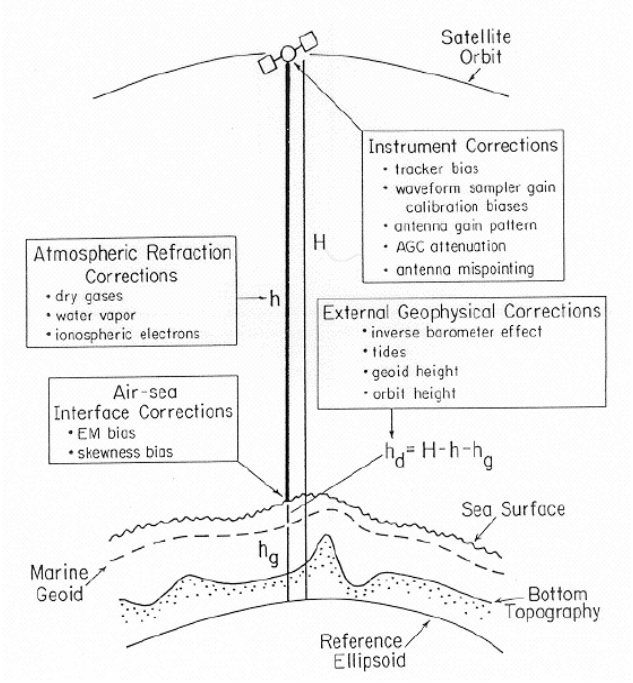

***Figure 1**: Measurement principles of satellite altimeter*

sophisticated algorithms. The third quantity of interest is ocean surface wind speed, which is empirically related to the backscattered power. Measurement principles of altimeter and associated corrections involved in accurately determining the SSH are shown in Figure 1.

A typical waveform or the radar return pulse from ISRO-CNES joint mission, SARAL/AltiKa 40-Hz data has been shown in Figure 2:

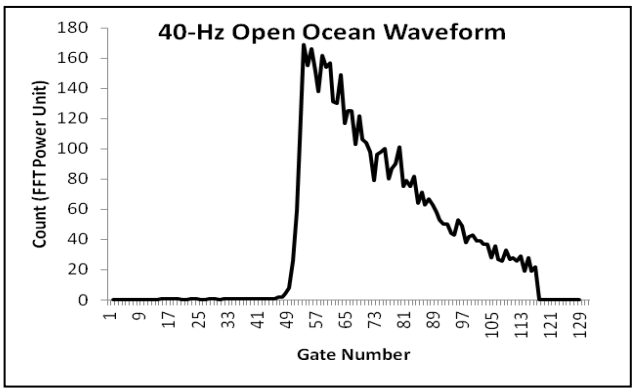

***Figure 2**: Typical waveform of open Ocean region*

Radar return pulse W (t) is a convolution of three terms; a) the flat sea surface response (FSSR), b) the sea surface elevation probability distribution (PDF), and c) the radar system point target response (PTR) (transmitted pulse as affected by the receiver bandwidth). The first term a) includes the effects of antenna beam width and the off-nadir pointing angle. The mean return waveform as a function of time t, (generally measured in nanoseconds), is expressed as the following convolution:

$$W(t) = FSSR(t)^* PDF(t)^* PTR(t)$$

Calculation of the convolution with the assumption that mispointing angle is less than 0.3 degrees gives the analytical expression:

$$W(t) = (A/2) \exp(-v) [1+ erf(u)]$$

where, the auxiliary parameters u and v depend on the oceanic parameters of our interest. Retrieval algorithms employed are physically-based type like, maximum likelihood estimator. The algorithm retrieves mainly three parameters, namely the amplitude, the epoch and backscatter coefficient from the analytical model. More complex waveforms are retracked using empirical algorithms.

Scatterometer: A radar scatterometer uses its own source of electromagnetic energy (hence an active sensor) at microwave wavelengths to illuminate the target and detects the backscattered energy. It operates either on ground or air-borne/space-borne platforms to measure the scattering or reflective properties of the target from an oblique angle. It is a non-imaging sensor, since it measures the average backscattered energy over relatively broad areas. A space-borne scatterometers use the same antenna for transmission and reception of electromagnetic signals. Scatterometers employ multiple fan-shaped or pencil beam antenna to measure the directional property of the backscattered energy in order to remove ambiguities in derivation of physical processes. It may also use different polarizations for transmitted and received signals. Sensitivity of scatterometer to winds and waves depends on the frequency or wavelength of the operation. Bragg scattering for incidence angle in excess of 20^o predominantly controls backscattering of microwave energy from ocean surface. The backscatter energy from the ocean surface is dependent on wind speed, relative wind direction and the incidence angle and polarization. The backscatter energy from the ocean surface is related to wind speed as:

$$BE = A + B \cos \varphi + C \cos 2\varphi$$

where, φ is the azimuth angle between radar look-direction and the upwind direction, A, B and C are constants which depend upon wind speed, its direction and incidence angle.

The radar backscatter has a harmonic dependence on wind direction which results into multiple solutions of wind vector from a given radar backscatter data. As the radar backscatter depends upon both wind speed and direction, at least two measurements of radar backscatter are required to determine the two parameters. However, unique solutions are not possible due to the harmonicity and the noise in the data. Among these multiple wind vector solutions, only one solution corresponds to true wind vector while others are ambiguous, which are called aliases. Although, the wind speed solutions are very close to each other, the direction solutions are quite apart. An algorithm with certain criterion prioritizes the solutions and the performance of the algorithm is evaluated in terms of percentage of highest priority solutions, correctly identifying the true directions out of the total number of data cases processed. The retrieval algorithms yield multiple solutions of wind vector along with their priority in identifying the true wind vector from a given set of radar backscatter measurements. Under noise-free conditions, the highest priority solution always represents the true wind vector but for noisy or real data, it is not always so. However, the first two highest priority solutions contain the true direction most of the times. The directional ambiguity removal algorithm performs the selection of true wind solution. Geometry of the pencil-beam scatterometer onboard Oceansat-2 is shown in Figure 3.

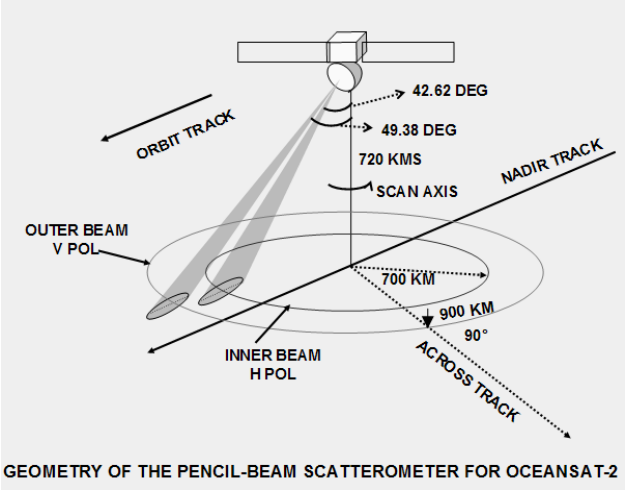

***Figure 3**: Geometry and scan mechanism of scatterometer onboard Oceansat-2*

Synthetic Aperture Radar (SAR): The resolutions of microwave radar are different in the azimuth and range directions and depend upon a number of antenna parameters such as antenna length, pulse, look-angle, frequency of electromagnetic radiation used and processing scheme adopted. For a side-looking or real-aperture radar, the azimuthal (R_a) and range resolutions (R_r) are given as,

$$Ra = \beta R; \quad R_r = c\,\tau / (2 \sin \theta)$$

where, τ : the pulse width, θ : the incidence angle for the radar beam, c : speed of propagation of electromagnetic radiation, R : range, β : the beam width, which is directly proportional to the antenna length of electromagnetic radiation used. Real aperture radars are characterized by coarse azimuthal resolution due to limitation on the antenna length for a radar operating on a space platform.

Along track or azimuth resolution of the radar is defined as β R, where β is the beam-width of the antenna and R is the range of the target. Beamwidth β depends upon wavelength λ of the

transmitted signal and aperture D of the antenna as λ/D. Hence, azimuth resolution will be defined as λR/D. For, a radar operating at frequency 6 GHz (5 cm wavelength) on a spacecraft at height of 800 km, to achieve ground resolution of 10m, an antenna of size of 4km will be needed, which is clearly impracticable with present technology, so an alternative approach of synthesising the larger antenna is developed.

The way to understand the operation of large real aperture and SAR is as follows. Suppose a signal is emitted from radar and it reflects back from different targets. The signal from point opposite the antenna reaches first to the centre of antenna and later to ends of antenna i.e. small phase change will occur along the aperture but phase distribution will be symmetrical about the centre and overall summation of signal across the aperture will be constructive. But if the target is towards one end of antenna, the phase change around centre of antenna will not be symmetric and hence destructive interference will occur and when signal is integrated, it will not contribute to the signal. Similar things will happen for targets between these two points. The larger the aperture of antenna, the closer the point from centre will try to create destructive interference and will not contribute to received signal, hence resolution will be higher. SAR uses the same principle, but instead of using larger antenna, it uses smaller antenna and signal is integrated over a large period of time by moving the antenna. Synthetic aperture radar uses coherent processing of backscattered signals using the amplitude as well as the phase information from the target, as the beam travels across the targets to generate high azimuthal resolution comparable with that of the optical sensors. In synthetic aperture the length of aperture can be synthesised depends upon the distance while a particular point is seen. In the Fig.4 it is AB = ρ_R. Thus azimuth resolution achievable with AR is $\rho_a = \lambda R/2\rho_R$. Hence $\rho_a = \lambda R/2\rho_R = \lambda RD/2\lambda R = D/2$. Like scatterometer, SAR may also use multiple polarization concepts.

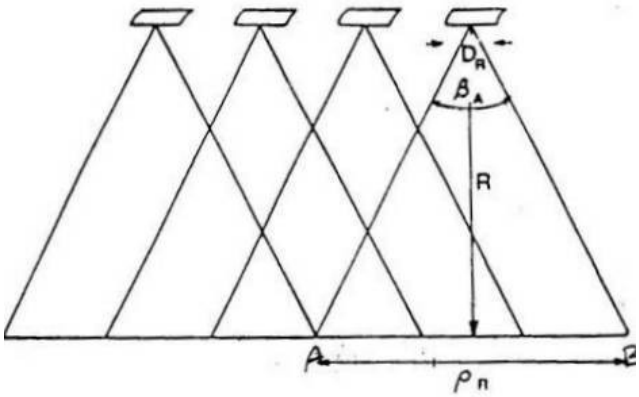

***Figure 4**: SAR Antenna Synthesis*

SATELLITE DERIVED OCEANOGRAPHIC PARAMETERS

Important oceanographic parameters and processes where remote sensing can help are as follows:

Sea surface temperature: Since sea surface is defined as the boundary between the ocean and the atmosphere, SST is the main parameter of air-sea interaction. This parameter is used in studying the climate and monsoons. Equatorial waves, eddies, thermal fronts and upwelling regions can be detected from SST observations. This parameter is also required for fishery resource studies.

Sea Surface wind vector: Wind affects ocean surface to a great extent and causes oceanic mixing and surface currents. This parameter is a crucial input to the numerical modelling of the ocean and atmospheric dynamical processes.

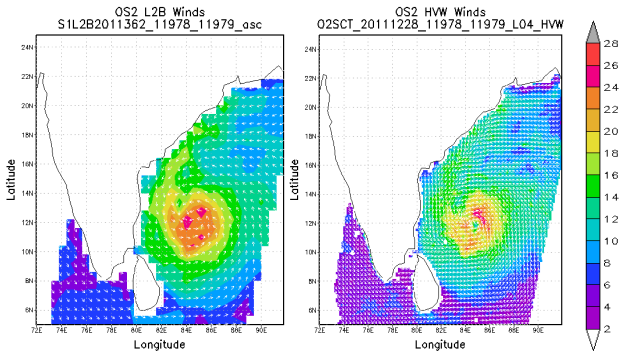

***Figure 5**: Scatterometer derived operational and high resolution winds*

Sea surface height: This parameter represents the dynamic and thermodynamic nature of the oceanic top layers, since both heat content and dynamic forcing change the sea surface height. Due to the Ekman divergence, the sea surface slopes up to the right in the Northern Hemisphere. Similarly the sea level rises due to the thermal expansion of water. Sea level is also affected by the atmospheric pressure. The sea surface height variations are measurable only from MW altimeters requiring a very high degree of satellite orbital information.

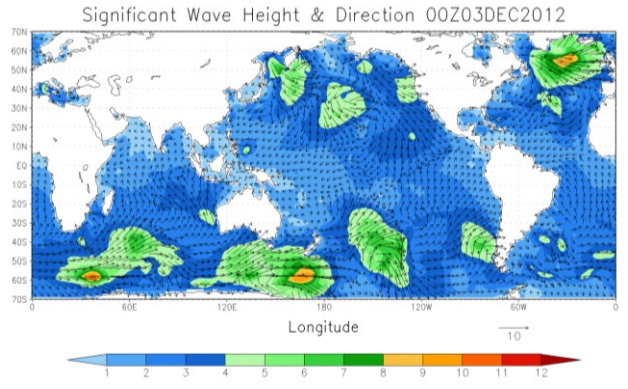

***Figure 6**: Significant wave height and direction*

Sea Surface waves: This is one of the most important parameters where MW information is the only source because microwave instruments are particularly capable of measuring the roughness of the sea surface in a variety of ways. With quantitative global measurements of the significant wave height through an altimeter, and two-dimensional wave spectrum through synthetic aperture radar, and availability of new generation Wave models, it is now possible to provide very reliable wave forecast over global oceans.

Mixed layer depth: Mixed layer is that portion of the oceans which directly interacts with the atmosphere. Oceans having deeper mixed layer have more thermal inertia compared to the places where mixed layer is shallower. Thus, MLD has a direct role to play in climatological behaviour of a particular region. It also influences cyclogenesis at least to some extent. Bay of Bengal has deeper mixed layer compared to the Arabian Sea and this is considered as one of the factors for Bay of Bengal to be more susceptible for the cyclone formations.

Sea Surface Salinity: Salinity is also important parameter from the point of view of ocean circulation. The degree of salinity in oceans is a driver of the world's ocean circulation, where density changes due to both salinity and temperature changes at the surface of the ocean produce changes in buoyancy, which cause the sinking and rising of water masses. Salinity is also an ecological factor of considerable importance, influencing the types of organisms that live in a body of water. As well, salinity influences the kinds of plants that will grow either in a water body.

Ocean Circulation: The main features of the mean ocean circulation are a series of gyres which extend longitudinally across the entire ocean, and which vary with latitude in their sense of rotation. The rotation sense is correlated with the latitudinal shears of the prevailing wind stress. This makes the wind stress or surface

wind measurements by microwave scatterometer very relevant. An important feature of this wind-driven circulation is the longitudinal asymmetry. The Ocean tends to be composed of distinct water masses, with distinct temperature, salinity, and chemical constituents, and often-distinct biological populations too.

APPLICATION AREAS OF SATELLITE OCEANOGRAPHY

Ocean State Forecast: Ocean state is one of the principal information required by shipping, off-shore industries as well as pollution monitoring. The physical state of the ocean viz. surface wind, surface humidity, surface waves, surface currents, mixed layer depth, storm surge, upwelling in coastal regions, etc. are some of the information which are required not only on near-real time basis, but also a forecast for at least next 3-5 days.

Monitoring El-Nino and Indian Ocean Dipole: Ocean-atmosphere is a coupled system. They exchange energy and momentum at interact with each other at various temporal and spatial scales. El-Nino in Pacific and Indian Ocean Dipole are two strong interannual mode and are the result of air-sea interaction processes. These two events have strong societal and climatic implications. These events can be easily monitored by SSH and SST signatures. Strong anomaly in the SSH is observed during these two events, with a see-saw kind of pattern having positive sea level anomaly at one side of the basin and negative at the other side. These two events have co-occurred in many years. Space borne sensors like, altimeter and radiometer are of immense use to monitor such events.

Monitoring Global Mean Sea level: Global mean sea level rise as a consequence of increasing earth's surface temperature is a major threat to coastal regions of the world. It becomes increasingly important to monitor this rise. Satellite altimeter is the most important tool to measure global sea level, which otherwise is very difficult to observe using tide gauges.

SATELLITE MISSIONS FOR PHYSICAL OCEANOGRAPHY

It has been realized that satellites represent a very important (in many situations, even critical) tool to complement existing in-situ techniques, such as ships and buoys, and contribute to a better understanding and monitoring of ocean processes, not only for research and climate studies, but also for better management of activities on and in the oceans. For the first time, it is possible to contemplate synoptic observations of geostrophic surface currents, wind stress and sea surface temperature over an ocean network routinely. These data when combined appropriately with subsurface density and current measurements should provide global information on the general circulation of the ocean and its primary driving forces. Some of the new systems for Sea Surface Height, under consideration are 'Multi-beam interferometric Altimeter', 'Large dish beam limited Altimeter', 'Scanned-beam-limited phases array altimeter', 'Interferometric side-looking imaging radar', 'Synthetic - Aperture Altimeter', etc. Present capability of scatterometer systems are of the order of 2 ms-1 and 20o. It will be desirable to achieve 1 ms-1 and 10o unambiguous directions. Increasing interest in the global climate problem has tended to focus attention upon the very large-scale components of the ocean circulation. The climate studies seek estimates of the quantities of heat stored in the surface layers of

the ocean and the rate at which the heat is exchanged with the atmosphere or advected to other regions by currents. In this context, measurements of surface wind, sea temperature, and the distribution of clouds are particularly important.

Indian Scenario

Bhaskara I and II carrying satellite microwave radiometer operating at three frequencies launched in 1979 and 1981 marked the beginning of satellite oceanography in India. Sensors on board the Indian Remote Sensing Satellites (IRS -1A, 1B, 1C, 1D) have been essentially designed for land applications. IRS - P3 carrying German-built eighteen channel Modular Opto-electronics Scanner is the first in the series aimed at oceanographic research. The data from these provided impetus for scientific investigations. Data at high radiometric resolution and at narrow spectral bands placed appropriately are learnt for retrieval of ocean colour and atmospheric parameters. Development of suitable algorithms and their validation through in-situ ship measurements has taken place. Small swath (200 km) and 24 - day repeativity prevented it being used for operational applications. IRS-P4 (Oceansat - I) carrying two payloads Ocean Colour Monitor (OCM) and Multi-frequency Scanning Microwave Radiometer (MSMR) was launched in 1999. Oceansat - 2 carrying active microwave sensor, scatterometer (OSCAT) and OCM was launched in 2009. Wind data from OSCAT is now routinely assimilated in to weather model for providing accurate prediction with lead time of few days. Several parameters are being derived from OCM, like diffuse attenuation coefficient, suspended sediment, chlorophyll concentration, which is helping scientists to study the biological processes and also coupled bio-physical processes. Another microwave sensor, Altimeter (AltiKa) onboard SARAL operating in Ka-band in the framework of collaboration between ISRO and CNES was launched this year. This is the first time that high frequency altimeter has been put in orbit. The small footprint in Ka-band will be highly beneficial for coastal applications. INSAT-3D, primarily for atmospheric applications and forecasting, will also give SST, very useful for ocean applications, has been launched. Need for new sensors such as LIDAR and multi-frequency, multi- polarization synthetic aperture radar are constantly being reviewed. Table 2 provides broad specifications of Indian satellites, sensors and parameters.

Table 2: Indian Remote Sensing Satellite for Physical Oceanographic parameters

Satellite Mission	Sensor	Parameters
Oceansat-1 (1999)	MSMR, OCM	SST, Surface wind speed, integrated water vapour, cloud liquid water
Oceansat-2 (2009)	Scatterometer (Ku), OCM	Ocean surface wind vector, ocean color
SARAL (2013)	AltiKa	SSH, wind speed, SWH
RISAT-1 (2012)	SAR	Ocean waves, Winds
INSAT-3D (2013)	Imager	SST

International Scenario

At the international level too, the past and the coming decade has/will witness the launch of a series of advanced satellite systems capable of providing unique oceanographic measurements. There are roughly about eighty missions

carrying more than two hundred instruments launched/planned by various member countries of the Committee on Earth Observation systems (CEOS). These instruments include high-resolution multi-spectral radiometers in visible, infrared and microwave spectrum, active imaging radars and lidars, multi-directional radiometers, polarimeter radiometers, radar altimeters and wind scatterometers etc. In the last few years, yet another microwave instrument that operates at low frequency (L-band, 1.4 GHz) has been put onboard NASA's satellite Aquarius and ESA's SMOS. These instruments for the first time are giving useful information about the sea surface salinity for understanding the global water cycle. Some of the international missions, sensors and parameters are listed in Table 3. This list is just an indicative one and by no means is exhaustive.

Table 3: Major International Space Missions related to Physical Oceanography

Satellite Mission (Year of launch)	Sensor	Parameters
NOAA 9, 10,11, 12,14,15,16,17 (1983-present)	AVHRR	SST
SeaWIFS (1997)	Radiometer	Ocean colour parameters
ERS 1,2 (1991-1995)	SAR, AMI, ATSR,ALT	SSH, Waves, SST, wind speed
ADEOS-1 (1996)	OCTS	SST, chlorophyll
TERRA (2000)	MODIS	SST, chlorophyll
Envisat (2002)	ALT,AAT SR,ASAR	SSH, SST,waves
TOPEX/ POSEIDON, JASON 1/2 (1992, 1998, 2008)	ALT	SSH
QuikSCAT (1999)	SCAT	Wind vector
Seasat (1978)	SMMR, SASS	SST, wind vector
Nimbus (1978)	SMMR	SST
DMSP (1987)	SSM/I	SST
TRMM (1997)	TMI	SST, wind
AQUA (2002)	AMSR-E	SST
Radarsat (1995)	SAR	Surface waves
HY-2/3 series (Starting 2011)	Alt, Rad, Scat	Wind, wave, SSH, SST
SMOS (2009)	Radiometer	Sea surface salinity
Cryosat 2 (2010)	Altimeter	Sea/land Ice thickness
Aquarius (2011)	Radiometer	Sea surface salinity
Sentinel-3 (2014)	Radiometer, altimeter, scatterometer	SSH, SST, Wind

Design and development of innovative sensors such as multi-beam interferrometric altimeter, synthetic aperture altimeter, interferrometric side- looking imaging radar etc. are also in progress. It would be up to the oceanographers to make use of this wealth of information to study the ocean and also critically evaluate the gaps and provide feedback towards the definition of newer ocean observation systems.

Applications of satellite altimetry in geodynamics

K. M. Sreejith and A. S. Rajawat

Space Applications Centre, ISRO, Ahmedabad, India
E-mail: sreejith81@gmail.com

MARINE GRAVITY FROM SATELLITE ALTIMETRY

The calculation of marine gravity field of the Earth from radar altimetry data is based on the principle that the sea surface corresponds to an equipotential surface of the gravity field. The presence of lateral density variations (e.g. seabed morphology and varying density of subsurface masses) distorts the shape of the gravity field and, by implication, the shape of the equipotential surface. The sea surface (or geoid) will bulge upwards over excess mass (gravity high) and will dip downwards over a mass deficit (gravity low). The Sea surface height (SSH) measurements from satellite altimeters averaged over a period of time represent the marine geoid. However, SSH need to be corrected for dynamic components introduced by currents, tides and other oceanographic and atmospheric phenomena. The deflection of geoid from the reference ellipsoid or geoid undulation could be calculated as the height of the satellite above the reference ellipsoid is precisely known (Figure 1).

To date, nine high-precision radar altimeter missions have logged sea surface height measurements since last 25 years. However, only a small fraction of these data have spatially dense ground tracks that are suitable for gravity field recovery. Most of the altimeter data were collected from the repeat orbit configuration that is optimal for recovering changes in ocean surface height associated with currents and tides. The sources of non-repeat altimeter data are the geodetic phases of Geosat (18 months) and ERS-1 (11 months), Jason-1 (16 months) and CryoSat-2 (since 2010). These non-repeat profiles, combined with ‘‘stacks’’ (temporal averages) of repeat profiles from the other altimeters, have been used in numerous studies to estimate the short wavelengths (<400 km) of the marine gravity field. The addition of new satellite altimeter data in geodetic orbits like Jason-1, Cryosat-2 along with ISRO’s Ka band SARAL/AltiKa altimeter is expected to improve the marine gravity field in the 14-km to 40-km wavelength band, which is of interest for investigation of sedimentary basins as small as 7 km. Based on expected future data acquisitions and improved processing, the accuracy of the gravity field is expected to be to be better than 1.4 mGal.

APPLICATIONS IN GEODYNAMICS

About two thirds of the Earth's surface lies beneath the oceans and most of the geologic processes occurring on land are linked, directly or indirectly, to the dynamics of the ocean floor. However, the knowledge of ocean floor has been highly depended on limited ship-borne geophysical surveys and selected drill sites.

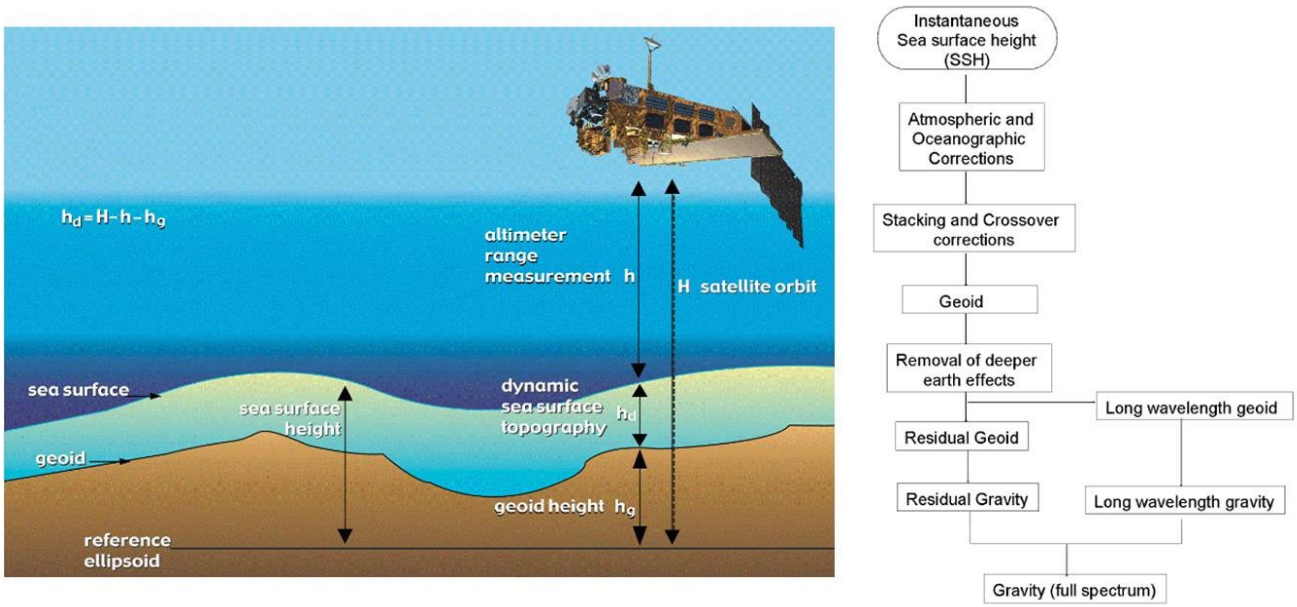

***Figure 1**: Measurement of Sea Surface Height from radar altimeter and retrieval of marine gravity*

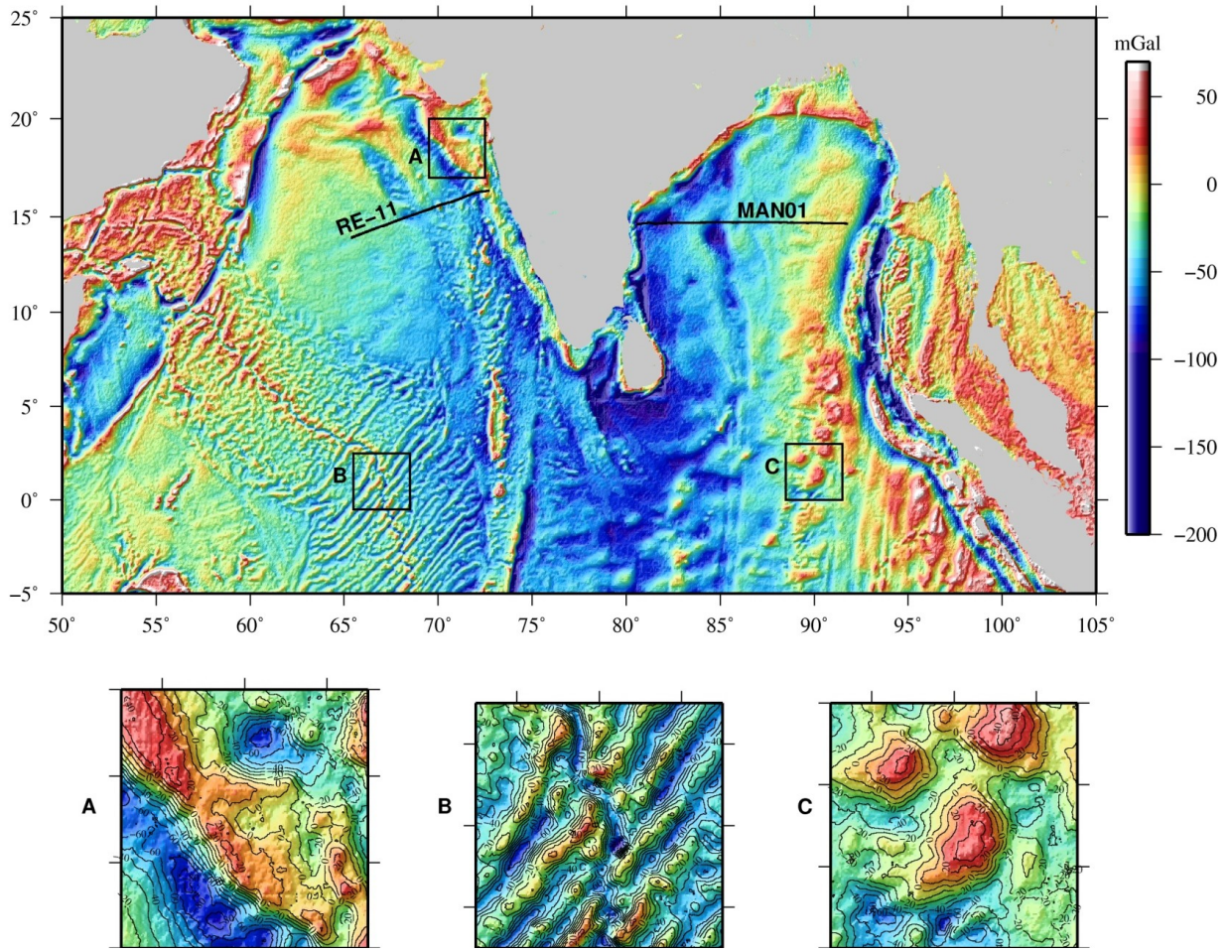

***Figure 2**: Free-air gravity anomaly of Northern Indian Ocean. Three Subsets of gravity data from various tectonic domains - A (Continental Margin), B (Central Indian Ridge), C (Ninetyeast Ridge) are shown separately.*

Satellite altimetry revolutionized our understanding of the shape and structure of the world's sea floor and the geodynamic processes that form it. Satellite altimeter data provide an important and definitive confirmation of the theory of plate tectonics which suggest that suggests that the outer most layer of the Earth is fragmented into numerous segments of varying size and the segments are being moved relative to each other over a fluid substratum (asthenosphere). Satellite gravity maps provided direct evidences for plate tectonic process like sea-floor spreading, subduction of plates, under sea volcanism and fracture zones on seafloor etc. Further, satellite gravity data are used to estimate the thickness of the elastic portion of the tectonic plates. When a volcano forms on the ocean floor it provides a large downward load on the plate causing it to deform. This deformation is appears in the gravity field as gravity low surrounding the gravity high associated with the volcano itself. By measuring the amplitude and width of the gravity low and relating this to the size of the volcano, one can establish the thickness and strength of the elastic plate. Elastic plate thickness provides direct information regarding the isostasy and sub-surface structure of the volcanoes, and thereby to understand their geological evolution. Dense satellite altimeter measurements in combination with sparse measurements of seafloor depth could be used to construct a uniform resolution map of the seafloor topography.

In India, the retrieval of satellite gravity from satellite altimetry has been attempted at Space Application Centre, Ahmedabad since late nineties. The retrieval techniques have been improved time to time leading to the generation of high resolution geoid and gravity maps of the Indian Ocean. These datasets were extensively utilized for geodynamic studies and contributed significantly in understanding the structure and evolution of the Indian Ocean. The latest version of gravity data of the Indian Ocean depicting major structural and tectonic features are given in Figure 2. 3D crustal structure map of the Ninetyeast Ridge – the longest linear volcanic feature on the globe produced by inversion of satellite gravity data is given in Figure 3. The thick crust of 15-19 km beneath the ridge is produced by the enormous volcanism of the Kerguelen hotspot during the evolution of the lithosphere.

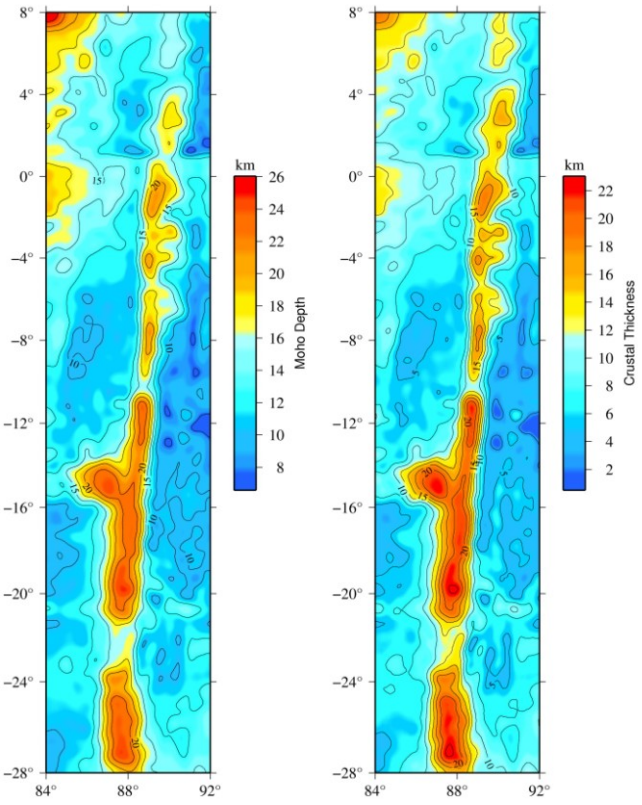

***Figure 3**: Moho topography and crustal thickness maps of the NER obtained from the inversion of Satellite derived gravity data.*

Tropical Cyclone Monitoring and Prediction using Remote Sensing Satellite Observations

Neeru Jaiswal and C. M. Kishtawal

Space Applications Centre, ISRO, Ahmedabad, India
Email: neeru@sac.isro.gov.in

The Indian sub-continent is one of the active cyclone basins of the world that experiences on average 4-5 cyclones every year. In comparison to other cyclone basins this region is the most vulnerable as the large population lives in the coastal areas. These cyclones are associated with high winds, heavy rains, storm surge and flood that cause great loss of life and properties near the coastal areas. The number of deaths in the Bay of Bengal region is highest in the globe (3, 00,000 people are estimated to have died from tropical cyclone associated storm surge in Bangladesh in 1970). Out of 9 recorded cases of heavy loss of human lives (>= 40,000) by cyclones during last 300 hundred years, 7 cases (77%) occurred in the Bay of Bengal region. Much of this contributed by the relatively dense and poor economic condition of the coastal population, shallow bottom topography and coastal configuration and also due to reluctance of the people to vacate the area under the cyclone threat.

Timely information of cyclone alert and warnings are very important to save the life of people and to take the preventive measures like evacuation. Considering the gigantic destructive power associated with the tropical cyclone winds, it is not very convenient to make the observations of a cyclone with conventional surface based observation network. Moreover, over the vast oceanic regions where these cyclones originate, develop, and intensify, there are very few observation sites, and these are far too insufficient for making routine observations for monitoring the tropical cyclone developments.

The remote sensing satellite data plays very important role in the cyclone monitoring and predictions. The microwave, infra-red and visible channel sensors onboard the remote sensing geostationary and polar orbiting satellite provide very useful data that is integrated in the models to provide the cyclone predictions. Satellite data from microwave sensors can penetrate through the clouds and provide the eye structure of the cyclone which is very useful to estimate the cyclone intensity and rain associated to the system. Visible channels provide very high spatial and temporal resolution data which is used to estimate the structure of cyclone very accurately. The infra-red channels provide the high temporal acquisitions with high resolution during day and night which is used for continuous monitoring of the cyclone and to determine the various cyclone structural parameters for its intensity estimation. The data from the currently active Indian

satellites viz., Oceansat-2, Megha-tropiques, Kalpana, INSAT-3D and RISAT is being used for the cyclone monitoring and predictions. Scatterometer on board Oceansat-2 provide the surface wind structure of the cyclone which is used to detect the cyclone formation. The SAPHIR sensor from Megha-Tropique satellite provides the vertical profile of humidity that is employed to evaluate the net moisture content in the cyclone structure which is the indicator of cyclone intensification. The INSAT-3D and Kalpana derived images from IR and visible channels provide the continuous monitoring of the development of any convective activity in the Indian-sub-continent.

***Figure 1**: Disasters due to Cyclone events (Heavy Rain, Flood, High Winds, trees uprooting)*

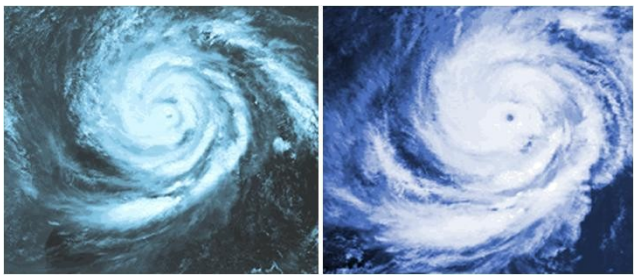

***Figure 2**: Visible and TIR-1 image of cyclone PHAILIN (11 OCT, 2013, 06UTC)*

On October 9th a historically intense cyclone "Phailin" formed in the south Bay of Bengal that hit the Odisha coast where a massive super cyclone badly affected the human and property in 1999. Due to the advancement in the cyclone prediction models the alerts were timely generated and government took the preventive measures. The cyclone track and intensity till the landfall was continuously broadcasted via media channels, which made the wide publicity and awareness among the people. The timely information saved the human loss and results the better preparedness to overcome the post-cyclone impacts. These accurate and reliable forecasts were due to advancements in the satellite observations and the development of sophisticated cyclone prediction models. The cyclone track was predicted by using the models in the real time and was disseminated through the web and media. This was the most intense cyclone in the last 14 years which raises a very hot discussion about the impact of climate change on the cyclones. The latest studies discuss the impact of climate change on the cyclones with their increase in the intensity. Throughout the world, impacts of natural hazards are getting more and more vulnerable. One of the reasons may be the human impact upon the environment, which has contributed to the climate change as mentioned in the IPCC report. The studies have been performed to show the impact of climate change on tropical cyclones. Cyclones derive their energy from the warm waters of ocean and do not form unless the temperatures are over 26.5 ^{0}C. The recorded

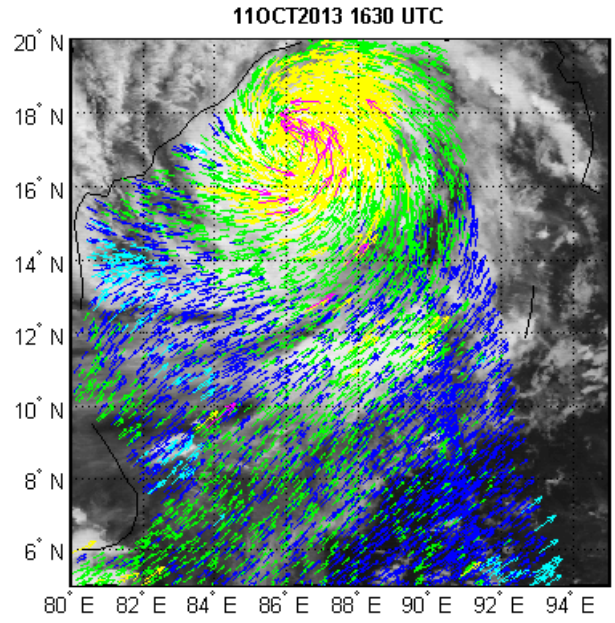

Figure 3: *OSCAT derived winds of cyclone Phailin overlaid on the TIR-1 image INSAT-3D (11-OCT-1630 UTC)*

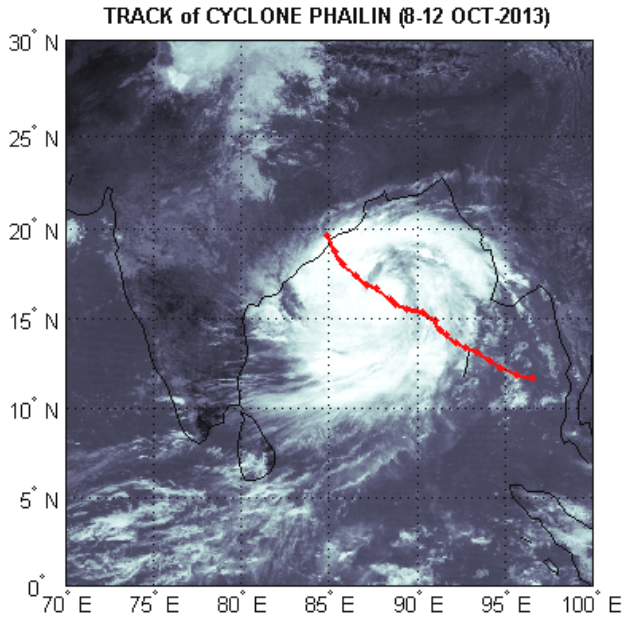

Figure 4*: Observed Track of Cyclone Phailin (8-12 October, 2013)*

temperature in the Bay of Bengal where Phailin developed was 28-29 ^{0}C with very high Ocean heat content. These conditions are favourable for the intensification of cyclone systems. PHAILIN was the first cyclone in the North Indian Ocean which was continuously monitored by the new Indian geostationary satellite INSAT-3D. The winds of cyclone Phailin derived by Indian satellite Oceansat-2 scatterometer are overlaid on the TIR-1 image of recently launched new Indian Satellite INSAT-3D (11-OCT-1630 UTC) have been shown in the Fig. 3.

Table 1: Some of the currently active ISRO satellites being used for Cyclone Monitoring and Prediction

Satellite	Sensor	Applications in Cyclone Monitoring & Prediction
INSAT-Series of satellites (Kalpana, INSAT-3A, INSAT-3D)	Visible/ Infrared Imager	Continuous monitoring of cyclone
		Cyclone centre determination
		Intensity estimation
		Structure of cyclone
		Upper level winds
Oceansat-2	Oceansat-2 Scattero-meter (OSCAT)	Surface wind observations to detect cyclone formation and cyclone wind structure
MT	SAPHIR	To estimate the vertical structure of humidity profile for cyclone intensification
RISAT	SAR	Post-cyclone damage analysis

Study of Tuna forage using IRS P4 OCM

Beena Kumari

Space Applications Centre, ISRO, Ahmedabad, India
E-mail: beena@sac.isro.gov.in

ABSTRACT

Chlorophyll-*a* (chl-*a*), which can be detected from satellite sensor is considered as the index of phytoplankton in the ocean. This study focuses on understanding the distribution and persistence of phytoplankton patch and formation of tuna forage on a spatial and temporal scale in the waters of India's Exclusive Economic Zone (EEZ) using time series chlorophyll-*a* images derived from Indian Remote Sensing Satellite P4 - Ocean Colour Monitor (IRS P4 - OCM). Results indicate that phytoplankton patch and its persistence depends on both the length and the concentration of chl-*a* within the patch. Study reveals that a minimum of 7 days is required for a phytoplankton patch to mature to the tuna forage ground. This has been validated using tuna catch data acquired from Fishery Survey of India. Validation results based on hindcasting indicate that the tuna forage ground derived from satellite data yielded high catch of tuna (> 2% hooking rate).

INTRODUCTION

Study of phytoplankton is indispensable for understanding the marine living resources. They form the base of the marine food chain. Phytoplankton occurs in heterogeneous patches on a continuum scales throughout the world ocean.

Phytoplankton patchiness and heterogeneity

Formation of phytoplankton patches is believed to be the result of a strong linkage between the biological and physical dynamics, affecting nutrient fluxes across the pycnocline and the coupling between trophic levels (Franks and Walstad, 1997). These patches can inhabit surface or the subsurface regions of the ocean. Since this study is based on satellite derived ocean colour information, it is not taking care of the subsurface patches, which are invisible to most satellite sensors.

These patches are in general dynamic, continually responding to temporal and spatial changes in physical processes that create, maintain and disperse them. Recent studies suggest that biological growth increases the population, which leads to patchiness and its persistence and sustainability depends on dispersion by physical forces (Slobodkin, 1999). The scale of patchiness can range from millimetres to kilometres (Franks and Jaffe, 2001). At the micro-scale (<1 m) interactions between biotic and abiotic factors generate spatial variability in the distribution of phytoplankton (Plat, 1972; Abraham, 1998).

Understanding the extent and nature of this spatial variability is essential for determining the processes and mechanisms controlling plankton ecology and has direct consequences for population dynamics, planktonic ecosystem functioning, and biogeochemical fluxes. This

study eventually aims at the development of a technique for tuna forecasting system in the waters of India's EEZ.

Tuna physiology and distribution

Tunas are highly mobile, economically exploitable resources because of their tendency to aggregate into schools and the school's tendency to aggregate at specific oceanographic features such as thermal fronts and upwelling filaments, which are known to be areas of increased productivity and relatively high prey abundance (Kumari et al. 1993; Holland and Grubbs, 2001; Santos et al. 2006). Numerous investigators have tried to determine the effect of environmental conditions on depth distribution, migratory speed, residency time, tendency to aggregate and eventually the vulnerability to specific fishing gears over time and space (Grudinin, 1989; Dagorn et al. 2000).

Food also is an important factor influencing the growth, migration and abundance of fish stocks in time and space. By identifying the feeding ground and feeding habit, exploitation strategy can be refined and improved upon. Several authors have reported on the food and feeding habits of yellow-fin tunas from different Oceans as well as from the Indian waters. Various studies have indicated observations on the feeding habits of yellowfin tunas caught on longline gears in the Indian waters (Vijaykumar et al. 1992; Govindraj et al. 2000). All these studies suggest that plankton rich areas are suitable ground for tuna forage.

Phytoplankton is the basis of marine food chain. They grow at a rapid rate and are constantly being produced and consumed in huge amounts by other forms of marine life or die and sink to the ocean bottom. Apparently there is a very tight coupling between phytoplankton production, its consumption, death and the environment (Figure 1). The constant swimming life style and the rapid growth characteristics have made tuna an eating machine. They need to consume great amount of food to fuel this life style. Thus, tunas are likely to be encountered near the forage ground where feeding can be accomplished with a minimum expenditure of energy.

Trophodynamic structure of the tuna food chain is driven by the phytoplankton through the process of photosynthesis. They form the base of food chain or food web. The zooplankton and certain other pelagic herbivores consume phytoplankton, which in turn are preyed upon by secondary carnivores. In this study we are dealing with open ocean tunas so the food chain is long with low transfer efficiency. Tuna being

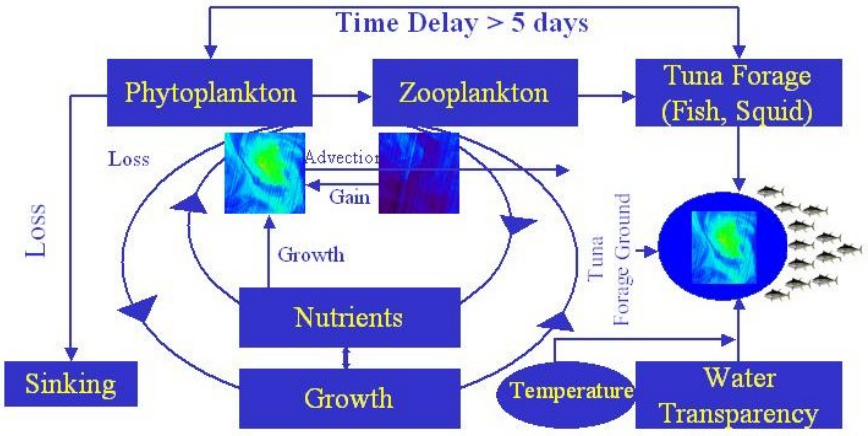

Figure 1*: Tuna forage ground formation showing the coupling between phytoplankton productions, its consumption, death and the role of environment in the formation of tuna forage ground.*

an apex predator, the food chain involves three or four level of carnivorous feeding. The forage constitutes smaller fishes, mesopelagic fishes (myctophids), squids, upper ocean zooplankton and larger zooplankton of deep scattering layer. Aggregation and growth of forage primarily depends on the spatial and temporal concentration of primary biomass. India's annual tuna production of 0.0035 million metric tons (Somvanshi et al., 1998) is insignificant as compared to the world tuna production of 3.6 million metric tons (Lehodey, 2001). This study aims at developing a technique for finding out potential tuna habitat to facilitate the fishing community of India to go for economically viable tuna fishing in the high seas.

The distribution of tuna forage within this potential habitat probably has the major influence on tuna distribution. Surface tuna like skipjack and yellowfin feed visually, mainly during the daylight hours. For this reason, water clarity is also likely to influence their distribution. Therefore, the habitat of surface tuna could be defined in general terms as water masses with a combination of suitable temperature, high forage biomass and also clear water.

Scientific rationale

The scientific approach involves determination of critical patch length and spatial and temporal concentration of chl-a within the patch using satellite derived ocean colour data in the open ocean. This forms the primary biomass. Spatial and temporal resolution for the biomass quantification has been decided based on the evolution and stability of primary biomass using time series data on ocean colour.

Patchiness produced by individual physical features such as fronts and eddies or at a specific geographical location is not discussed explicitly. The advent of a new generation of colour-sensing satellites means that global data of phytoplankton distributions is now easily available on a daily basis barring the inevitable cloud problem. The main debate in patchiness has centered on whether biological or physical processes are responsible for the observed spatial structure. This work is confined to understanding patchiness in general, its persistence and sustainability in spatial and temporal domain, which leads to the formation of tuna forage ground.

STUDY AREA

The technique development and the validation experiment for this was carried out in the Arabian Sea, one of the basins of the northern Indian Ocean. All the images and its subsets used in this study are from various regions of the Arabian Sea (Figure 2). Arabian Sea is land-locked in the north by the Asian continent which separates the northern Indian Ocean from the deep-reaching vertical convective areas of the Arctic Seas and the cold climatic regions of the northern hemisphere. Arabian Sea experiences unique oceanographic features and events compared to other world oceans, The semi-annual reversal of monsoon winds are divided into southwest (June-September) and northeast (December-February) monsoon phases with two transition periods, spring inter monsoon (March-April-May) and fall inter monsoon (October-November). Southwest (SW) monsoon winds cause vigorous and deep anti-cyclonic surface circulation in the Arabian Sea, inducing both coastal and open ocean upwelling (Shetye et al., 1993). During northeast (NE) monsoon, cold dry northeast winds blow over the Arabian Sea

causing cyclonic circulation. Accordingly, waters north of 15°N experiences densification and sinking of surface waters leading to convective mixing and deepening of the mixed layer (Prasanna and Prasad, 1996). Surface currents dissipate and hydrographic conditions in the Arabian Sea approach those of a well-stratified and unperturbed tropical ocean during the transition period between the two monsoon phases. The SW and NE monsoon periods drive the biological production in the Arabian Sea. During SW monsoon intense upwelling both in the coastal waters off Somalia, Arabia and in the adjacent open ocean waters causes deepening of mixed layer and injection of nutrients from thermocline. This process results in very high levels of biological production in the western Arabian Sea (Brock et al. 1991). Similarly wind driven upwelling and consequently high production is observed during the SW monsoon in the southeastern part of the Arabian Sea. However during rest of the season, this region is almost oligotrophic. In the NE monsoon phase, surface cooling and densification leads to sinking and convective mixing triggering intense biological production in the northern Arabian Sea (Prasanna and Prasad, 1996).

DATA

Chlorophyll- a concentration

In this study chlorophyll-a (chl-a) data received from IRS P4 OCM have been used extensively. The OCM is the first instrument to take advantage of push broom technology for achieving higher radiometric performance and higher spatial resolution while maintaining a large swath to provide high revisit time for ocean observations (Navalgund and Kiran Kumar, 1999).

Tuna catch data

This study makes use of the tuna Longline data collected by Fishery Survey of India as well as the longliner operated by the private fishermen of India. Longline gear consists of a continuous monofilament mainline to reduce drag and visibility supported by float lines, with regularly spaced leaders that end with about 600-1000 baited hooks. Catch rate of tuna is expressed as % hooking rate, number of fish caught by 100 hooks. The Indian tuna fishery comprises coastal as well oceanic fishery. In this study we have considered all the dominant species of tuna caught in Indian waters by longliners especially yellow-fin and big eye.

METHOD

Chl-a retrieval involves atmospheric correction of visible channels to obtain normalised water leaving radiances, and the application of bio-optical algorithm (Gordon and Wang, 1994).

SeaWiFS operational OC2 (modified cubic polynomial) algorithm (O'Reilly et al. 1998) which is fine-tuned for chl-a concentration retrieval in the waters of Arabian Sea and Bay of Bengal using IRS-P4 OCM data (Prakash et al. 2002), have been used to generate chl-a images. This algorithm captures the inherent sigmoid relationship through the remote sensing reflectance ratio between the bands of 490 and 555 nm. This algorithm facilitates the retrieval of low as well as high concentration of chl-a. The algorithm operates with five coefficients and has following mathematical form:

$$C = 10^{(0.319 - 2.336 \times R + 0.879 \times R^2 - 0.135 \times R^3) - 0.071} \quad (1)$$

Where, C is chl-*a* concentration in mg m^{-3} and $R = \log_{10} [R_{rs}(490)/R_{rs}(555)]$, where R_{rs} is remote sensing reflectance at 490nm and 550nm bands of IRS P4 OCM.

Prior to the in-depth study of phytoplankton patch and its persistence, critical phytoplankton patch size was estimated using equation developed by Wroblewski, O'Brien and Platt (Wroblewski et al. 1975). The basic equation is given below.

$$L_c = 2\pi[D/(b - R_m\lambda)]^{1/2} \quad (2)$$

Where L_c is critical patch length, D is eddy diffusivity, b is the phytoplankton growth rate, R_m is the herbivore maximum grazing ration and λ is the Ivlev constant. To maintain the initial concentration of phytoplankton after a given period of time, the phytoplankton patch size has to be more than the critical patch length (Lc). Based on the above equation the minimum phytoplankton patch size in the waters if India's exclusive economic zone is found to be about 22 km. Following this exercise a detailed analysis have been carried using about 150 time series OCM derived chl-*a* images of Arabian Sea and Bay of Bengal to understand the patch length, initial concentration, maturation, stabilization and obliteration of chl-*a* within the patch.

RESULTS AND DISCUSSION

Figure 2 shows sustainability and variation in chlorophyll-*a* (chl-*a*), concentration of 15 patches of varying length from 13 km to 37 km observed in the Arabian Sea. Detailed analysis of these patches shows that for a patch to persist,

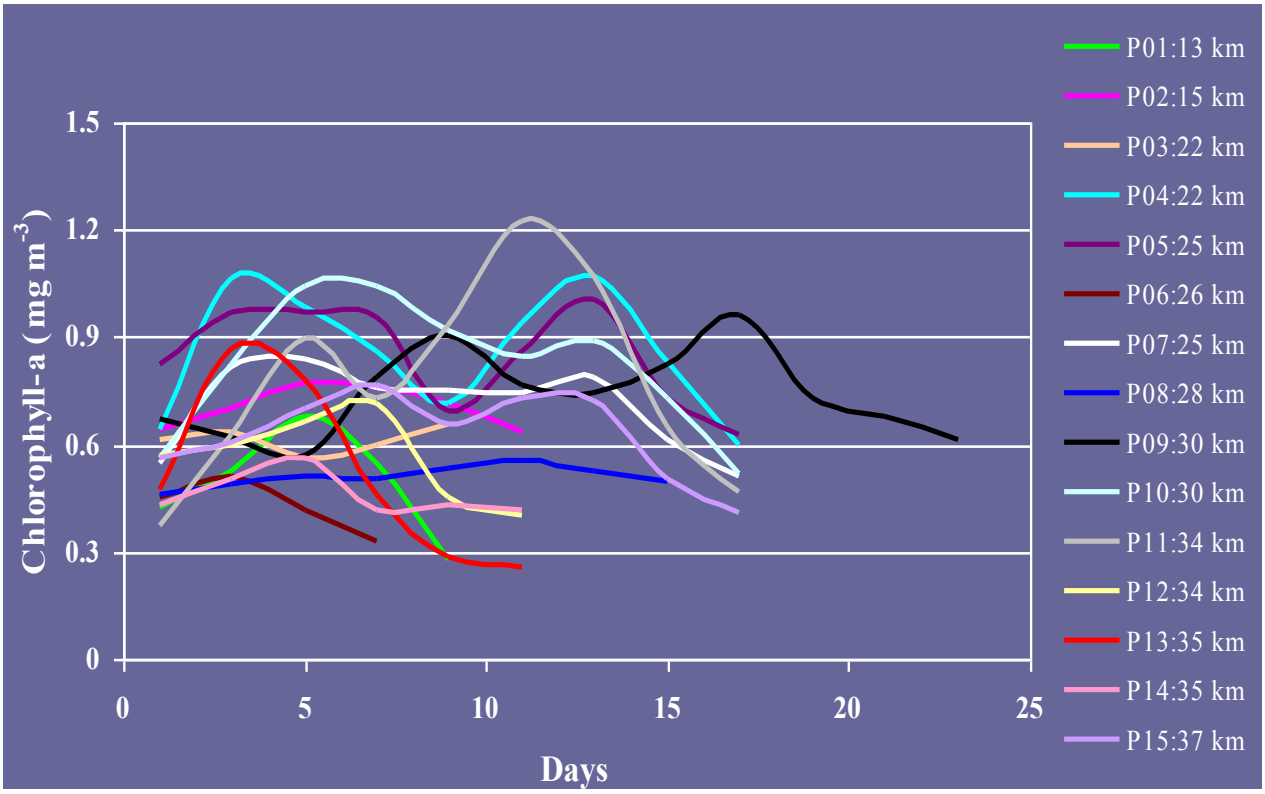

***Figure 2**: Shows sustainability and variation in chlorophyll-*a *(chl-a), concentration of 15 patches of different length observed in the Arabian Sea.*

both the concentration and a minimum length are important. Henceforth in the discussion, patch would be denoted as "P", and "days" are in reference to the first appearance of the patch (day 1), its evolution and dismissal (day 4,5,6,7…till it last). Numbers succeeding P (01, 02, 03, 04….) represents the patch number. P01 having a length of 13 km shows 0.5 mg m^{-3} as initial concentration of chl-*a*. The concentration peaks on day 5 (0.7 mg m^{-3}) and then starts declining with a minimum of 0.3 mg m^{-3} on day 9 and dissolute on day 10. P02 of 15 km length persists for about 11 days with chl-*a* concentration ranging from 0.6 mg m^{-3} to 0.8 mg m^{-3}, peaking on day 6. P03 and P04 are of 22 km in length. P03 is a uniform patch without much variation in chl-a (0.62 mg m^{-3} to 0.7 mg/m^3). Where as P04, sustains for a period of 18 days before dissipation. Chl-*a* concentration ranges from 0.61 mg m^{-3} to 1.1 mg m^{-3} with two peaks, the first on day 4 and the second peak on day 13. P05, P06 and P07 are of 25 km in length with varying concentration of chl-*a*. P05 persist for 18 days with a chl-*a* concentration ranging from 0.7 mg m^{-3} to 1.15 mg m^{-3}. Like the previous patch this one also shows two peaks. P06 persists only for 7 days. This may be because of the low concentration of chl-*a* (0.34 mg m^{-3} to 0.5 mg m^{-3}) without any significant peak. P07 also doesn't show a significant range in chl-*a*. P08 is a uniform stable patch of 28 km length persisting for 15 days with chl-*a* ranging from 0.4 mg m^{-3} to 0.5 mg m^{-3}. Two patches of 30 km length (P09 and P10) persist for more then 15 days. P09 persist for 24 days and the chl-*a* concentration ranges from 0.7 mg m^{-3} to 1.0 mg m^{-3}. Whereas P10 persist for 17 days and chl-*a* concentration ranges from 0.7 mg m^{-3} to 1.1 mg m^{-3}. P11 is of 34 km in length and persist for 17 days and peaking on day 11 with chl-*a* concentration of 1.22 mg m^{-3}. P12 is also of 34 km in length and the chl-*a* concentrations range from 0.4 mg m^{-3} to 0.8 mg m^{-3} and the patch persist for about 13 days. P13 and P14 are of 35 km in length and persist for 12 days. The chl-*a* concentration ranges from 0.2 mg m^{-3} to 0.9 mg m^{-3} in case of P13 where as P14 shows a range of 0.4 mg m^{-3} to 0.55 mg m^{-3}. P15 is of 37 km in length and persist for about 17 days and the chl-*a* concentration ranges from 0.4 mg m^{-3} to 0.8 mg m^{-3}. The essence of above description is given in table 1.

Table 1: Description of patches depicted in Figure 2

Patch No.	Patch Length (km)	Chl-*a* concentration range (mg m^{-3})	Peaking (Day)	Persistence (Days)
P01	13	0.3-0.7	5	9
P02	15	0.6-0.8	6	6
P03	22	0.62-0.67	No peak	9
P04	22	0.61-1.1	4 & 13	18
P05	25	0.7-1.1	8 & 13	18
P06	25	0.34-0.5	No peak	7
P07	25	0.5-0.8	No peak	18
P08	28	0.4-0.5	No peak	15
P09	30	0.7-1.0	9 & 17	24
P10	30	0.7-1.1	5 & 12	17
P11	34	0.5-1.22	11	17
P12	34	0.4-0.8	No peak	13
P13	35	0.2-0.9	4	12
P14	35	0.4-0.55	5	12
P15	37	0.4-0.8	7 & 13	17

Figure 3 explains 8 patches of 50-150 km in

length observed in the Bay of Bengal and off the east and west coast of Andaman. P01 in figure 3 is of 50 km length with a chl-*a* range from 0.3 mg m^{-3} to 0.79 mg m^{-3} persists for about 21 days. P02 of 58 km with a chl-*a* range from 0.3 mg m^{-3} to 0.9 mg m^{-3} persists for about 11 days. P03 of 66 km with a chl-*a* range from 0.41 mg m^{-3} to 0.61 mg m^{-3} persists for about 13 days. P04 is of 67 km in length and persist for about 9 days. Chl-*a* concentration ranges from 0.5 mg m^{-3} to 0.7 mg m^{-3}. P05 of the same length persist for about 13 days showing a high peak on day 5 (0.95 mg m^{-3}). P06 is of 75 km in length and persist for about 19 days. Chl-*a* concentration ranges from 0.55 mg m^{-3} to 0.82 mg m^{-3}. P07 in figure 3 is of 116 km in length and persist for about 32 days. Chl-*a* concentration ranges from 0.4 mg m^{-3} to 0.7 mg m^{-3}. This particular patch shows 4 peaks (on day 5, 9, 15 and 21). P08 is of 150 km in length and persist for about 18 days. Chl-*a* concentration ranges from 0.5 mg m^{-3} to 0.7 mg m^{-3}. It shows two peaks, the first on day 5 and the second peak on day 10. The essence of above description is given in table 2.

Table 2: Description of the patches depicted in Figure 3

Patch No.	Patch Length (km)	Chl-*a* concentration range (mg m^{-3})	Peaking (Day)	Persistence (Days)
P01	50	0.3-0.79	5 & 16	21
P02	58	0.3-0.9	7	11
P03	66	0.41-0.61	4 & 8	13
P04	67	0.5-0.7	4	9
P05	67	0.3-0.9	5	13
P06	75	0.55-0.82	7	19
P07	116	0.4-0.7	5,9,15 &21	32
P08	150	0.5-0.7	5 & 12	18

After studying in detail the chl-a patches and its persistence it was compared with the tuna catch data obtained from Fishery Survey of India.

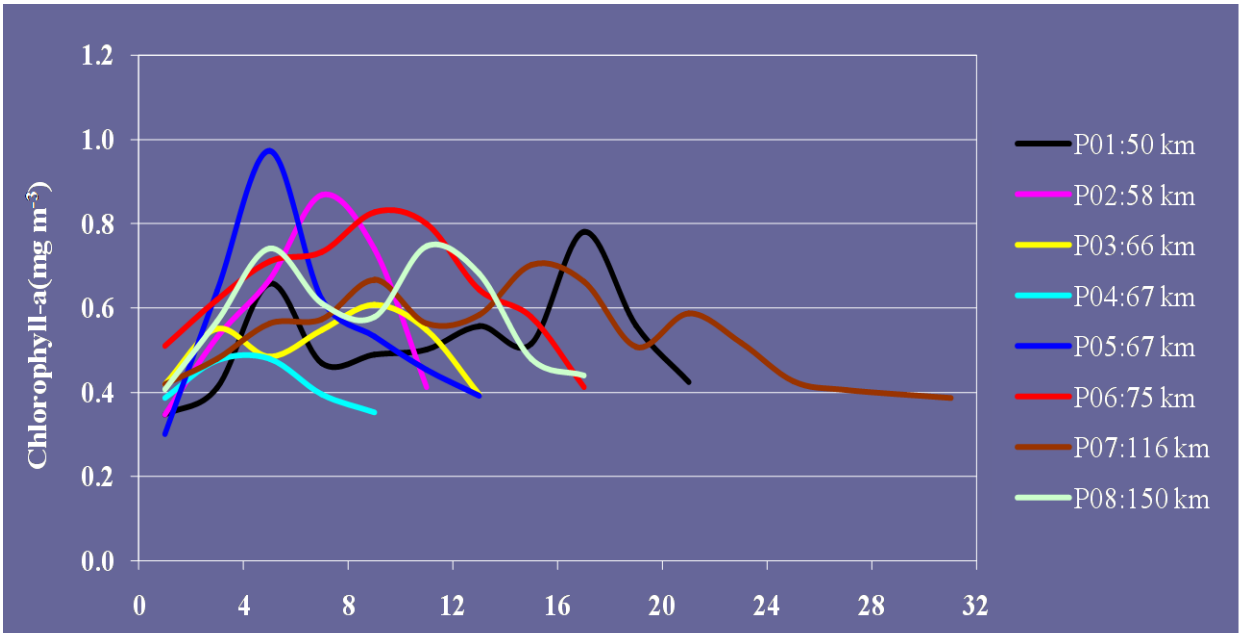

***Figure 3**: Shows sustainability and variation in chlorophyll-*a *(chl-*a*), concentration of 15 patches of different length observed in the Bay of Bengal and off the east and west coast of Andaman.*

Tuna catch data was converted to % hooking rate before comparing it with chl-a images generated for March 2005. The patch observed on March 10, 2005 image (Figure 4 (a)) shows a 3 fold increase on day 3 and declines on day 5 but the chlorophyll concentration on day 5 is still higher then what was observed on day 1 and then it declines further and stabilizes on day 7, yielding high catch of tuna (1.8% hooking rate). The patch shown on the bottom image of figure 5 (b) doesn't show any significant increase even after day 10, yielding very low catch of tuna (0.2% hooking rate). This analysis explains the time lag for tertiary production, the ideal time for tuna aggregation.

CONCLUSION

The study shows that both the length of the patch and its chl-a concentration determines the longevity of the patch. The longevity is high when chl-a concentration of the patch is high. Patch showing chl-a concentration ≥ 0.8 mg m-3 sustained for more than 15 days. And patch showing chl-a concentration ≤ 0.3 mg m-3 sustained for ≤ 7 days. Patch length ranging from 1-25 km normally sustained for 9-12 days. 25-50 km patches sustained for more then 15 days. 50-75 sq km patches sustained for17-23 days. 100-150 sq km patches sustained for17-32 days. The result of the extensive spatial and temporal data analysis across the Indian EEZ (Arabian Sea, Bay of Bengal and Andaman Sea) indicates that location and season doesn't play a significant role in the sustainability of the patch. The study also indicates that the phytoplankton patches in general evolve to the probable tuna forage ground. The time lag for the forage ground formation is > 5 days. This has been validated using concurrent data on tuna catch.

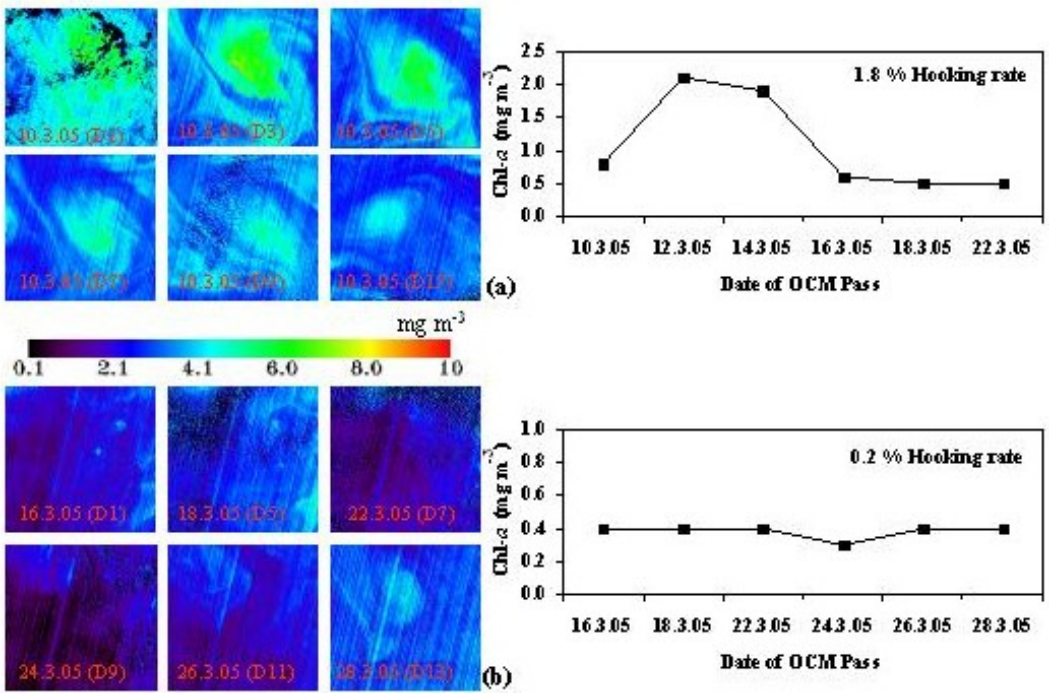

***Figure 4**: Depicts two sets of time series chlorophyll images. The patch observed in figure 4 (a) shows a 3-fold increase on day 3 and declines on day 5 yielding high catch of tuna. The patch observed figure 4 (b) doesn't show any significant increase even after day 10 yielding very low catch of tuna.*

References

Abraham, E. R., 1998, The generation of plankton patchiness by turbulent stirring. Nature, 391,577-580.

Beena Kumari, Mini Raman, Narain, A. and Sivaprakasam, T. E., 1993, Location of tuna resources in Indian waters using NOAA AVHRR data, International Journal of Remote Sensing, 14, 3305-3309.

Brock J. C., McClain C.R., Luther M.E., Hay W.W., 1991, The phytoplankton bloom in the north-western Arabian Sea during the southwest monsoon of 1979. J Geophys Res, 96: 20623-20642.

Dagorn, L. Bach P. and Josse, E., 2000, Movement patterns of large big eye tuna (Thunnus obesus) in the open ocean determined using ultrasonic telemetry. Marine Biology, 136, 361-371.

Franks, P. J. S. and Jaffe, I.S., 2001, Microscale distributions of phytoplankton: initial results from a two-dimensional imaging fluorometer. Marine Ecology Progressive Series, 222, 59-72.

Franks P.J.S. and Walstad L. J., 1997, Phytoplankton patches at fronts: a model of formation and response to wind events. Journal of Marine Research, 55, 1-29.

Gordon, H.R. and Wang, M., 1994, Retrieval of water leaving radiance and aerosol optical thickness over the oceans with SeaWiFS: a preliminary algorithm. Applied Optics, 33, 443-452.

Govindraj, John, M.E. Premchand, Unnikrishnan, N. Jacob Thomas and Somvanshi, V.S., 2000, Oceanic Tuna resources in the north west region of India EEZ, Bulletin of Fishery Survey of India, 27, 20-24.

Grudinin, V.B., 1989, On the ecology of yellowfin tuna (Thunnus albacares) and big eye tuna (Thunnus obesus), Journal of Ichthyology, 29, 22-29.

Holland, K.N. and Grubbs, R.D., 2001, The trophic ecology of tuna aggregations: rationale, experimental design and early results, 52nd Annual Tuna Conference, Lake Arrowhead, California. May 2001.

Santos, A.M.P., Fuza, A.F.G. and Laurs, R. M., 2006, Influence of SST on catches of swordfish and tuna in the Portuguese domestic longline fishery, International Journal of Remote Sensing, 27.

Shetye, S. R., Gouveia, A. D. and Shenoi, S. S. C., 1994, Circulation and water masses of the Arabian Sea. In Proc. Indian Acad. Sci. (Earth Planet. Sci.) 107-123.

Slobodkin, L. B., 1999, Akiro Okubo and the theory of blooms. Oceanography, 12, 9-14.

Navalgund, R. R. and Kiran Kumar, A S., 1999, Ocean colour monitor (OCM) on Indian remote sensing satellite IRS-P4. Available online at: http://www.IOCCG.org. (accessed: July 17 2009).

O' Reilly, J.E., Maritonena, B. G., Mitchel, D.A., Siegal, K. L., Carder, S. A., Graver, M., Kahru, M. and Mcclain, C.R., 1998, Ocean colour chlorophyll algorithms for SeaWiFS. Journal of Geophysics, 103, 24937-24963.

Prakash, C., Mohan, M., Sarangi, R. K., Beena K. and Nayak, S., 2002, Surface chlorophyll-a estimation in the Arabian Sea using IRS-P4 Ocean Colour Monitor (OCM) satellite data. International Journal of Remote Sensing, 23, 1663-1676.

Prasanna Kumar, S. and Prasad, T.G., 1996, Winter cooling in the northern Arabian Sea. Current Science, 71, 834-841.

Vijayakumar, K. Parasuraman, P.S. Rajakumar, S.A. and Nagarajan, g., 1992, A study on the food and feeding habits of Yellowfin tuna (Thunnus albacares) caught in Andaman waters of Indian EEZ by tuna long lining, Bulletin of Fishery Survey of India, 24, 40-44.

Wroblewski, J.S. O'brien, J.J. and Trevor Platt, 1975, On the physical and biological scales of phytoplankton patchiness in the ocean, Memoires Societe Royale des Sciences de Liege, 6 (VII), 43-57.

Bleaching Forewarning: A Space-based Capability towards Reef Ecosystem Management

Nandini Ray Chaudhury

Space Applications Centre, ISRO, Ahmedabad, India
Email: nandinirc@sac.isro.gov.in

BLEACHING: STRESS RESPONSE OF REEF ORGANISMS

As a functional group, scleractinian reef-building corals are central to coral reef ecosystems: a major feature of the tropical oceans within 30° north and south latitudes. The global distribution of these hermatypic corals coincides with seawater temperatures ranging between 16° C to 34.4 ° C (Kleypas et al., 1999). Reef-building corals as well as numerous species of reef-dwelling invertebrate organisms (like sea anemones, snails, clams, sponges and even some single-celled ciliates) are host to unicellular microalgae commonly referred as 'zooxanthellae' due to their yellow-brown colour (Stambler, 2011). Zooxanthellae are mainly classified as dinoflagellate algae belonging to the genus Symbiodinium sp. Ecological success of corals and other reef invertebrates in nutrient-poor or oligotrophic environment is widely attributed to this unique symbiosis between host organisms and their endo-symbiont microalgae. Autotrophic zooxanthellae photosynthesize and contribute photosynthates (sugars, amino acids, etc.) to their invertebrate hosts while hosts in addition to shelter supply zooxanthellae crucial plant nutrients (ammonia and phosphate) from their waste metabolism (Lesser, 2004). For their life, colour and skeletal growth, corals and many of the reef invertebrates depend on zooxanthellae.

In cases of environmental stresses like high seawater temperature and high solar radiation zooxanthellae's photosynthetic machinery gets damaged and leads to cellular damage in the symbionts and/or their hosts (Baker et al., 2008). This in turn leads to the expulsion of zooxanthellae from their hosts and eventually the symbiosis breaks down. The loss of zooxanthellae (and/or a reduction in their pigment concentrations) as a result of this process is referred to as 'bleaching' (Baker et al., 2008). Bleaching leads to visible paling/fading/whitening of the host organism as the yellow-brown pigment of the symbiont is lost. Reef-scale bleaching events not only confine to the principal reef-builders or the corals but also involve numerous other invertebrates (Figure 1). Accordingly, coral reef bleaching is considered to be a better descriptor of these reef scale events rather than the restrictive term: coral bleaching (Baker et al., 2008). Bleaching may occur at local scales or as Mass Bleaching at geographic scales that may involve entire reef systems and geographic realms (Hoegh-Guldberg, 1999). A key

characteristic of mass bleaching events is that the host tissue remains on the skeleton but is relatively free of zooxanthellae (Hoegh-Guldberg, 1999).

Elevated seawater temperature is known to be the most common driver of mass bleaching events followed by other known causes of high solar radiation and a lethal combination of both (Baker et al., 2008; Lesser, 2004; Hoegh-Guldberg, 1999; Brown, 1997; Glynn, 1993). Other stressors like decreased seawater temperature or cold stress, heavy downpour, bacterial infection and coral diseases, excessive sedimentation, marine pollution, exposure and desiccation have also been documented (Lesser, 2004; Brown, 1997; Glynn, 1993) as factors leading to more restricted coral bleaching and successive coral mortality. However, the physiological and cellular mechanisms by which these stressors cause coral bleaching are not yet well understood (Baker et al., 2008). The worldwide phenomenon of mass bleaching has more been an effect of combination of abnormally high seawater temperatures and high solar irradiance (Veron et al., 2009; Hoegh-Guldberg, 1999).

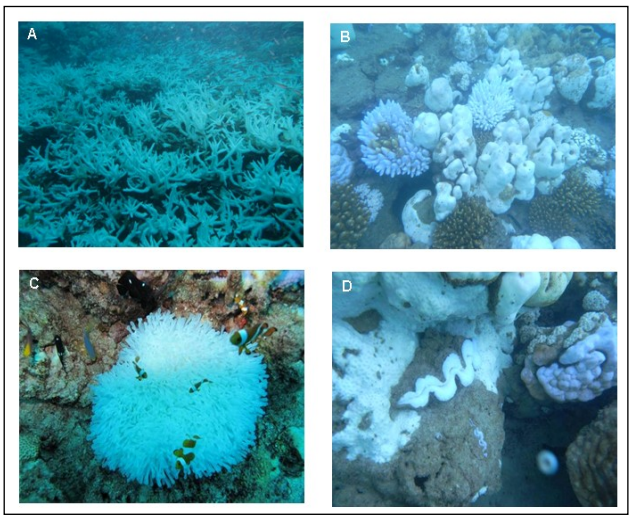

***Figure 1**: In situ photographs of Mass Bleaching observed in Andaman reefs, India, April-May, 2010: A) Mass bleaching of branching coral species Acropora, B) Mass bleaching of massive (Porites sp.) and branching (Acropora sp.) corals, C) Fully bleached Sea-Anemone and D) Fully bleached Giant Clam.*

MASS BLEACHING: HOW FAR A PREDICTABLE DISASTER?

The number and severity of mass bleaching events have been considered as a biological signal of the consequences of global climate change on world's coral reefs (Lesser, 2004; Hughes, 2000). Global warming through its evil twins: ocean warming and acidification has now overtaken all other stress-impacts (in importance) on tropical coral reefs. It is the principal cause of widespread and increasingly severe mass bleaching events (Veron et al., 2009; Hoegh-Guldberg et al., 2007; Hughes et al., 2003). Mass bleaching events can be considered as catastrophic expressions of environmental or more precisely climate change disasters with reference to their episodic nature, magnitude (geographical and ecological scales), intensity (mass mortality effect on reef corals and other taxa) and frequency in spatio-temporal domain. What makes mass bleaching unique from other environmental disasters is their relatively slow and long-term impact on humankind.

Coral reefs are high-value ecosystem for many of the tropical nations owing to their intrinsic contribution to coastline protection, human subsistence and commercial exploitation in marine tourism and fisheries (Hoegh-Guldberg et al., 2007; Sheppard, 2003). According to Global Coral Reef Monitoring Network's (GCRMN) latest estimate, the world has already

lost 19% of its functional coral reef area while an additional 35% of reef area is seriously threatened (Wilkinson, 2008). It has also been reported that one-third of the reef building corals face extinction risk from climate change and localized environmental impacts (Carpenter et al., 2008). Climate change is expected to fundamentally alter the attractiveness of coral reefs through inevitable reduction in biodiversity and may affect the economic interest of tourism (Hoegh-Guldberg et al., 2007). Productivity of reef-based fisheries at subsistence, industrial or even for aquarium trade will also be affected due to declining reef rugosity (Hoegh-Guldberg et al., 2007). With acidic and warmer oceans, reef accretion is expected to reduce and hence natural advantage of coastline protection from increasingly fragile reef frameworks will also get reduced. Loss of coral reefs not only gets limited to the loss of these essential ecosystem goods and services to humankind but would encompass extinction of a large part of earth's total biodiversity – an experience unprecedented in human history (Veron et al., 2009).

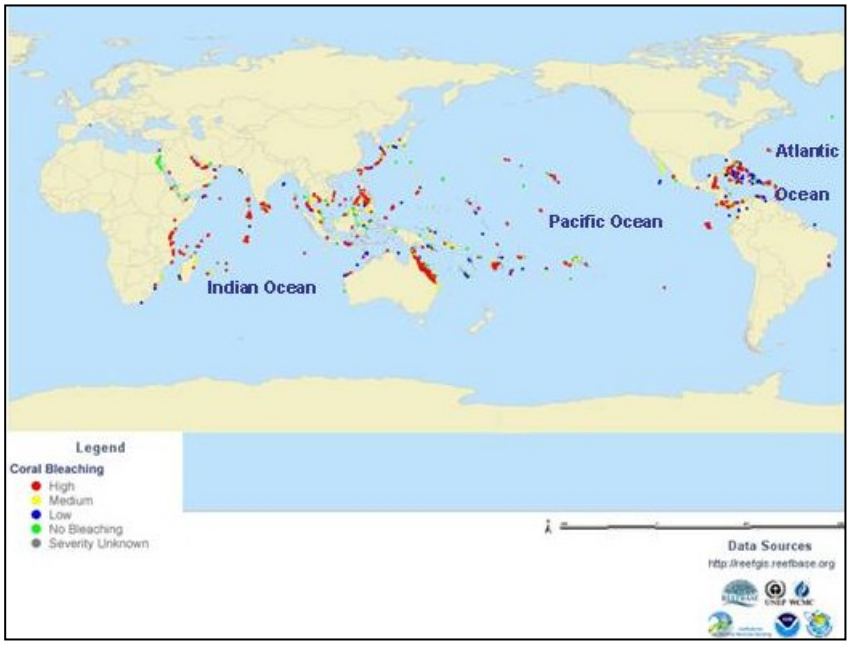

***Figure 2**: Reefbase data on locations of worldwide bleaching records and their severity (Since January, 1963 to July, 2013) (Adapted from http://www.reefbase.org).*

Mass mortalities of corals from major reef regions have been reported since 1870s (Glynn, 1993). However, the earliest comprehensive report of temperature-related bleaching came from a study on the Great Barrier Reef of Australia from 1928 to 1929 by Yonge and Nichols in 1931 (Lesser, 2011). Yonge and Nichols recorded a mass bleaching event during the Austral summer of 1929 when the seawater temperatures reached 35.1° C and surmised that elevated seawater temperature was the main cause of coral mortality. They further carried out controlled experiments on coral samples of Favia species and reported that the duration and the intensity of thermal stress were the critical factors affecting both bleaching and mortality. The number of coral reef bleaching reports (Figure 2) associated with elevated seawater temperatures) has increased dramatically since the early 1980s (Lesser, 2011; Veron et al., 2009; Baker et al., 2008; Hoegh-Guldberg, 2007; Lesser 2004; Hughes et al., 2003; Hoegh-Guldberg, 1999; Brown, 1997; Glynn 1993). Over the last three decades, the phenomenon of mass bleaching has been studied in detail from different academic perspectives (Lesser, 2011; Baker et al., 2008). In 1990s correlative field studies from different parts of the world consolidated the strong association between 'warmer than normal conditions' and the incidences of mass bleaching (Hoegh-Guldberg, 1999; Brown, 1997; Goreau and Hayes, 1994; Glynn, 1993). This strong

correlation made prediction of mass bleaching events a reality which subsequently placed coral reef bleaching and climate change squarely at the centre of the coral reef conservation debate.

SATELLITE BLEACHING ALERT! : A SUCCESS STORY

January, 1997 ushered in a new era in coral reef bleaching prediction when USA's National Oceanic and Atmospheric Administration (NOAA)/ National Environmental Satellite Data and Information Service (NESDIS) established an interactive website to predict global bleaching 'HotSpot'(s). NOAA/NESDIS' prediction of 1998 mass bleaching episode specially with reference to Great Barrier Reef, Australia became the historic success story of this experimental attempt when reports of in situ mass bleaching started flooding Coral Health and Monitoring (CHAM) Network within a week's time (Hoegh-Guldberg, 1999). NOAA/NESDIS' 'HotSpot' suite of products are the most graphic examples of space borne remote sensing data getting translated into a meaningful data product for coral reef management and conservation. This 'HotSpot' suite of products popularized the application of Advanced Very High Resolution Radiometer (AVHRR) sensor onboard NOAA's Polar-orbiting Operational Environmental Satellite (POES) series which forms the backbone of United State's Low Earth Orbit (LEO) meteorological programme. AVHRR sensor is a broad-band, four or five channel across-track scanner, sensing in the visible, near-infrared and thermal infrared portions of the electromagnetic spectrum with a spatial resolution of 1.1 km at nadir. The POES satellite system offers the advantage of daily global coverage and thus AVHRR sensor can provide daily information on global day and night time Sea Surface Temperature (SST). The at-sensor radiance observations are converted into surface temperatures of seawater in degree Celsius using a multi-channel algorithm. In simple terms, this method uses the relative radiances obtained in the near-infrared and thermal infrared regions to correct for atmospheric attenuation and calculate the ocean surface temperature. The cloudy areas are detected by their comparatively cold temperatures and masked out. The satellite SST algorithms are calibrated and routinely validated against the in situ buoy data to ensure their accuracy.

NOAA's Coral Reef Watch (CRW) (http://coralreefwatch.noaa.gov) operational SST product which goes as an input to generate global bleaching HotSpot maps uses only night-time satellite SST observations. Daytime SST observations are excluded to eliminate the diurnal variation caused by solar heating of the near-surface skin interface (10-20 µm) during the day and to avoid contamination from solar glare. It has been observed that when compared with day-time and day-night blended SST, night-time SST provides more conservative and stable estimate of thermal stress triggering coral bleaching. The spatial resolution of this dataset is 0.5 x 0.5 degree. The product is updated bi-weekly once on Monday morning and next on Thursday morning. This SST product is used for bi-weekly SST Anomaly product generation. SST Anomaly is recorded for those pixels where the current SST is found to be higher than the long-term (ten years) mean SST or the "climatology". This climatology is static in time but varies in space (Liu and Strong, 2003). Next in chain is the concept of 'Bleaching threshold' (BT) which is defined as the SST condition exceeding the climatological mean temperature of the climatologically hottest month (popularly referred to as Maximum Monthly Mean or

MMM climatology) by 1° C. Based on this the global Bleaching HotSpot maps/products are generated where pixels equalling BT become Bleaching HotSpot(s) while the rest of the pixels which record SSTs exceeding the MMM climatology indicate only thermal stress. These data products were outcome of works pioneered by Goreau and Hayes (1994) and Montgomery and Strong (1994).

HotSpot values indeed provide a spatial measure of the intensity of thermal stress but do not consider the cumulative effect of that thermal stress on a biological system like coral reefs (Liu and Strong, 2003). In order to monitor this cumulative effect new thermal stress indices like "Degree Heating Month" (DHM) (Goreau and Hayes, 1994), "Degree days" (DD) (Podesta´ and Glynn, 1997) started getting developed (Baker et al., 2008). Liu et al., (2003) developed a Degree Heating Week (DHW) index which measures accumulated thermal stress over a 12-week period by calculating the number of degree- weeks by which SST exceeds the mean annual maximum temperature: 2 DHW is equivalent to either 2 weeks continuous time when the SST remains 1°C above the mean summer maximum or 1 week time when the SST remains 2°C above the mean summer maximum. DHWs have been fairly successful in predicting coral bleaching events barring their sensitivity to the baseline definition of mean summer maxima and have been incorporated into NOAA's CRW programme as an operational product. DHW values reaching 8.0 signal a likelihood of widespread bleaching event followed by coral mortality (Liu and Strong, 2003). NOAA/NESDIS' 'Bleaching Alert Area' maps (Figure 3) classify the global ocean pixels into five classes of bleaching alerts (as No Stress, Watch, Warning, Alert Level 1 and 2). The first two classes consider only HotSpot values while the latter three classes consider HotSpot and DHW criteria in combination.

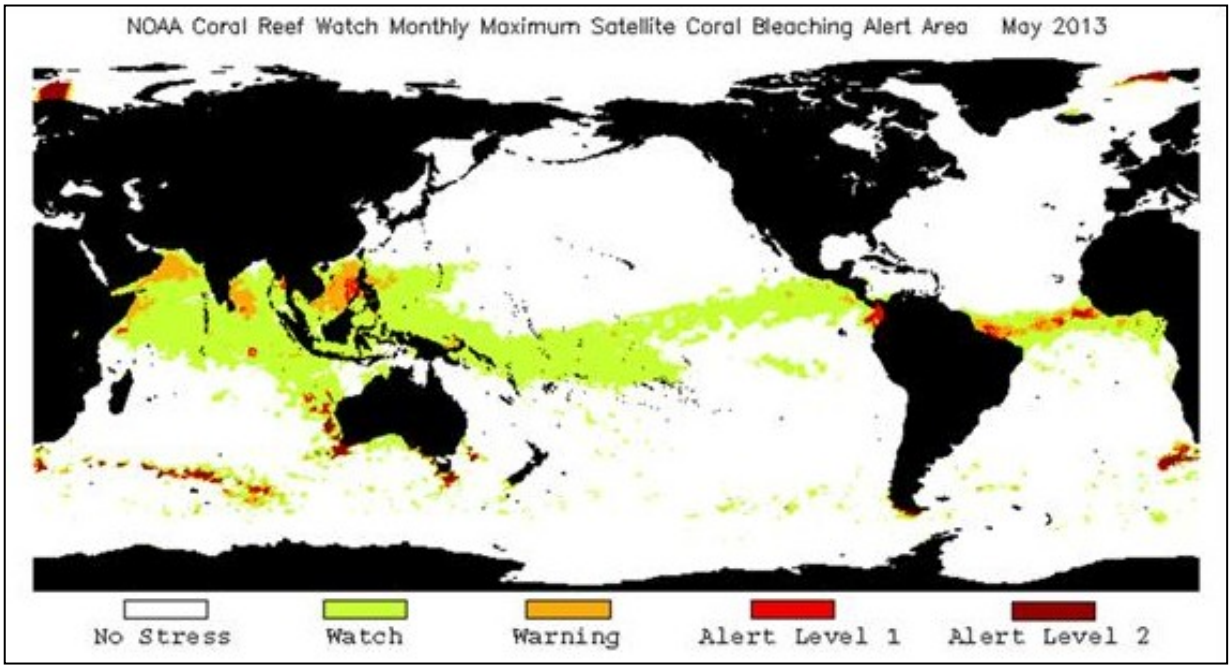

***Figure 3**: NOAA CRW global product of Coral Bleaching Alert Area for May, 2013 (Source: http://coralreefwatch.noaa.gov/satellite/composites/monthly/images/crw_oper50km_monthlymax_alertarea)*

In July, 2005, CRW launched an automated operational Satellite Bleaching Alert (SBA) e-mail based system for 24 reef sites (subscribed virtual stations) of the world. This attempt demonstrated the potential of synergistic use of space data in near-real time ecosystem management. By 14th March, 2013 CRW has upgraded and expanded their SBA system to include 227 virtual stations across the global reef sites. Three point locations or stations from coral reef regions of India (Lakshadweep, North Andaman and Great Nicobar) have so far been covered in CRW's 227 virtual station's network!

INDIAN INITIATIVES ON BLEACHING FOREWARNING

As a maritime nation, Indian coast is blessed with strategically located coral reef systems: both in its continental shelf and oceanic settings in Arabian Sea and Bay of Bengal. Amidst the threats of coastal development, fringing reefs thrive in Gulf of Kachchh and Gulf Mannar while far from the Indian peninsula, Indian island groups of Andaman and Nicobar and atolls of Lakshadweep foster great reef biodiversity. Indian coral reefs share sixty genera of reef-building corals out of one hundred and eleven genera reported in the world (Venkataraman, 2003) and thus share 54% of global coral diversity at genera level. Indian coral reefs have experienced twenty-nine widespread bleaching events since 1989 with intense bleaching in 1998 and 2002 (Vivekanandan et al., 2009) and in 2010. Reefbase data of worldwide bleaching records classify Andaman, Gulf of Mannar and Lakshadweep reef regions as sites of high bleaching events while already degraded reefs of Gulf of Kachchh are depicted as reefs recording medium to low bleaching (Figure 2). The unprecedented MCB event of 1997-98 had greatly destroyed the live coral cover of shallow water coral reefs of India (Venkataraman, 2011; Wilkinson, 2000). Field surveys conducted during or after the bleaching events reported a 20% to 30% reduction of live coral cover in Gulf of Kachchh and Gulf of Mannar, 20% to 30% in Lakshadweep and less than 10% in Andaman and Nicobar Islands (Venkataraman, 2011). In the last decade Indian reef regions experienced local to regional scale, severe bleaching episodes during 2002 (Gulf of Mannar: Kumaraguru et al., 2003; Andaman: Krishnan et al., 2011), 2004-05 (Gulf of Kachchh: Bahuguna, 2008) and in 2010 (Andaman: Krishnan et al., 2011; Lakshadweep: Ajith Kumar and Balasubramanian, 2012).

Space Applications Centre (SAC) of Indian Space Research Organisation (ISRO) has developed a two-stage conceptual model on coral reef health (Ajai et al., 2012; Bahuguna et al., 2008). This two-stage Coral Reef Health Model has been conceptualized and designed to assess reef health using an archive of multi-spectral IRS satellite imageries as well as field / in situ data. In order to evolve a multi-metric, holistic approach to test the diverse conditions of Indian coral reef regions, certain ecological as well as environmental parameters have been chosen as Operational Ecosystem Reference Points (OERPs) in the design of Coral Reef Health Model. In this model, ecological and environmental parameters in the form of Operational Ecosystem Reference Points or OERPs, collectively define a Reef Health Index (RHI). On the basis of RHI, an early Warning Index (WI) can be generated using the environmental parameters for the concerned reef in order to adopt proper management action. Conceptually the model involves critical reef health parameters for Indian reefs and can assess reef health considering both reef-habitat and

environmental conditions.

The OERPs have been classified into Environmental, Ecological and Damage Indicators. Each OERP has been assigned a weightage (Wt) that adds up to 100% scaled to 1 for simplifying the computation purpose. As per the scaled condition of the parameter, each parametric condition is then ranked into categories. Rank x Weightage gives Composite Scores (CS) of OERPs that go as an input to generate the respective indices. In the first stage, the model computes a 7-parameter based Ecological Index and 4-parameter based Damage Index. Additively these two indices give a holistic statement on reef health condition in the form of Reef Health Index (RHI). The model can also generate a 3- parameter based Warning Index for the stressed, degrading and degraded reefs specifying different levels of alert actions for reef managers and planners.

The model has been customized on IGIS software platform using Visual Basic scripting language and Visual Basic Development Tool (version 6.4). User can run, prepare and provide inputs to the model and generate Report on Reef Health Index (RHI) and subsequently on Warning Index (WI) for particular point-location of the concerned reef (Ajai et al., 2012; Figure 4). The report has the provision of hard copy printing as well as e-mail attachment. This multi-parameter based reef health model concept is first of its kind in the world. The model has a potential to be operationally utilized for generating periodic reef health bulletins. This multi-parameter, reef health model concept is first of its kind in the world as it considers the impact of oceanographic parameters concurrent to the ecosystem health unlike bleaching forecast models focusing only on SST parameter.

Indian National Centre for Ocean Information Services (INCOIS), Hyderabad has experimentally established a Coral Bleaching Alert System link (http://www.incois.gov.in /Incois/coralwarning.jsp) under Advisory Services based on NOAA's CRW product generation protocols. Bi-weekly products of HotSpot (Figure 5), DHW (at 1° x 1° and ~ 0.5° x 0.5° resolution) and time series plots of SST, generated from NOAA AVHRR daily night-time SST are available since 2010 for the five major coral reef regions of India. Web-release of the complete annual cycle of

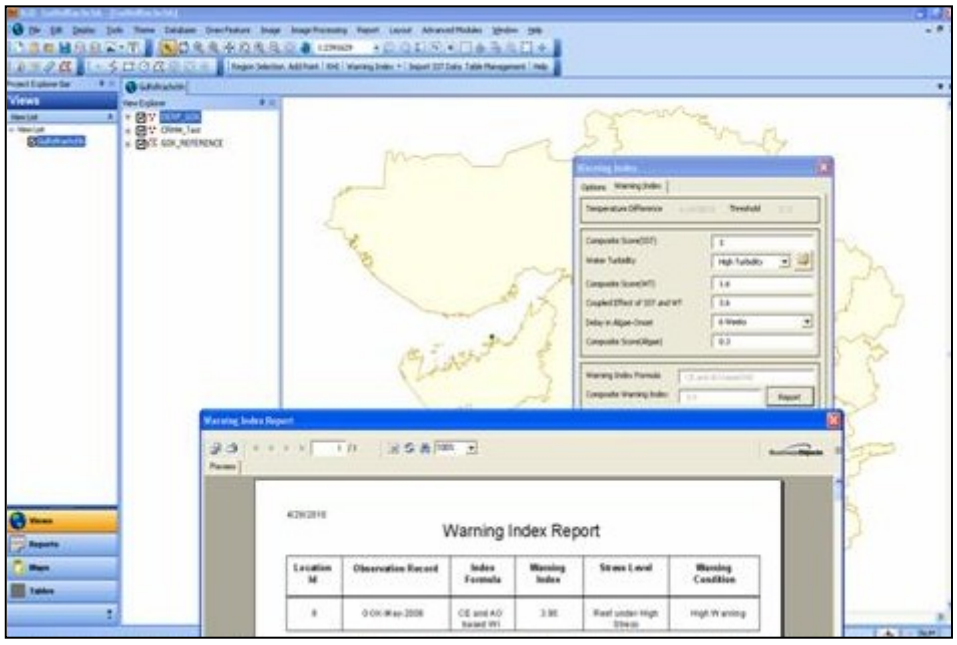

***Figure 4**: Screen-shot of Coral Reef Health Model run on IGIS software and generation of Warning Index Report (Source: Ajai et al., 2012)*

DHW and time series SST plot products from 2011 to 2013 is however awaited from this link.

Currently SAC, ISRO is working towards determining region-specific, bleaching thresholds for Indian coral reef regions by analyzing historic SST datasets following MMM climatology and MMMmax climatology models. Considering the current scenario of ocean warming there is a definite need of defining a more dynamic Bleaching Threshold as compared to the existing, static threshold. A more robust satellite bleaching alert system can be developed based upon these dynamic bleaching thresholds

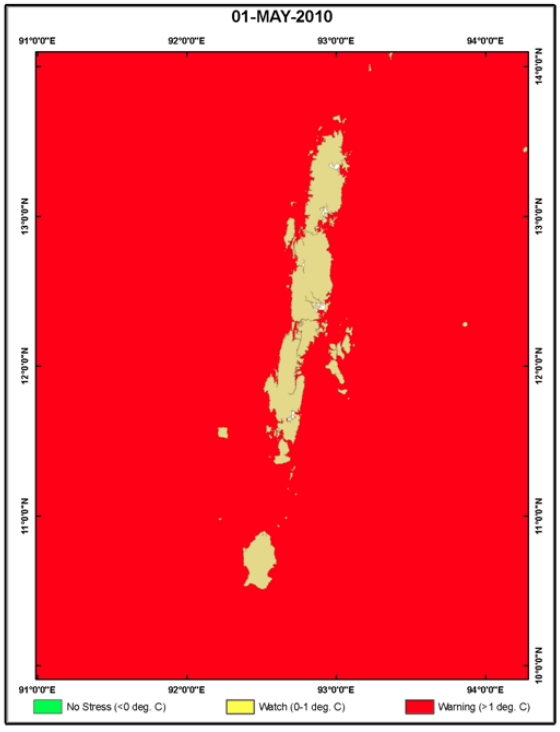

Figure 5 *HotSpot Map of Andaman Islands showing Warning status during Mass Bleaching episode of April-May, 2010 (Source: http://www.incois.gov.in/Incois/coralwarning.jsp)*

which will take into account the spatio-temporal variability of regional responses to global bleaching events.

BLEACHING PREDICTION: TRAJECTORIES FOR FUTURE

The field of bleaching prediction whose theoretical and operational development spans over two decades is still evolving. The significant challenges this young field encounters today come from a wide array of unanswered questions. The predictive power of global bleaching from satellite observations is continuously debated with respect to spatial and temporal resolution of the input data, climatology and observational time period (Logan et al., 2012; Donner, 2009). The usage of static thermal threshold (i.e. 1° C above climatological summer maximum) under MMM climatology model of bleaching prediction has already been challenged by an alternate method of MMMmax climatology (Donner, 2009) which shows greater robustness in terms of variability statistics (Logan et al., 2012). Predictive modeling of mass bleaching gets also limited by i) insufficient real time data of in situ seawater temperatures corresponding to satellite SSTs during bleaching events; ii) marginal knowledge on species specific bleaching response; iii) decoupling capability of thermal stress from other, coincident environmental stresses like photo-bleaching, pollution, diseases, etc.

Prediction of recurrence frequency and intensity of global mass bleaching events has found a new dimension in climate modeling when analysed in the light of coupled atmosphere-ocean General Circulation Models (GCM) and IPCC (Intergovernmental Panel on Climate Change) projections on different climate change scenarios. The model outputs have indicated that mass bleaching of corals remains the most severe threat for global tropical reefs for the next thirty to forty years even under the most optimistic climate scenarios (Donner, 2009;

Veron et al., 2009; Baker et al., 2008; Hoegh-Guldberg et al., 2007; Donner et al., 2005; Sheppard, 2003; Hoegh-Guldberg, 1999). Global mass bleaching episodes have coincided with intensified El Niño-Southern Oscillation (ENSO) events: the principal source of inter-annual global climate variability (Lough, 2011; Parry et al., 2007). Projected frequency of mass bleaching episodes breaching the recurrence interval of ENSO events however remains an interesting debate. Another aspect that needs crucial attention in future bleaching modeling and predictions is adaptation and acclimatization of corals and their endo-symbionts to thermal stress (Thompson and Woesik, 2009, McClanahan et al., 2007).

Forewarning of mass bleaching events presents a horizon of hope for the people associated with the protection aspect of this beautiful but fragile ecosystem: the reef managers. Improvisation in the existing models of bleaching prediction is always a welcome step to ensure timely and effective management strategies for real-time ecosystem management. From management perspective, mass bleaching events consequent upon climate-driven warming rather present a limited capacity to reduce perturbations or disturbances on reef ecosystem (Mumby and Steneck, 2011). However, at the same time its forewarning on a spatial framework can help in planning complementary approaches (like reducing human stress, physical closure of the protected reef area, ecological interventions like reduction in sea urchin population, etc.) to speed up reef recovery and strengthen resilience in the long run.

Acknowledgements

Author thanks Director, Space Applications Centre, ISRO and Deputy Director, EPSA for their overall guidance, continuous encouragement and support to study coral reef ecosystems through various projects under Earth Observation Applications Mission programme of ISRO. Author is indebted to Dr. R. P. Singh, Head, Environment and Hydrology Division for his valuable inputs towards this topic. Field support and contribution of in situ photographs used in Figure 1 by the collaborating research team from Division of Fisheries Science, Central Agricultural Research Institute (CARI), Port Blair, Andaman is acknowledged with thanks.

References

Ajai, Nayak, S., Tamilarasan V., Chauhan, H. B., Bahuguna, A., Gupta, C., Rajawat, A. S., Ray Chaudhury, N., Kumar, T., Rao R. S., Bhattacharya, S., Ramakrishnan, R., Bhanderi, R. J., Mahapatra, M. et al. 2012. Coastal Zones of India. Space Applications Centre, (ISRO). Ahmedabad, 597 p. (ISBN No. 978-81-90-9978-9-8).

Ajith Kumar, T. T. and Balasubramanian T. 2012. Bleaching of corals in Agatti-Lakshadweep, India: A window view. Proceeding of the 12th Intl. Coral Reef Symposium, Caims, Australia, 9-13 July, 2012 (http://www.icrs.2012.com/proceedings/manuscript/icrs2012 9A/1.pdf)

Bahuguna, A. 2008. Impact of climate change on coral reefs. ISG Newsletter, 14: 44-48.

Bahuguna, A., Nayak, S., Ray Chaudhury, N., Sharma, S., Bhanderi, R. J. 2008 Assessment of coral reef health using satellite data. Space Applications Centre, (ISRO), Ahmedabad, SAC/ RESA/ MESG/ MCED/SN/62/2008, 14p.

Baker, A. C., Glynn, P. W. and Riegl, B. 2008. Climate Change and coral reef bleaching: An ecological assessment of long-term impacts, recovery trends and future outlook. Estaurine, Coastal and Shelf Science, 18: 1-37.

Brown B. E. 1997. Coral bleaching: causes and consequences. Coral Reefs. 16: S129 – S138.

Carpenter, K. E., Abrar, M., Aeby, G. et al. 2008. One third of reef-building corals face elevated extinction risk from climate change and local impacts. Science. 321: 560-563.

Donner, S. D. 2009. Coping with commitment: Projected thermal stress on coral reefs under different future scenarios. PLoS ONE 4(6): e5712. doi: 10.1371/journal.pone.0005712

Donner, S. D., Skirving W. J., Little, C., M., Oppenheimer, M. and Hoegh-Guldberg, O. 2005. Global assessment of coral bleaching and required rates of adaptation under climate change. Global Change Biology 11: 2251-2265.

Glynn, P.W. 1993. Coral reef bleaching: ecological perspectives. Coral Reefs, 12: 1-17

Goreau, T. J. and Hayes, R. L. 1994. Coral bleaching and ocean "HotSpots". Ambio, 23: 176-180.

Hoegh-Guldberg, O. 1999. Climate change, coral bleaching and the future of the world's coral reefs. Review. Marine and Freshwater Research, 50: 839-866.

Hoegh-Guldberg, O., Mumby, P.J., Hooten, A.J., Steneck, R.S., Greenfield, P., Gomez, E., Harvell, C.D., Sale, P.F., Edwards, A.J., Caldeira, K., Knowlton, N., Eakin, C.M., Iglesias-Prieto, R., Muthiga, N., Bradbury, R.H., Dubi, A., Hatziolos, M.E. 2007. Coral reefs under rapid climate change and ocean acidification. Science, 318: 1737–1742.

http://coralreefwatch.noaa.gov

http://coralreefwatch.noaa.gov/satellite/composites/monthly/images/crw_oper50km_monthlymax_alertarea

http://www.incois.gov.in/Incois/coralwarning.jsp

http://www.reefbase.org

Hughes, T. P., Baird, A. H., Bellwood, D. R., Card, M., Connolly, S. R., Folke, C., Grosberg, R., Hoegh-Guldberg, O., Jackson, J. B. C., Kleypas, J., Lough, J.M., Marshall, P., Nystro¨m, M., Palumbi, S.R., Pandolfi, J.M., Rosen, B., Roughgarden, J. 2003. Climate change, human impacts, and the resilience of coral reefs. Science, 301: 929–933

Hughes, L. 2000. Biological consequences of global warming: is the signal already apparent. Trends in Ecology and Evolution, 15: 56–61.

Kleypas, A., Mcmanus, J. W. and Meñez, A. B. 1999. Environmental limits to coral reef development: Where do we draw the line? American Zoology, 39: 146-159.

Krishnan, P., Dam Roy, S., George, G., Srivastava, R. C., Anand, A. Murugesan, A. Kaliyamoorthy, M., Vikas, N. and Soundararajan, R. 2011. Elevated sea surface temperature during May 2010 induces mass bleaching of corals in the Andaman. Current Science. 100: 111-117.

Kumaraguru, A. K., Jayakumar, K. and Ramakritinan, C. M. 2003. Coral bleaching 2002 in the Palk Bay, southeast coast of India. Current Science, 85: 1787-1793.

Lesser, M. P. 2004. Experimental biology of coral reef ecosystems. Journal of Experimental Marine Biology and Ecology. 300: 217-252.

Lesser, M. P. 2011. Coral bleaching: Causes and mechanisms. In Coral Reefs: An Ecosystems in Transition, Dubinsky Z. and Stambler, N. (eds). pp. 405-419.

Liu, G. and Strong, A. E. 2003. Remote sensing of sea surface temperature during 2002 Barrier Reef coral bleaching. Eos, Transactions, American Geophysical Union, 84: 137-141

Logan, C. A., Dunne J. P., Eakin, C. M., Donner S. D. 2012. A framework for comparing coral bleaching thresholds. Proceeding of the 12th International Coral Reef Symposium, Caims, Australia, 9-13 July, 2012. (http://www.icrs2012.com/proceedings/manuscripts/ICRS2012_10A_3.pdf)

Lough, J. M. 2011.Climate change and coral reefs. In In David Hopley (ed.) Encyclopedia of Modern Coral Reefs. Springer. pp. 198-210.

McClanahan, T. R., Ateweberhan M., Muhando C. A., Aina J. M. and Mohammed M. S. 2007. Effects of climate and seawater temperature variation on coral bleaching and mortality. Ecological Monographs, 77: 503-525.

Montgomery, R.S. and Strong, A.E. 1994.Coral bleaching threatens ocean,life, Eos, Transactions, American Geophysical Union, 75: 145–147

Mumby, P.J. and Steneck, R.S. 2011. The resilience of coral reefs and its implications for reef management. In Coral Reefs: An Ecosystems in Transition, Dubinsky Z. and Stambler, N. (eds). pp. 509-519.

Parry, M.L., Canziani, O. F., Palutikof, J. P., Linden van der P. J., & Hanson, C. E., Eds. 2007. Cross-chapter case study. In: Climate Change 2007: Impacts, Adaptation and Vulnerability. Contribution of Working Group II to the Fourth Assessment Report of the Intergovernmental Panel on Climate Change, Cambridge University Press, Cambridge, UK, pp. 843-868.

Podesta´ , G.P., Glynn, P.W. 1997. Sea surface temperature variability in Panama´ and Gala´ pagos: extreme temperatures causing coral bleaching. Journal of Geophysical Research, 102:15749–15759.

Sheppard, C. R.C. 2003. Predicted recurrences of mass coral mortality in the Indian Ocean. Nature, 425: 294-299.

Stambler, N. 2011. Zooxanthellae: The yellow symbionts inside animals. In Coral Reefs: An Ecosystems in Transition, Dubinsky Z. and Stambler, N. (eds). pp. 87-106.

Thompson, D.M. and Woesik, R. van 2009. Corals escape bleaching in regions that recently and historically experienced frequent thermal stress. Proceedings of the Royal Society B. 276: 2893-2901.

Venkataraman K. 2011. Coral reefs of India. In David Hopley (ed.) Encyclopedia of Modern Coral Reefs. Springer. pp. 267-275

Venkataraman, K., Satyanarayana, Ch., Alfred, J.R.B. and Wolstenholme, J. 2003. Handbook on Hard Corals of India, Zoological Survey of India, Kolkata, 266 p.

Veron J.E.N., Hoegh-Guldberg O., Lenton T.M., Lough J.M., Obura D.O., Pearce-Kelly, P., Sheppard, C.R.C., Spalding, M., Stafford-Smith M.G., Rogers A. D. 2009. The coral reef crisis: The critical importance of <350 ppm CO2. Marine Pollution Bulletin 58: 1428-1436.

Vivekanandan, E., Ali M. H., Jasper, B. and Rajagopalan, M. 2009. Vulnerability of corals to warming of the Indian seas: a projection for the 21st century. Current Science. 97: 1654 -1658.

Wilkinson, C. R. 2000. Status of Coral Reefs of the World: 2000. Australian Institute of Marine Science. Townsville. Australia,. 361 p.

Wilkinson, C. R. 2008. Status of coral reefs of the world: 2008. Global Coral Reef Monitoring Network and Reef and Rainforest Research Centre, Townsville, Australia, 296 p.

Healthy Mangrove Ecosystem: Saviour of Mankind from Natural Disasters

Anjali Bahuguna

Scientist (Retd. ISRO), Ahmedabad, India
Email: anjalibahuguna30@gmail.com

Mangroves comprise several species of trees and shrubs that grow along sheltered intertidal shores, mainly in tropical and subtropical coastal zone. In certain areas mangroves do extend along temperate coastlines where their distribution overlaps with salt marsh communities. A mangrove is not just a tree; it is a whole forest community which lives between the sea and the land. Mangroves can be found in all major subclasses of coastal waterways including: tide-dominated deltas, tide-dominated estuaries, tidal creeks, wave-dominated deltas, wave-dominated estuaries and strand plains. However, they are most common in tide-dominated waterways (e.g. deltas, estuaries and tidal creeks) and in wave-dominated deltas.

Mangrove forests are one of the most important habitats in the world. Ecologically mangroves are important in maintaining and building the soil, as a reservoir in the tertiary assimilation of waste, and in the global cycle of carbon dioxide, nitrogen, and sulphur. The protection against: cyclones are a "free" benefit. They play a significant role in coastal stabilization and promoting land accretion, fixation of mud banks, dissipation of winds, tidal and wave energy. Use of mangroves as natural sewage-treatment plants has been considered. Mangroves trap sediments and so contribute to land building, preventing erosion and excessive shifting of coastlines.

75% of the commercially caught fish and prawns spend atleast some part of their life cycle living in the mangroves. For many species of fish, like the sea mullet and barramundi, the muddy waters of the mangroves are the nurseries where they raise their young. Mangrove forests also provide safe nesting and feeding sites for herons, egrets and other birds. Mangroves are also home to lots of snakes and spiders, flying foxes and a favourite niche for salt water crocodiles. Mangroves have been exploited for timber for building dwellings and boats and fuel-wood for cooking and heating. In Indonesia, commercial exploitation of mangroves for charcoal is reported from 1887. In Central America, the direct use for charcoal production and the extraction of tannin has been responsible for large-scale mangrove removal and degradation. Large-scale conversion of mangroves for wood chip production began in East Malaysia and Indonesia during the 1970s. Cottage industries flourish in Malaysia, Philippines, Sri Lanka and Japan where mangroves are used for making roof thatching material, basketry, floats, textile industry, pulp for paper, utensils, production of honey and wax. They are also used as staple food in Papua New Guineas. Intoxicating drinks are made from the sap of the "coconut" of Nypa and Borassus. Their use for medicinal purposes has also been demonstrated. A relatively recent

commercial use of mangroves is for recreation and ecotourism. For their vast economic importance they have been unsustainably exploited and destroyed world-wide.

The mangrove flora of the world is represented by about 65 species. Most of the species are strongly represented in South East Asia and the Eastern coast of Africa. The floral diversity of mangroves in India is great. The Indian mangroves are represented by approximately 59 species from 29 families. Of the 59 species, 34 species belonging to 21 families are present along the west coast. There are a few species of which are indigenous to the west coast, e.g., Sonneratia caseolaris, Sueda fruticosa, Urochondra setulosa etc. The east coast of India and the Andaman and Nicobar Islands shows a higher species diversity as well as unique distribution of mangrove flora. The east coast is represented by 48 species belonging to 32 genera. Maximum area is occupied by mangroves in West Bengal, followed by Gujarat (Table 1).

Table 1: State-wise area (in sq km) occupied by mangroves on the Indian coast

State/UT	Area in Sq Km	
	1990-93	2005-07
Gujarat	1014.6	890.7
Maharashtra	222.6	270.9
Goa	6.7	34.6
Karnataka	8.7	6.0
Kerala	10.0	6.6
Tamil Nadu including Puducherry	23.6	57.3
Andhra Pradesh	380	351.3
Orissa	187	221.1
West Bengal	1838	2529.3
Andaman	679	566.6
Nicobar	70.9	21.7
	4441.1	**4956.2**

HEALTHY MANGROVE ECOSYSTEM

Health describes an environment that maintains its biodiversity, is stable over time and is resilient to change (Rapport et al., 1998),shows diversity, complexity and robustness, because the critical ecological components of the ecosystem are well preserved and exhibit no symptoms. Biological or ecological indicators are used that reflect community derived environmental values to infer overall ecosystem health. For evaluating the ecosystem health of a wetland, the selection of the assessment indicators should take account of the dynamics of ecological processes, economic structures and societal dimensions under differing management mechanisms, and incorporate the temporal or spatial scales at study because a wetland is a complex ecosystem with compounding interactions among natural, economic, and social aspects.

In the present paper I am describing the health of Orissa mangroves and their role in saving the coastal population from the recent cyclone Phailin.

Orissa is located in the eastern part of the country, with a geographic area of 155,707 sq km, which constitutes 4.74 % area of the country. It lies between latitude 17°47' and 22°34' N and longitude 81°22' and 87°29' E. The forest cover of the state is 48,374 sq km which is 31.07% of the geographic area of the state. The total length of the coast line in Orissa is about 430 km.The three major rivers of the state are Mahanadi, Brahmani, and Baitarni. Mangroves of the Orissa coast are mainly tide dominated. Dominant features are high tidal range with strong bi-directional current, river channels are funnel shaped with extensive tidal flats dominated by mangroves. There are 36

mangrove communities in Orissa. The three species of Avicennia viz, A. officinalis, A. marina and A. alba dominate in majority of the mangrove forest areas.

Bhitarkanika is the third important mangrove habitat (Fig.1) among the Indian mangroves with respect to mangrove species diversity and the most dominant and diverse mangrove habitat of the Orissa coast. Important mangrove and mangrove associate species are Avicennia alba, A. officinalis, Aegiceras corniculatum, Aegialitis rotundifolia, Acrostichum aureum, Bruguiera parviflora, B. gymnorrhiza, B. cylindrica, Ceriops decandra, Excoecaria agallocha, Heritiera kanikensis (rare & endemic), Heritiera fomes, Kandelia candel, Phoenix paludosa, Porteresia coarctata, Sonneratia apetala, Rhizophora mucronata, R. apiculata, and Salvadora persica. Bhitarkanika is the important natural breeding place of estuarine crocodiles (Crocodilus porosus) and several species of threatened sea turtles, Lepidochelys olivacea, batagur baska and the king crab, Carcinoscopius rotundicanda and Tachypleus gigas.

***Figure 1**: Distribution of Mangroves in Orissa State*

Other important mangrove ecosystem of Orissa (Fig.1) include the Mahanadi Mangroves (Kendrapara district), the Kantilo Forest Block, the Jambu Forest Block, the Bhitar Karnasi Forest Block, the Bahar Kharnasi Forest Block, the Kansardia Forest Block, the Hukitola Forest Block, the Dhamara RF, the Kalibhanjdia RF, the Katikhaal RF, the Sunirupi RF, the Kantika RF, Devi Mouth Mangrove Wetland, the Salio Forest Block, the Boruan Forest Block, the Bandar Forest Block and the Subarnrekha Mangrove Wetland.

Due to their importance for the state of Orissa, the Bhitarkanika mangroves, their density diversity, area and health has been studied using satellite data (Nayak et al., 1992, Nayak and Bahuguna 2001, Nayak et al., 2003, SAC 2007, and Ajai et al., 2012).In 1975 Bhitarakanika was declared as a sanctuary under the Wild Life protection act, 1972 and comprises Bhitarakanika, Kalibhanjadian and Gahirmatha mangrove area. It is fed by the Dhamara River, Manipura River and Bhitarakanika River. The Dhamara River in the north, the Hansua in the west and the Bay of Bengal in the east and south bound the sanctuary. Gahirmatha mangrove area comprises Sunirupi R.F, Habilikunti P.F and Gahirmatha P.F.The area is under laid by alluvial deposits, which are brought down by the rivers. The area is also prone to severe cyclonic storms during April to June and October to November. Tidal level varies from estuarine mouth towards the inland areas subjected to wide seasonal variation. The area is influenced by high tides and low tides twice a day at an interval of 12 hours. The tidal amplitude ranges from 2 - 3.5 m upstream and 3.5 – 6 m near the river mouth (MSSRF 2002). Due to regular inundation through tidal action the soil is mostly clayey loam and highly slushy. The surface soil is composed of silt loam and clayey loam and is

about three to four meter in depth. The soil though well aerated is saline. In the elevated areas away from the creeks and channels the soil is more sandy and comparatively less moist and saline. The soil pH varies from 6.73 to 7.3 (MSSRF, 2002). Due to constant deposition of humus the soil is fertile even though it is saline. Out of the 215 sq km of mangrove forest of Orissa, Bhitarakanika occupies 202 sq km. The Kendrapara district has 184 sq km and Bhadrak district has 18 sq km of mangrove vegetation cover. The mangrove species are mostly concentrated along only the network of creeks and channels and extend from the sheltered bay to the elevated banks of the upper riparian zone. The diversity in fauna is very high. In Bhitarakanika the fauna is distributed throughout the sanctuary often in distinct zones related to frequency of tidal flooding, soil type, salinity and the type of surrounding plant community. There are several species of mammals, birds, amphibians, reptiles, fish that live in Bhitarakanika.

There are 10 types of major and associate mangroves and non-mangrove classes identified in the Bitarakanika (Fig.2).According to Kanvinde (2003) the mangroves of Bhitarakanika comprises 70 species, including mangrove and their associates with 4 species of Brugueira, 3 species of each Avicennia, Sonneratia, Heritiera, Rhizophora and Xylocarpus.

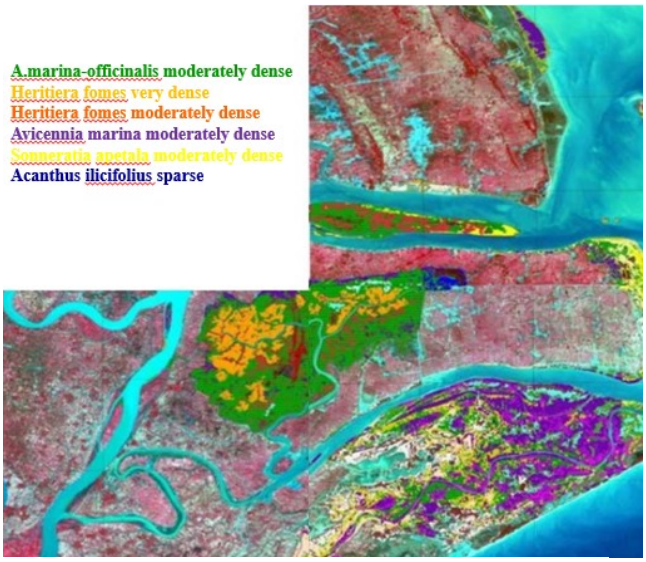

***Figure 2**: Mangroves of the Bhitarkanika RF mapped using satellite data (Ajai et al., 2012)*

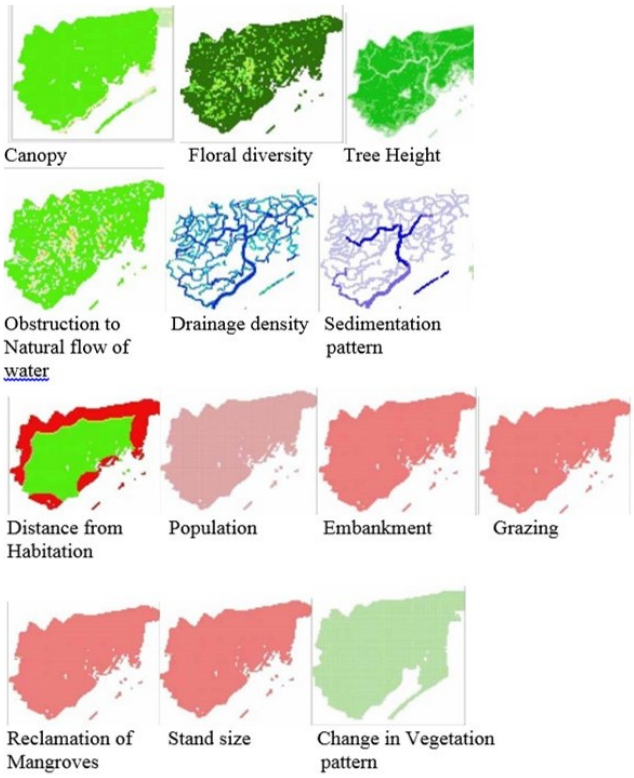

***Figure 3**: Maps of environmental indicators*

Space Applications Centre (Ajai et al., 2012) developed a multi-parameter health model using twelve environmental indicators of health in a cell-based grid analysis in a GIS environment. The twelve environmental indicators of health included canopy cover, floral diversity, obstruction to natural flow, drainage density, natural regeneration, anthropogenic stress, stand size fragmentation, change in vegetation patter, height, defoliation, erosion/accretion and sedimentation. Giving weightages to each indicator a cell based grid analysis was carried

out to yield health of each grid in the study area. Health of mangroves was then indicated as Mangroves in i) pristine health, ii) vulnerable to degradation, iii) degrading and iv) degraded mangroves. The model developed for assessing the health of mangroves was applied for Bhitarkanika RF and is being discussed here.

Maps were generated for the twelve environmental indicators (Fig.3) affecting the health of mangroves and corresponding values in the scale 1 to 100 were given.

Table 2: Parameter Weightage

Parameter	Weightage
Canopy	12
Flora density	11
Obstruction to natural flow	10
Drainage density	9
Natural regeneration	8
Anthropogenic stress	7
Stand size / fragmentation	7
Change in vegetation pattern	6
Height	5
Defoliation	4
Erosion / accretion	3
Sedimentation	2

All four types of canopy cover (very dense, dense, sparse and degraded) were found and overall percentage cover is of dense mangroves. Mangrove zones comprise three-four mangrove communities in each zone. Maximum area is occupied by trees having more than 10 m height. There was no unseasonal defoliation. There was no obstruction to natural flow of water. There are adequate creek systems in the region and overall creek systems had less turbidity. Area was having more than 80% natural regeneration. The outer periphery has more anthropogenic influence with habitation residing in less than 100 m from the mangroves. The Bhitarkanika mangrove forest region has 100-500 human population. There are no embankments, no grazing, and no reclamation of mangroves. There has been no change in the size of the stand and no change in mangrove vegetation pattern from 2000-2005.

All intersected layers with grid generate a separate grid showing the averaged values for each indicators of health. Lastly, each grid is recalculated assigning weightages to each layer (as per Table 2) and the health of the mangrove is predicted as follows:

MH = ∑ (Map of each parameter (Rank) X Weightages/ sum of weightages (84))

(The sum of weightages is done here to bring the values in the range of 1-100.)

Thus, Mangrove Health (MH):

Mangroves in pristine health	80.1-100
Mangroves vulnerable to degradation	40.1-80
Mangroves degrading	10.1-40
Mangroves degraded	1 - 10

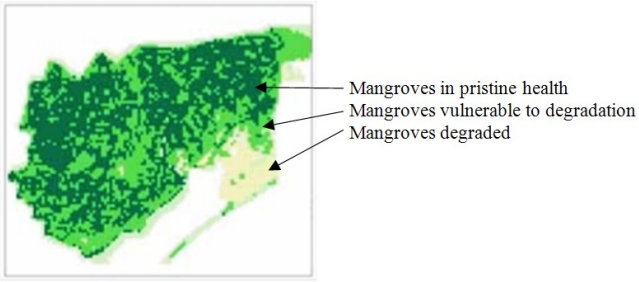

***Figure 4**: Mangrove Health Map*

The mangroves of the Bhitarkanika are in good condition. The central region has mangroves in pristine health. The mangroves near the outer periphery are vulnerable to degradation.

Measures should be taken to preserve and conserve these mangroves. It is very important that the mangroves are in a healthy state for them to act as saviours for mankind against natural disasters like cyclone and storm surge.

Cycolne Phailin hit the Orissa coast near Gopalpur on October 11, 2013. Fig. 5 depicts the worst affected and less affected areas due to the cyclone.

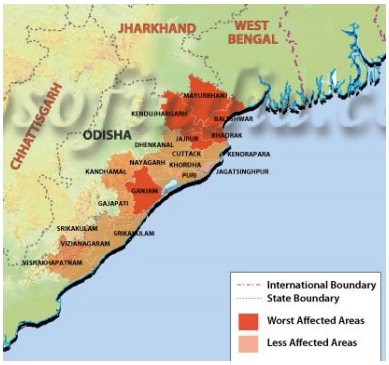

***Figure 5**: Impact of cyclone Phailin in Orissa state*

The coast from Kendrapara to Puri district is the mangrove dominated coast and is seen to be among the less affected area (Fig.5). Upton, J., 2013 (in an article in Down to Earth), says that the Paharajpur village was sheltered and saved from storm damage due to the mangrove belt on the seaward side of the village. About 40 of the village's 200 homes were damaged, but residents told that it would have been worse without the mangrove. In the nearby Sundrikhal and Pentha village, most of the houses have been washed away, however this village was saved because the mangrove forest bore the initial brunt of the storm. This mangrove area was planted and later grew into a thick forest. Thus proving the role of mangroves as the savoir of mankind from natural disasters like cyclone.

Acknowledgements

I am grateful to Dr.Shailesh Nayak, the then Group Director at Space Applications Centre and currently Secretary, Ministry of Earth Sciences, for his guidance and encouragement. Thanks are due to Dr R.R. Navalgund, the then Director, Space Applications Centre for motivating me throughout this work. I am also thankful to Dr. Ajai for guiding me in this study.

References

Rapport D. J., R. Costanza and A. J. McMicheal. 1998. Assessing ecosystem health. Trends Ecol. Evol. 13:397-402.

Nayak, S. R., Bahuguna, A., Shaikh, M. G., Chauhan, H. B., Rao, R. S. and Arya, A.S. (1992): Coastal Environment: Scientific Note, RSAM/SAC/COM/SN/11/92 (Space Applications Centre, Ahmedabad), 114 P.

Nayak S.R., and Bahuguna A (2001). Application of remote sensing data to monitor mangroves and other coastal vegetation of India. Indian Journal of Marine Sciences. 30(40): 195-213.

Nayak, S., Bahuguna, A, Shah, D. G. et. al. (2003): Community zonation of selected mangrove habitats of India using satellite data: Scientific note; Space Applications centre, Ahmedabad, p 108.

SAC 2007: Project Team: Coastal Habitat of Selected Marine Protected Areas: Atlas of India: Atlas; Space Applications Centre (ISRO), Ahmedabad. SAC/RESIPA/MESG/PR/59/2007, May, 2007, 77 p.

Ajai et al., 2012. Coastal zones of India. Space Applications Centre (ISRO), Ahmedabad.

MSSRF 2002: Atlas of mangrove wetlands of India part 1 Tamil Nadu. M.S. Swaminatham Research Foundation, Chennai, India.

Kanvinde H.S., 2003.Bhitarakanika, In: Bioresources status in select coastal locations. National Bioresource Development Board (Department of Biotechnology) Govt. of India. PP: 177 – 200.

Monitoring Marine Protected Areas (MPAs) using Geomatics: A Case Study in Gulf of Kachchh, Gujarat, India

Mohit Kumar, H. B. Chauhan, A. S. Rajawat, R.D. Kamboj[1] and Ajai

Space Applications Centre, ISRO, Ahmedabad, India
[1]Gulf of Kachchh Marine National Park and Sanctuary, Jamnagar, India
Email: mohitk@sac.isro.gov.in

INTRODUCTION

India has a coastline of about 7500 km of which the mainland accounts for about 5, 400 km and Lakshadweep and Andaman & Nicobar islands together constitute around 2, 100 km. The coastal zone comprises of wide range of coastal ecosystems such as creeks, mudflats, estuaries, beaches, backwaters, lagoons, deltas, mangroves and coral reefs, which are characterized by unique biotic and abiotic properties and coastal processes. Recognizing the need to conserve and protect coastal ecosystems, Ministry of Environment and Forests, Government of India has identified Marine Protected Areas (MPAs) under the Wildlife (Protection) Act, 1972, throughout the country, with the assistance of state governments. The Convention on Biological Diversity (CBD) defines an MPA as "any defined area within or adjacent to the marine environment, together with its overlying waters and associated flora, fauna, and historical and cultural features, which has been reserved by legislation or other effective means, including custom, with the effect that its marine and/or coastal biodiversity enjoys a higher level of protection than its surroundings". MPAs are notified either as 'National Parks' or 'Wildlife Sanctuaries' under the Wildlife (Protection) Act, 1972. There are 31 MPAs in the country covering an area of 6271.21 sq km. Monitoring Marine Protected Areas using geomatics provides accurate and cost effective method to the concerned authorities and this article provides salient highlights of the approach and observations through a case study carried out for the Gulf of Kachchh Marine National Park and Sanctuary.

The Gulf of Kachchh Marine National Park and Sanctuary (MNP&S), located along the southern shore of Gulf of Kachchh in the Jamnagar district of Gujarat, India (between 22° 15'N to 23° 00'N latitudes and 69° 00' E to 70° 30'E longitudes), is endowed with ecologically sensitive habitats such as mangroves, mudflats, coral reefs, seagrasses and sand dunes (Fig 1 and 2). It was established by a set of Government of Gujarat notifications during the period 1980 to 1982. Presently, the entire notified protected area comprises of 457.92 sq km of Marine Sanctuary and 162.89 sq km of Marine National Park. The MNP&S supports 215 species of molluscs including oysters, three species of sea turtles, three species of marine mammals (Dolphin, Porpoise and Dugong), 144 different

varieties of fishes, 27 species of commercially important prawns, 49 species of hard corals, 10 species of soft corals, 100 species of algae, six species of sea grasses along with few mangrove species. Since 1991, mangroves and coral reefs have been provided extra protection under the 1991 Coastal Regulation Zone (CRZ) notification of Government of India.

Coastal habitats of the MNP&S, Gulf of Kachchh (GoK) were monitored earlier at Space Applications Centre (SAC) for the period 1975-2001 using multi-temporal satellite data. In continuation to that work, coastal habitats, viz. mangroves and coral reefs, of the MNP&S, GoK, Gujarat were monitored using IRS P6 LISS-III (Linear Imaging Self Scanning-III) data for the years 2006, 2009 and 2011. Mangrove cover has been mapped and monitored for the year 2006, 2009 and 2011 while coral reefs have been mapped at eco-morphological level for 2006 and 2011.

STUDY AREA AND DATA USED

The study area covers a part of MNP&S (including islands such as Pirotan, Jindra-Chhad, Mundeka Bet and Dideka Bet) extending from 69° 49' to 70° 02' E longitude and from 22° 37' to 22° 29' N latitude (Fig 3). The vital habitats in the study area are: mangroves, mudflats, coral reefs, seagrasses, beaches and sand dunes. IRS P6 LISS-III digital data of 02 March 2006, 28 December 2009 and 11 January 2011 have been used to map and study the ecological changes in mangroves and coral reefs.

***Figure 1**: Mangrove in MNP&S, Jamnagar.*

***Figure 2**: Coral Reef in MNP&S, Jamnagar.*

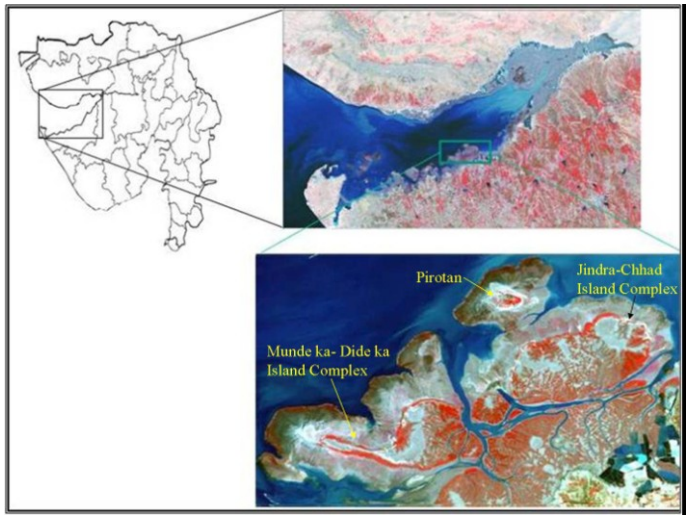

***Figure 3**: Study Area.*

METHODOLOGY

Satellite data of the year 2006, 2009 and 2011 were subjected to radiometric normalization and geometric correction. For radiometric normalization, the DN values of the images were converted to top-of-the-atmosphere reflectance values. The geometric correction was carried out by georeferencing the images using ground control points and all the images were assigned to a common projection system so that they could be mutually compared and analysed for change detection studies. The study area was then extracted from the satellite images. Mangrove mapping was done by analysing the satellite images of 2006, 2009 and 2011 using supervised classification technique.

The coral reef maps at ecomorphological level were prepared using 2006 and 2011 satellite data only, as the data of 2009 was of high tide period and the reef areas were completely submerged (Fig 4). These maps were prepared using visual interpretation technique. The coral reefs were classified into: Reef Slope, Reef Flat, Algae Dense, Algae Sparse, Muddy Reef Flat, Sandy Reef Flat, Moat and Sand Patch/Beach.

OBSERVATIONS

Mangroves: Prior to 1950 the entire gulf had very dense growth of mangroves, with individual plants reaching a height of 14 m. In the year 1975 entire intertidal area in and around core marine national park was occupied by dense mangroves. By the year 1982 there was a substantial reduction in the area under mangroves. In the year 1985, there was some improvement in dense mangrove category,

***Figure 4**: Satellite data used in the study for different periods*

however, the area under sparse mangrove reduced from 28.2 sq km in 1982 to 10 sq km. The degradation of mangroves was on account of their harvesting for fodder and fuel purposes, construction of saltpans, industrial development and establishment of a ship breaking yard near Bedi port.

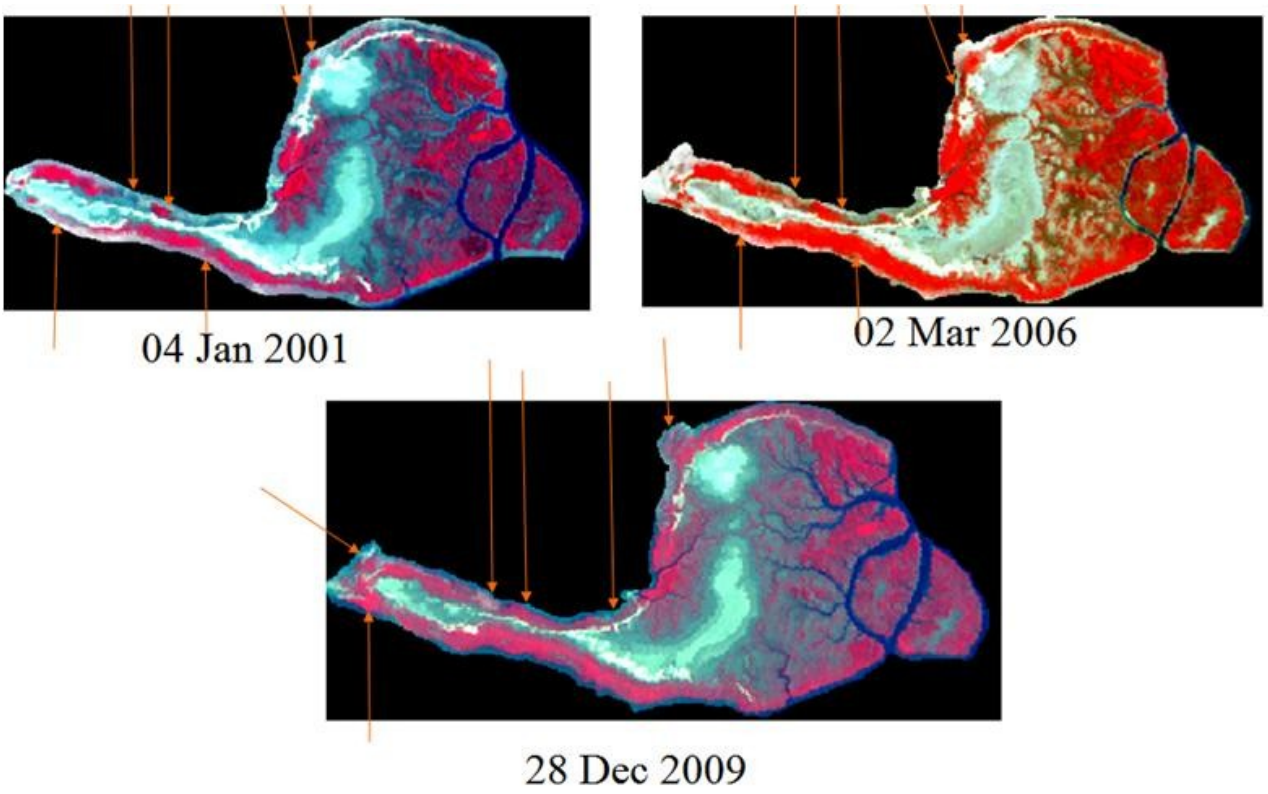

***Figure 5**: Increase in mangroves on Mundeka-Dideka island complex between 2001-2009 (Arrow indicates changes in mangrove cover).*

From 1985 onwards the condition of mangroves improved significantly because of establishment of MPA in the region. During the period 1985-1988, the total area under mangroves increased from 33 to roughly 50 sq km. Further till 1993 there was improvement noticed. However, mangrove density reduced sharply between 1993 and 1998. After 1998, there was significant deterioration, mainly because of recurrent oil spill incidents: one around March 1999, and the other on 15-16 November 1999. Mangroves on and around southeast of Jindra island suffered a loss of 14.7 sq km. Defoliation of mangroves was reported in this region in March 1999 and some regeneration was observed in July 2000. Till 2001 marginal improvement was observed, however, there was substantial increase in mangrove area when observed in 2006. The increase was more in case of sparse mangrove (7.05 sq km) than in case of dense mangrove (1.97 sq km). The mangroves have consistently increased on Mundeka-Dideka Islands between 2001 and 2009 (Fig 5). The area around southeast of Jindra, which was damaged due to oil spill in 1999, was observed under sparse mangrove cover in 2006. Increase in mangroves was also noticed on Pirotan Island (Fig 7). From

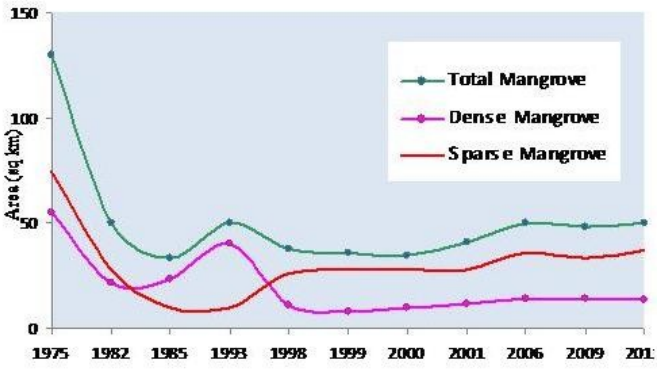

***Figure 6**: Variations in mangroves, in and around core Marine National Park, Jamnagar.*

2006 to 2011 the condition seems to be more or less stable. These variations in mangroves during 1975-2011 are represented in Fig 6.

Coral Reefs: The southern flank of GoK is inhabited by northernmost Indian reefs. These reefs have been classified into fringing reefs, platform reefs and coral pinnacles. The core area off the coast of Jamnagar has fringing reefs around Pirotan and Jindra-Chhad islands, where as the reef around Mundeka-Dideka bets are a platform reef. Among all the reef areas studied the one around Jindra-Chhad is in most degraded condition. Though a layer of mud has been mapped in all the three reef regions, the reef around Jindra-Chhad has been almost completely occupied by sediments and there is profuse growth of matty algae on the sediments. In1975 there was no mud mapped on Jindra-Chhad, which seems to have occupied reef flat area since 1982 onwards. It is believed that silt discharge brought by river Indus is one of the factors responsible for degradation of reefs. Pirotan reef, considered to be an atoll in earlier times the central portion of which has been filled gradually, has good reef portion on the northwestern, western and southwestern side. The entire eastern side is under mud on which algal development has been observed in 2006 and 2011 (Fig 7). There was an increase of 3.9 sq km in the reef flat area in 2001, relative to 1990. In 2006 there has been increase in the area under sediments by 2.84 sq km and consequently the area of reef flat has declined. The variation in reef substrates around Pirotan Island is shown in Fig 8. Much of northeastern and entire southern and south western part of reef around Mundeka-Dideka islands is under algal growth. The reef has been constantly experiencing sediment pressure from 1990 onwards. Matty algae such as Ulva colonise these muddy sandy substrata. Reef flat is narrow on all the reefs of GoK. It is widest on Mundeka-Dideka reef, among the different reefs studied. Live reef area is confined to the edges of the reef which are exposed to strong tidal currents and amount to 20-30 % of total reef area. A prominent narrow algal ridge zone of the reefs gets exposed during low tide period, which is more prominent in 2006. It mostly inhabits algae such as Sargassum and is composed of sandstone and calcareous deposits. The algal cover has increased over the years with matty and fleshy algae such as Ulva and filamentous Enteromorpha, dominating the

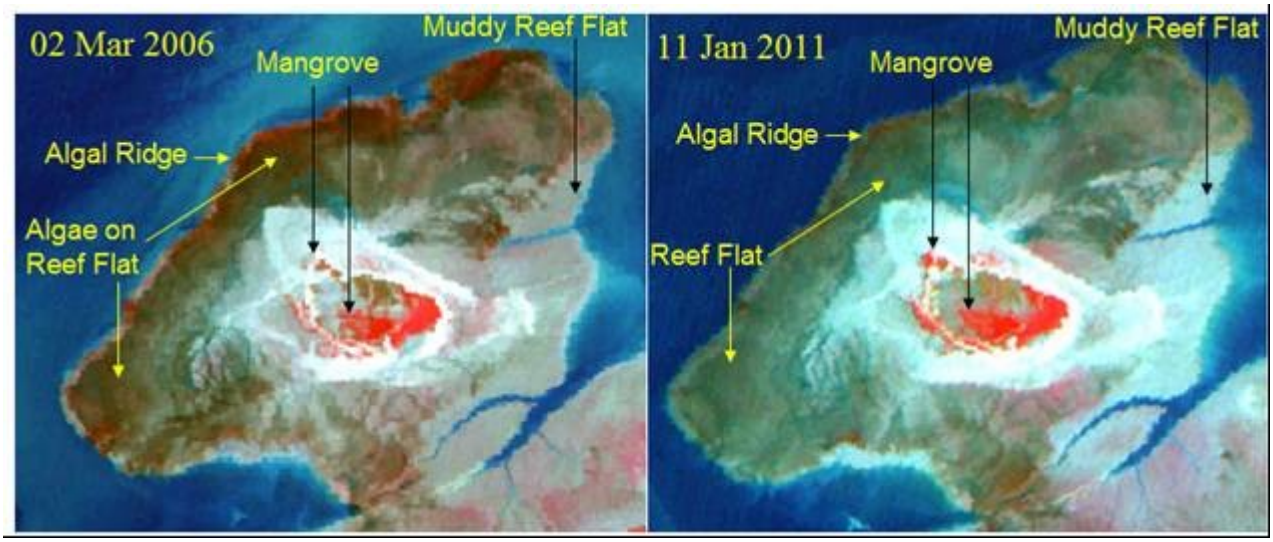

***Figure** 7: Ecological changes around Pirotan between 2006 and 2011.*

reef along with other members of chlorophyceae. It has been reported that onset of algae has been delayed by almost two months (from September-October to December) in the Gulf from the year 2002, which is an indication of degrading condition of reefs. Live coral cover is mainly confined to seaward region of the reef and mostly comprise of Porites, Favia, Favites, Montipora and other species.

Overall, between 2006 and 2011, there has been

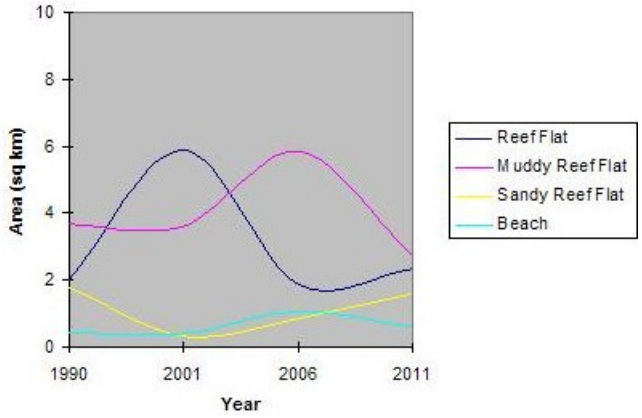

***Figure 8**: Variation in the area of Pirotan reef substrates between 1990 and 2011.*

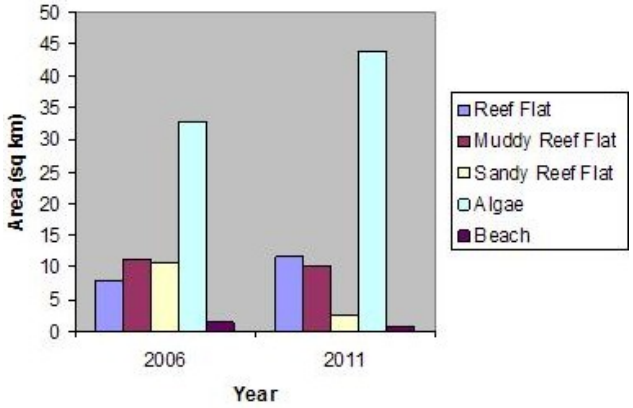

***Figure 9**: Variation in area of coral reef substrates in and around core MNP, Jamnagar between 2006 and 2011.*

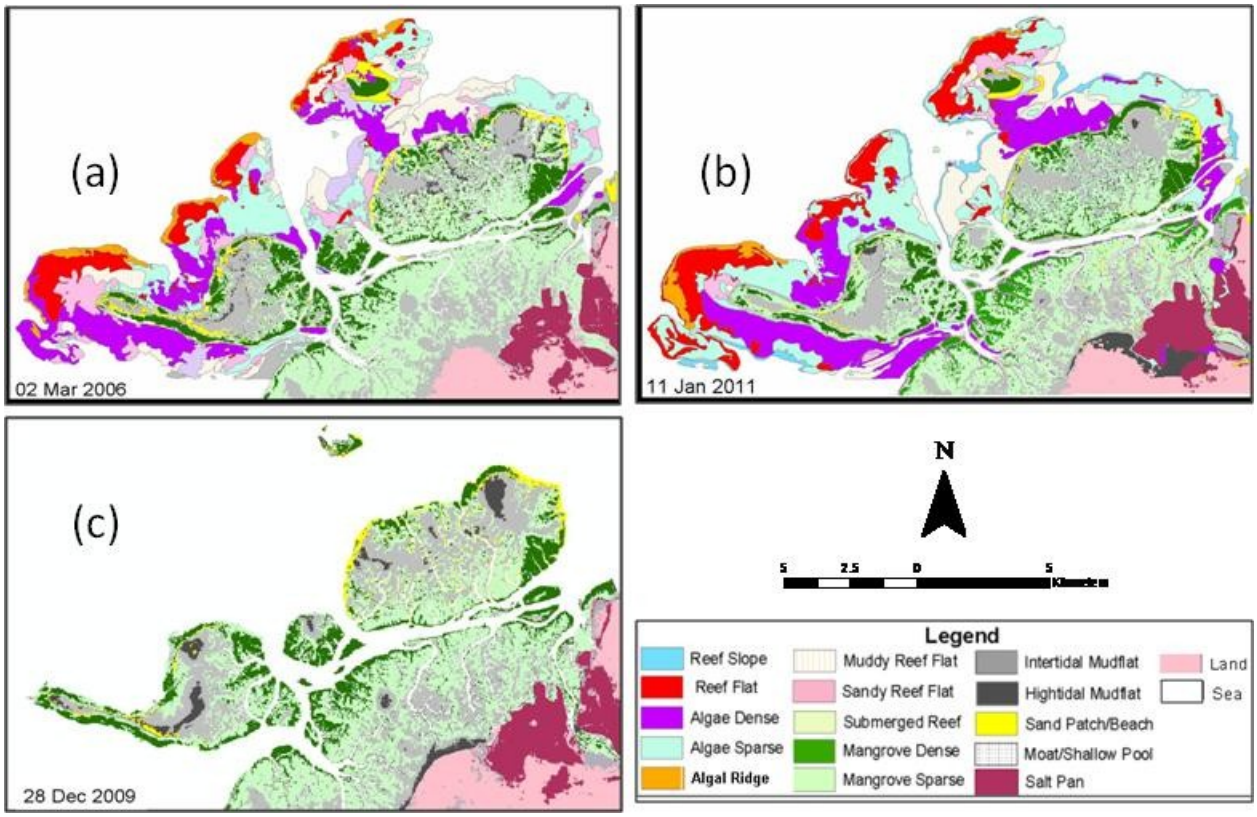

***Figure 10**: The coastal habitat maps of core MNP, Jamnagar for (a) 2006, (b) 2009 and (c) 2011.*

an increase in the algal cover by about 11 sq km. Algae have occupied new regions in 2011 such as south of Mundeka-Dideka and north of Jindra islands. There has been a little improvement in the area of reef flat, mainly on Pirotan and Mundeka-Dideka reef. The variation of different reef substrates is shown in Fig 9 and the complete coastal habitat maps for 2006, 2009 and 2011 is depicted in Fig 10.

CONCLUSIONS

Mangroves in and around the core MNP&S area have increased in 2006 relative to 2001, the increase being more in case of sparse mangrove than in case of dense mangrove. The regions which were damaged in 1999 oil spill have shown recovery and are stable. From 2006 to 2011 no marked change has happened in the study area. Mangroves have consistently increased on the Mundeka-Dideka island complex between 2001 and 2009. Algae have substantially increased, colonising new reef areas. There has also been an increase in the reef flat area as well between 2006 and 2011. Among the three reef regions studied, reef around Jindra-Chhad appears to be in most degraded state, with almost entire reef covered under the sediments.

WAY FORWARD

Work is in progress towards refining the methodology using multisensor and multidate satellite data for studying the coastal ecosystems. Efforts are also being made towards developing and validating models for assessing health of coral reefs and mangroves using Geomatics. Potentials of microwave and hyperspectral data are being explored for biomass estimation, community zonation and quantification of carbon stocks. Vulnerability of MPAs to coastal hazards is also being attempted.

Challenges of the Indian Coasts: Geomatics Solutions

S. M. Ramasamy

Former Vice Chancellor, Gandhigram Rural University, Gandhigram, Tamilnadu, India
Email:smrsamy@gmail.com

ABSTRACT

The coastal zones are very fragile owing to the reason that these form the junction between the continents and the oceans. Further the multi-variate tectonic, fluvial, marine and aeolian processes, which vary independently in their degrees and duration in space and time, act in different permutations and combinations with each other and keep on constructing and destroying the landforms along the coasts. Again as coastal zones are heavily populated; it adds further pressure on the coastal systems. The paper deals about the hierarchy of issues faced by the coastal zones like tectonic emergence and subsidence and it's impacts and the ways , means and needs for measuring the rate of such movements; marine regression and the need for the time series models on the land-ocean boundaries for drawing the sea level curve for India, the Quaternary deltas and the essentiality for understanding the mixture of fluvial and marine forces for the possible future fore casting models ;back water modifications , the related issues and the demands for the sediment-chemo dynamics modelling; disaster vulnerabilities and mapping methodologies etc; all using the unexplored vistas of geomatics technology. The concept has been explained by taking Tamilnadu coast as the reference region.

Key words: Indian coast, Taminadu coast, Geomatics-based coastal studies

INTRODUTION

The coastal zones are always fragile as these are formed by the tectonic, fluvial, marine and aeolian processes, which act independently in varying degrees and duration and occur cumulatively in different permutations and combinations along the different parts of the coasts. In addition to such inherent fragility, the coastal zones stand vulnerably exposed to various natural and anthropogenic disasters like seismicity and earth movements, tsunamis, floods, sea level rise, cyclones, coastal erosion etc. Further, owing to the enriched land and water resources, enjoyable eco systems and avenues for intra and intercontinental trades ,more than 70% of the global population and the related infrastructure are clustered in the coastal zones .Hence the scientists from all over the world have started showing more attention towards the coastal regions(Ahmed, 1972). The advent of Geomatics technology comprising multi spectral and hyper spectral remote sensing, GIS, GPS, Interferometry etc have opened up exhaustive newer vistas in unfurling the hidden complexities of the coastal zones and to provide solutions. From amongst many, the remote sensing based studies carried out by Shailesh

Nayak and his team (2004) have brought out many first time information to light about the Indian coasts. But still we will have to go a long way, as the global coasts in general and the Indian coasts in particular are confronted with a hierarchy of challenges and the Geomatics technology can provide answers for these challenging issues owing to its unique virtues.

The paper narrates the unique issues of the Indian coasts and how effectively the geomatics technology can be used in solving them .This has been done by taking Tamilnadu coast as the test area.

GENESIS OF THE INDIAN COASTS

The compressive force,which has originally drifted the Indian plate towards northerly to the distance of 6500 km, made it to collide with Eurasian plate and caused the rise of Mighty Himalayan mountains, is still active (Larson et al,1992).While it is pushing the Indian plate towards northerly , The Himalayas is obstructing from the north and as a consequence of which, the Indian plate is whirling with the a series of east-west alternate arches and deeps from Cape Comorin in the south to The Himalayas in the north (Fig.1) as demonstrated by Ramasamy (2006). Ramasamy (2006) has further inferred that the North-South faults are extension faults and block faulted, the Northeast-Southwest faults are sinisterly moving and the Northwest – Southeast faults are dextrally moving (Fig.2). Such an east- west arching phenomenon of the Quaternary period has been inferred by many; Ghosh (1976) in Amreli area of Saurashtra peninsula and Subrahmanya (1996) along Mangalore-Chennai. Overall, while such arching phenomenon has assigned convexities to the Chennai (1),Vedaranniyam (3) and Ramanathapuram (5) coasts, the complimentary deeps have yielded concavities to the Pondicherry/Cuddalore (2) and Manamelkudi (4) parts of the Tamilnadu coast (Fig.3). Whereas the multi directional faults and the geomorphic processes have configurated the coast with peaks, serrations, protrusions etc. Ramasamy (2006) has attributed such convexities and concavities to the structural culminations of the arches and deeps respectively .Thus, owing to the tectonic culminations, the convex coasts represent emerging coasts and the concave coasts symbolize subsiding coasts.

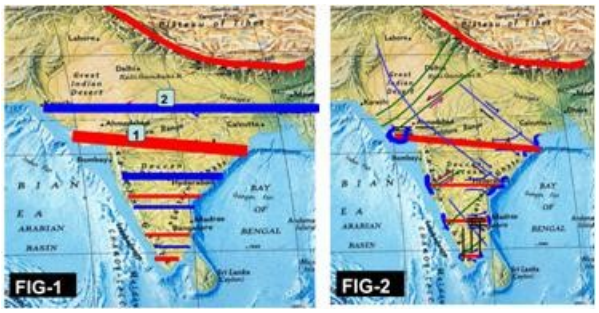

Figure 1*: Whirling Indian plate with East-West alternate arches and deeps due to post collision phenomenon.* ***Figure 2****: Post collision phenomenon and the fracturing Indian Plate with N-S extension /block faults, NE-SW sinistral faults and NW-SE dextral faults.*

THE CHALLENGES OF TAMILNADU COAST

The active post collision phenomenon and the related earth system processes like arching, deepening, faulting etc do pose a hierarchy of issues to the Indian coasts. For example, if Tamilnadu coast alone is taken up for discussion, along the emerging / convex coasts (1, 3 and 5, Fig-3), restricted marine regression, prograding deltas, sedimentation-shrinkage-defunct of back waters and creeks, modifying bay mouth bars, coastal erosion, formation of off shore sand bars and islands etc are common

issues . Whereas the subsiding concave coasts do witness drainage congestion and flooding ,accelerated tidal activities, marine incursion ,off shore shoal building etc. On the other side, the block faulted and the uplifted and the grabening parts of the coasts contribute in their own way to coastal emergence and subsidence .As the entire evolution and dynamics and there upon the natural resources, ecosystems and the disasters depend on this, the rate of emergence and subsidence need to be worked out and there from other related issues can be studied to provide solutions for sustainable coastal zone development.

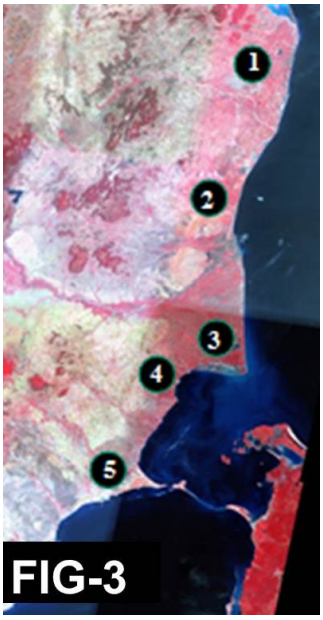

***Figure 3**: Alternate convex coasts (1-Chennai, 3-Vedaranniyam, 5- Ramanathapuram) and concave coasts (2-Pondicherry / Cuddalore, 4-Manamelkudi).*

GEOMATICS VIRTUES AND SOLUTIONS FOR COASTAL ISSUES

Estimation of rate of emergence of the coasts

All the above briefed issues are mostly due to the coastal emergence and subsidence related to post collision tectonics. Hence the estimation of such emergence and the subsidence need to be worked out holistically and the Geomatics technology is vested with exhaustive virtues for the same. The rate of emergence of the coasts can be worked out using the beach ridges, shrinkage of back waters, and withdrawal of creeks, dating of palaeo drainages and in areas of block faulting GPS based measurements.

Using beach ridges

In Chennai (1), Vedaranniyam (2) and Ramanathapuram (3) emerging coasts, bundles of beach ridges have developed to the breadth of respectively 2-3 km,50 km and 40-50 km due to the restricted marine regression related to post collision arching (Fig-4). These beach ridges can be mapped precisely using the digitally processed outputs of high resolution satellite data, samples can be collected from these ridges and their ages can be determined using 14C or TL dating. Such dating, coupled with elevations precisely measured using GPS in those sampled locations would give the rate of land emergence. Some attempts have been made by Ramasamy et al (1998) by dating the beach ridges of Vedaranniyam area which indicated the rate of land emergence of 1.5mm/yr and the land progradation and the withdrawal of the sea at the rate of 11 meters per year during the last 6000 years. At times, the sea level fall also could cause marine regression. However, after estimating the rate of coastal

***Figure 4**: Beach ridges showing the restricted marine regression in Chennai (1), Vedaranniyam (2) and Ramanathapuram (3) emerging coasts.*

emergence from the above geochronological dating of the beach ridges, it has to be calibrated with the local MSL to eliminate the input of sea level fall, if any.

Using shrinkage of back waters and creeks

Along the emerging coasts, the back waters will normally shrink due to the withdrawal of the sea and also due to sedimentation. However, the water spread areas of such back waters can be mapped using the multi dated topographic sheets and the satellite data and from the same, time series shrinkage of the back waters can be brought out as done in the case of Pulicat back water located in the Chennai emerging coast (Fig-5), which shows the pattern of shrinkage during 1915-2005. Now the GPS based

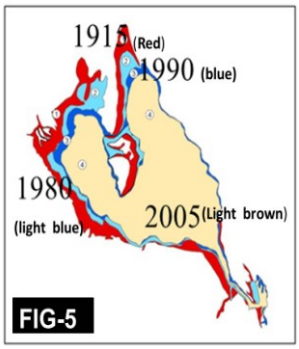

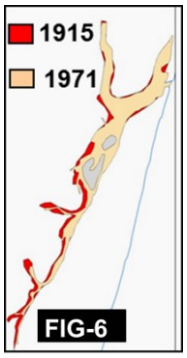

***Figure 5**: Limits of Pulicat lake from 1915 (toposheet data) to 2005 (satellite data);*

***Figure 6**: Limits of Ennore creek in 1915and 1971(toposheet data).*

elevations can be worked out in selected locations along the back water boundaries of different periods and from the same the rate of emergence can be worked out. This also needs to be caliberated for sedimentation and sea level fall.

The withdrawing Ennore creek of Chennai emerging coast during 1915-1971 is shown in Fig-6.The rate of coastal emergence can be worked out following the same methodology suggested for the back waters.

Using GPS measurements of tectonic uplifts

In areas of visible tectonic uplifts, continuous GPS based observations would provide better answer. However such areas of active tectonics with locations of the faults and zones of uplifts can be brought out precisely by studying the geology, tectonic frame work, geomorphic anomalies etc, of course for which the satellite multi spectral data could provide good base line support. For example, similar remote sensing based studies carried out by Ramasamy et al (2006a) in parts of Cauvery delta and Vedaranniyam area (Fig-7) showed that the two

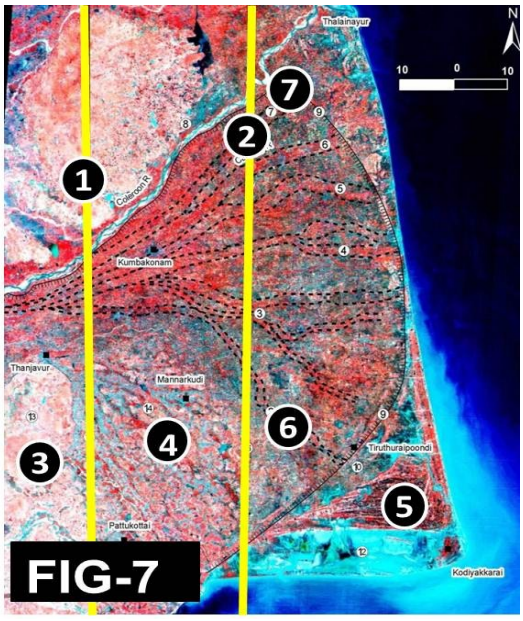

***Figure 7**: Satellite FCC of Tanjore delta-Vedaranniyam area showing N-S faults(1,2) with static Tertiary rocks(3) to its west and in between uplifting Tertiary rocks(4),Prograding Vedaranniyam(5)area and northerly migrating Cauvery river(6 ,7).*

sub parallel North- South faults (1,2) have cut the Mio-Pliocene sandstone(Tertiary formations) into two, with the western static (3) and the eastern bloc faulted and the uplifted segment(4). Ramasamy et al (2006a) further inferred that it is this uplift only has caused the land progradation /emergence in Vedaranniyam area (5) and the uplift is still going on. Now by doing continuous GPS observations in the faults trapped and uplifted sandstone block(4) and comparing it with similar GPS observations made in the western static block (3), the rate of uplift can be worked out. Such rate so worked out from GPS observations may be compared with beach ridge based land emergence of 1.5 mm/yr worked out by Ramasamy et al (1998) for Vedaranniyam area (5, Fig-7).

Using palaeo drainages

Again Ramasamy et al (2006c) have carried out selected 14C dating of the palaeo drainages of Cauvery delta (6, 7) and found that the palaeo drainages show gradual younger ages from the south to north from 1300 to 900 Y.B.P. (Fig-7). Ramasamy (2006), in his active tectonic model demonstrated that the river Cauvery has over all migrated towards northerly in Tanjore delta due to the above block faulting and uplift of the Mio Pliocene sandstones(4,Fig-7). In this context, the dating of the palaeo drainages and their elevation measurements can also give the rate of coastal emergence in Vedaranniyam area (Fig-7).

Estimation of rate of subsidence of the coast

Similarly the rate of subsidence can also be worked out for the subsiding coasts from the swelling back waters and creeks, accelerated tidal activities and mangroves etc mapped using the multi-dated topographic sheets and satellite data and GPS based elevation measurements of those boundaries of the water spread areas during the above different periods of the toposheets and satellite data sets. Besides, the natural resources, ecosystems and the disasters, this would provide vital information on tsunami, strom surge, tidal and flood inundation.

Time series models on land-ocean boundaries and the past and future sea levels

The phenomenon of global warming and the much apprehended sea level rise has started attracting the scientists from all over the world to study the land- ocean boundaries of the past, at least from 100 thousand years on wards. Though studies have been carried out in other parts of the world and the sea level curve has been brought out, it has been done only in a limited way in India and the sea level curve for the Indian coasts from 100 thousand years to till date is yet to be brought out. This is essential to understand the past climatic changes and the sea levels, so as to make future predictions there from and to visualize the different scenarios of sea water inundation/submergence for the different years in the future and further mitigation plans. Hence studies are required to bring out the coast line for the base of the Quaternary period, sea levels at different stages of prograded Quaternary deltas, the sea levels at different spatially distributed beach ridges etc. For example, the Pre Quaternary coastline drawn for Tamilnadu coast along the apex and the western limits of the deltas and the eastern limits of the Mio-Pliocene sandstone is shown in Fig-8. To the east of it a series of Quaternary deltas with differing morphologies viz. Vaigai lobate delta (1), Cauvery arcuate delta (2), Vedaranniyam cuspate delta (3), Ponnaiyar digitate delta (4) and Tamraparani estuarine delta (5) (Fig-9) were brought out by Ramasamy

(1992). These deltas also need to be studied for bringing out a time series model on the sea levels during the various time frame of the Quaternary period.

For example, the Vaigai lobate delta (1, Fig-9) has crescent shaped water bodies forming concentric rings encircling the apex of the delta located at Paramakkudi. This phenomenon suggests the gradual withdrawal of the sea from the apex of the delta and the corresponding progradation of the delta ring by ring ,which means the sea was in each ring in the process of withdrawal, from Paramakkudi to present day coast at Mandapam. Hence such lobate deltas need to be mapped using high resolution satellite data and dating and GPS measurements may be done along the selected rings of the delta. Similarly in arcuate deltas(2, Fig-9), the past sea might have been there within the arcuate delta and those must be located with the help of the caught up beach ridges. So, these ridges, if any and the outer most arc of the delta can be dated along with GPS based elevation measurements. In the same way, past levels can be traced along the rims of the east- west sand bodies in Ponnaiyar digitate delta (4, Fig-9) and dating and elevation measurements are to be done. The beach ridges along the coast also need to be dated and amalgamating all, sea level curve for India can be brought for the maximum possible time frame .Such past sea levels brought out from the local measurements are very vital to carry out any study related to global warming.

Quaternary deltas of Tamilnadu and land – ocean interactive dymamics

The Quaternary deltas stand as testimonies to the land ocean interactive dynamics. For example the Vaigai lobate delta(1) indicates turbulent fluvial activity with least marine forces acting on it (probably fluvial-90/ marine-10), the Cauvery arcuate delta(2) shows dominant fluvial forces with little rise in the marine dynamics (75/25), cuspate Vedaranniyam part of Cauvery delta(3), suggests the arresting of the delta progradation by the beach formation process(50/50), digitate Ponnaiyar delta (4) indicates the over powering and the incursion of the sea into the delta digitizing it (25/75) and estuarine

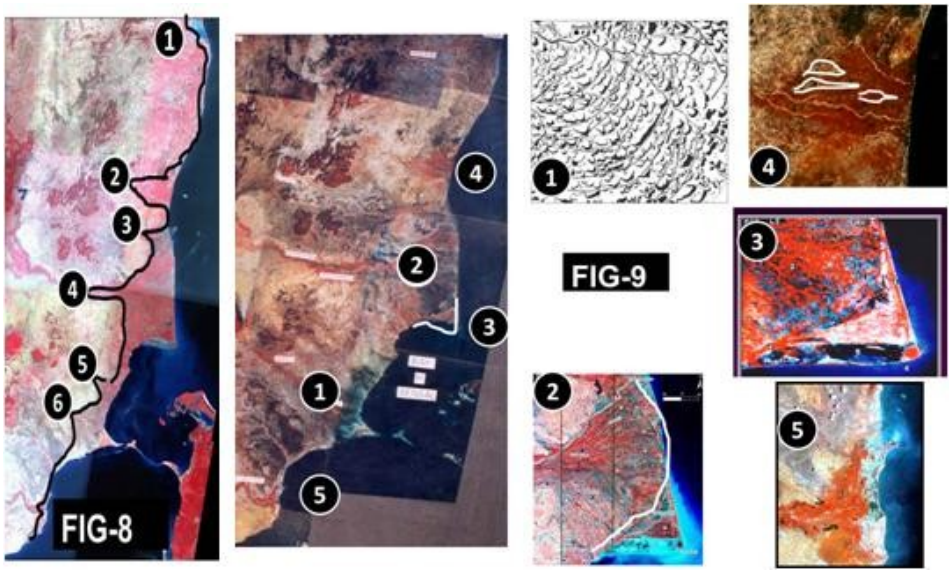

Figure 8*: Western limit of the sea during Pre Quaternary period along west of Pulicat Lake (1),apex and boundaries of Deltas of Ponnaiyar (2),Vellar (3),Cauvery (4), Manumuttar (5) and Vaigai (6) rivers and to the east of Mio-Pliocene sandstone;*

Figure 9*: Deltas of Tamilnadu .(1) Vaigai lobate,(2) Cauvery arcuate,(3) Vedaranniyam cuspate, (4) Ponnaiyar digitate and (5) Tamraparani*

Tamraparani delta(5) reveals that the river has almost surrendered to tidal activities without building any delta (10/90) (Fig 9). Again within the same delta also the different above morphologies may be there. So, the deltas are to be mapped in detail with finer geomorphology including the polygons of different fluvial and ocean energy levels and these polygons are to be dated so as to bring out the profile of the past fluvial and marine energy conditions, from which future predictions can be made.

Protruding deltas

While the Tamilnadu coast has large number of continental deltas as discussed above, in certain zones, like Pudukkottai coast, protruding deltas are seen to have developed in Agniar (1), Ambullar(2) and Vellar(3) rivers (Fig-10). Along Tamilnadu coast, the littoral currents are very active with northerly movement during March-Oct months and southerly movement during Nov-Feb north east monsoonic months (Sambasiva Rao, 1982;Ramasamy ,1992).So even the mighty rivers of Tamilnadu could not develop any protruding deltas. But in contrast, the above three small rivers have developed such protruding deltas. This indicates that either the catchment near the coast must be undergoing uplift or because of the embayed nature of the coast it must be a littoral current shadow zone facilitating the delta building. However, these protruding deltas are significant and form favourable areas for the harbours wherein littoral currents cannot cause any coastal erosion. However as significant sediment influx is there in such areas, when the harbour related constructions are proposed, detailed sediment budgeting needs to be done. Same is the case for tourism related industries. In this context there is a need to study these deltas along the entire stretch of Indian coasts using the digitally processed multi dated satellite data and GIS.

Backwater-creek ecosystems

The backwater ecosystems are unique and in emerging coasts and these stand prone for gradual defunct due to withdrawal of the sea and the creeks ,lack of fresh water supply into the back water, excessive sediment dump, later encroachment and abuse etc .In contrast, along the subsiding coasts, the back waters will be swelling due more influx of sea water. However, the shrinking and defunct of backwaters are to be studied with multi dated topographic sheets and satellite data to identify the pattern of shrinkage and

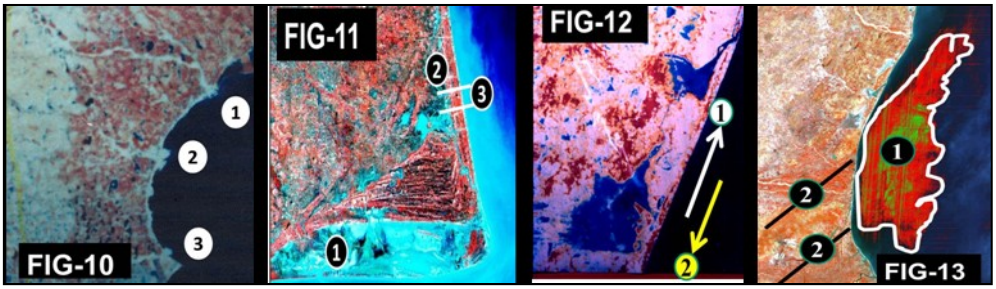

Figure 10*: Protruding deltas of Agniar (1), Ambullar (2) and Vellar (3) Rivers of Pudukkottai district.* ***Figure 11****: IRS FCC showing the silt choked Vedaranniyam backwater (1) Nagapattinam (2) and creeks (3).* ***Figure 12****: IRS FCC showing Marakkanam chain of backwaters and northerly moving littoral currents (1) of March-Oct and southerly moving littoral currents (2) of Nov-Feb months.* ***Figure 13****: IRS 1-A band 2 digitally processed image of Pondicherry area showing off shore shoals (1) and the bounding faults (2) of the graben.*

defunct along with causative factors so as to evolve strategies for their revival. For example, the studies carried out in Vedaranniyam backwater region showed that the back water (1) located just south of Nagapattinam (2, Fig-11) is heavily sediment choked because of the uplift of the Mio-Pliocene sandstone, the related intense gullying and the sediment supply into the back water, the progradation and emergence of the land in Vedaranniyam nose (5, Fig-7), withdrawal of the sea and the creeks and the later misuse of the backwater for salt and marine chemical industries. On the basis of the above preliminary studies the Vedaranniyam back water can be rejuvanated by desiltation and also pushing the sea water into the back water through the swarms of creeks (3,Fig-11) seen to the north of the back water. In the context of the observations made in Vedaranniyam back water, all the back waters of India need to be studied under multi- disciplinary mission mode program using Geomatics technology.

Sediment-Chemo dynamics of backwaters

The sediment –chemo dynamics of the backwaters is one of the vital parameters of the backwater and also the creek ecosystems. For example along the east coast of India, as briefed above, the littoral currents move in northerly direction(1) during Oct-March and in southerly direction(2) during the north east monsoonal months of Nov-Feb (Fig-12). During the above non monsoonal months, sediments and water get into the ocean and where as during the monsoonal months, as the currents flow towards southerly, the sediments brought by the littoral currents and the coastal waters enter into the back waters. This can be seen from the lesser and more water covered areas respectively in pre and post monsoonal seasons as seen in Marakkanam chain of back waters (Fig-12). Thus the sediment-chemo dynamics of the backwater keep on changing in seasonal cycle of a year which need to be studied in conjunction with ground based spectral measurements on the date of satellite pass and the sediment and water chemistry analysis so that, not only remote sensing based models can be developed on the aquatic dynamics , but also the optimum seasons can be identified for the various utilities of the back waters in India.

Off shore shoals

The off shore shoals are the unique geomorphic features found in the off shore regions. The digital image processing of IRS band -2 data of the Pondicherry-Cuddalore concave coastal region revealed the occurrence of a major off shore shoal (sub aqueous sand bar)in the off shore region(1,Fig-13).This has been built by the above said bi-directional littoral currents by dumping the sands it is carrying , taking advantage of the concavity of the coast. In addition, the two NE-SW sub parallel faults (2, Fig-13) which act as bounding surfaces of the in between graben continue into the off shore region too, further facilitating the accumulation of sands and the growth of the shoal. These off shore shoals have positive and negative impacts viz; concentration of heavy minerals, tsunami dissipaters, fish diversity, harbour sedimentation etc. Hence all the concave coasts warrant detailed studies using Geomatics.

Off shore sand bars

Almost along most of the global coasts, off shore sand bars will be found. Though they appear to occur randomly , they will be found more along the emerging coasts and also in areas where the littoral currents are active along serrated , etched

and embayed coasts . These are very significant and need to be studied. For example along Ramanathapuram (1)-Tuticorin (2) emerging segment of the coasts a chain of over 20-21 small islands are found parallel to the coast(3) also falling in conformity to the littoral currents which are very active in this region (Fig-14).In course of time , further sands will be dumped enveloping these islands by the north-easterly moving littoral currents , which will ultimately lead to the formation of a long northeast-southwest island (3, Fig-14) with the narrow sea in between it and the main coast. This would change the ecosystem and earth system processes along the present shoreline.

This might also lead to a condition that only sediment dumping by the rivers will be the dominant process and ultimately the narrow sea will be filled and the present Ramanathapuram – Tuticorin coast will get shifted to position -3 (Fig-14).As this has greater significance not only to the eco system but also to the Tuticorin

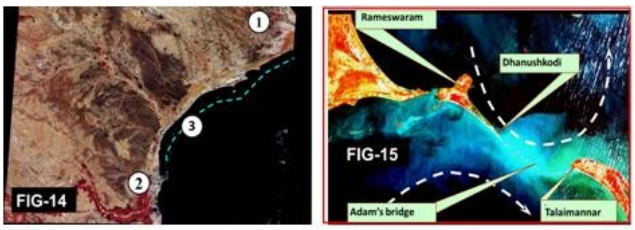

Figure 14*: IRS FCC showing 20-21 tiny islands in the off shore region of Ramanathapuram (1)-Tuticorin (2) along which linear land (3) may form linking these islands.* ***Figure 15****: IRS FCC showing the divergent littoral currents north and south of Rameswaram Island causing sand accumulation leading to the formation of Rameswaram and a chain of over 30 islands between Dhanushkodi and Talaimannar called Adam's bridge along current shadow zone.*

harbour ,this phenomenon needs to be studied on geology, geomorphology, morphodynamic processes , physical oceanographic processes etc using Geomatics technology.

Origin of Adam's Bridge

Recently, NASA has created a sensation that it has located a land bridge between India and Sri lanka. Whereas the fact is, this is known since historical times and mentioned in ancient literature too. Again using remote sensing, Shailesh Nayak and his team from SAC, Ahmedabad have brought out information that these are sandy islands with the corals over them. Ramasamy (2003) has explained that the anti-clockwise and clockwise moving littoral currents respectively in the north and south of Rameswaram region has provided a current shadow zone in between Ramanathapuram and Talaimannar of Sri Lanka (Fig -15) and hence taking advantage of the littoral current shadowiness and also the positive land provided by the Cochin- Ramanathapuram arch related to the post collision tectonics, the Ramanathapuram part of the coast has developed with the easterly nose up to Uchchipuli- Madapam in the east , further built Rameswaram island with the same configuration and continued to accumulate sand bodies numbering over 30 in between Dhanush Kodi and Talaimannar of Sri Lanka with same configuration.As the Uchchipuli beach ridges do give a 14c date of more than 3500 years Before Present, the Adam's bridge might have formed only after that. However, as the geo-mythological debates are still going on it needs to be studied by a multi disciplinary team from geology, geomorphology, history, archaeology, Tamil literature etc and the geomatics can play a vital role in this too.

Possible new land bridge between Vedaranniyam (India) and Jaffna (Sri Lanka)

Ramasamy et al (1998) carried out ^{14}C dating studies of the beach ridges grown to a distance of 55 kms from Thirutturaipoondi in the north west to Kodiayakkarai in the south east in Vedaranniyam area (3,Fig-8;fig-16). Amongst the bundles of large number of beach ridges, samples were collected from five beach ridges and dated using ^{14}C dating which revealed the gradual young age to the beach ridges from around 6000 years before present to the oldest in the north west to 1100 y.b.p to the youngest beach ridges in the south east. Using this Ramasamy and Ravikumar (2002) made a GIS based visualization which revealed that Vedaranniyam will get welded with Jaffna peninsula by a land bridge around 2750-2800 AD if the same current pattern and the processes continue. As such land welding is expected to cause major changes in the ecosystem of the region and further will bring in geo political issues, this warrant fine resolution studies.

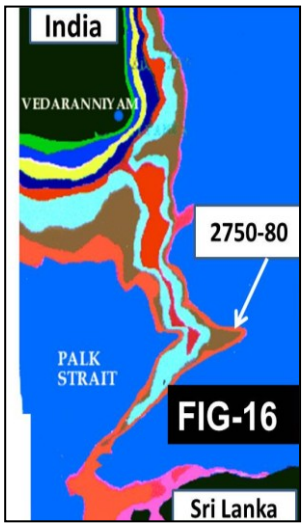

***Figure 16**: GIS based visualization done on the basis of dating of beach ridges in Vedaranniyam area showing the possible land bridge between India and Sri Lanka around 2750 AD.*

Natural resources

The costal zones in general are endowed with rich resources like placer mineral deposits in the beach ridges developed to a wider breadth all along the emerging coasts, potable ground water potential in the beach ridges, oil and gas etc. Though these have been studied, no comprehensive and holistic studies have been made. This needs to be done in the context of availability of hyper spectral remote sensing and other GIS based Decision Support systems.

Ancient river mouth civilization

The river mouths along the coasts have always remained as ports and related flourishing civilization and the recent remote sensing based observations indicate that most of the rivers show tail end migrations along Tamilandu coast. For example, the river Pudukkottai Vellar has earlier flowed southeasterly from its apex Chettiyanendal (1) and met the sea at Pudupattinam (2), migrated anticlockwise and flowed along path-3 and met the sea near Kottaipatttinam and further migrated northerly and now stabilized along path -4 confluence at Manamelkudi (Fig-17). Hence there are possibilities for the existence of ancient ports and the related civilisations at the old river

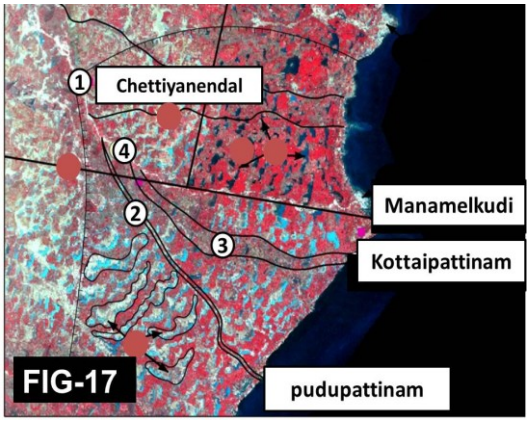

***Figure 17**: IRS FCC showing anticlockwise rotational migration of Vellar along Pudupattinam (2), Kottaipattinam (3) and present flow along Manamelkudi (4).*

mouths at Pudupattinam and Kottaipattinam , as also implied by their names. So these aspects need to be studied along the entire Indian coasts.

Since the river mouths are being contemplated for the existence of ancient civilisations, there are possibilities for the ancient port based civilisations along the apex of the rivers also, whereever these show well developed continental deltas. And if so, the apex of Ponnaiyar river at Tirukkoviloor(2), Cauvery at Tiruchirapalli(4),Manimuttar at Devakottai (5) (Fig-8) etc too need to be studied for such civilisations.

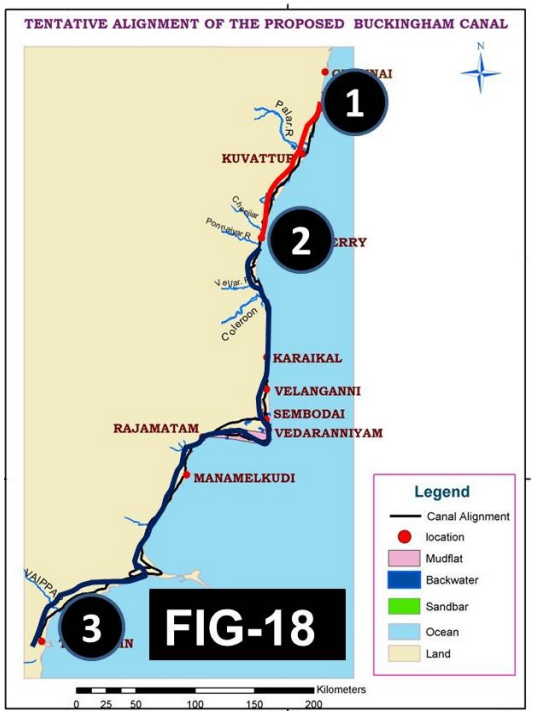

***Figure 18**: Possibility of resurrecting the Buckingham canal from Kovalam (1) south of Chennai to Pondicherry (2) and extending it upto Tuticorin (3)*

Inland Transport System

The Indian coasts have remained as an excellent candidate for inland water transport due to natural morpho-dynamics. The backwaters of Kerala are the popular inland transport systems in the world. Similarly along the east coast of India also there existed the Buckingham canal from Kakinada in the north to Pondicherry in the south and remained as an excellent water ways for transporting the materials. (Fig-18).This became defunct 50 -60 years ago due to due natural morpho dynamic processes and also due to anthropogenic activities. This can be revived by studying the coastal morpho tectonic and morpho dynamic processes and resurrect the existing canal in between Kovalam (south of Chennai) to Pondicherry(1 to 2,Fig-18) and can be extended up to Tuticorin(3,Fig-18) along the suitable geomorphic zones /depressions(swales, back waters, coast parallel creeks etc). The water for the canal can be brought in through the creeks in the upstream, made to flow for some distance and let out into the ocean in the downstream and again get the sea water from the downstream creeks in a cyclic pattern. The surplus fresh water coming from the rivers can also be lead into the canal .Once the canal is revived , it can not only be used for the pollution free transport , but also development of micro harbours ,mangroves, salt and marine chemical industries , fish feed industries, aqua culture, coastal tourism , revival of back water ecosystems etc are possible(Fig-18). This is again an yet another major aspect to be studied by inter disciplinary teams capitalizing the virtues of Geomatics technology.

Coastal disasters

The coastal zones stand prone for various natural and anthropogenic disasters like seismicity and earth movements, flooding, tsunamis and storm surges, sea level rise, landslides, coastal erosion etc. The vulnerability for such disasters is more in the coastal regions because of its inherent fragility as briefed above. So it requires detailed

studies for the preparation of vulnerability maps for different disasters, along with their causative factors and factor controlled mitigation and management models for which Geomatics has enormous potentials.

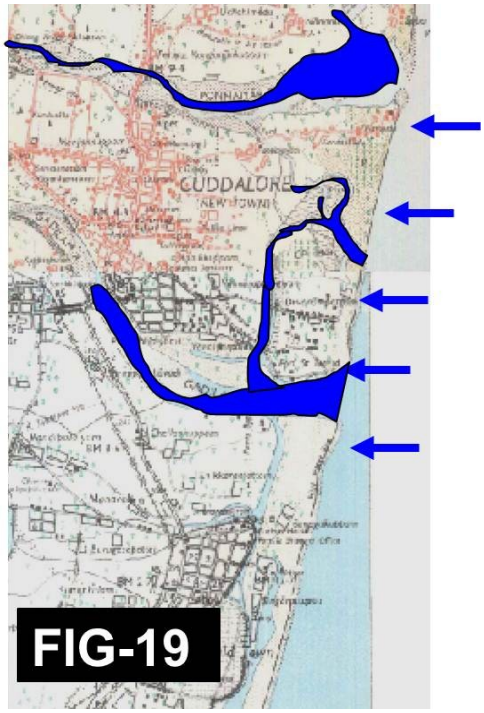

***Figure 19**: Geomatics based interface dynamics studies between tsunami and geomorphology.*

For example, the GIS based studies carried out by Ramasamy et al (2006b) on the interface dynamics between tsunami (2004) inundation and the geomorphic features indicated that various landforms have responded differently to tsunami inundation that (1) mudflats as facilitators, (2) river and creek mouths as carriers, as revealed by the Ponnaiyar river for example (Fig-19), (3) backwaters as accommodators, (4) beaches as absorbers, (5) beach ridges as barriers, (6) mangrove swamps as dissipaters etc. Similarly several workers have come out with different tsunami mitigation strategies. But, since the geomorphology plays the vital role, the studies must be carried out and GIS databases need to be brought out for the entire vulnerable coastal segments of India fragmenting the coasts into different polygons of tsunami responses. In addition models also need to be developed to forewarn the coastal zones to be affected by the tsunami under different seismogenic, sea bed topographic, physical oceanographic, coastal geomorphic and land use cover conditions. In this study geomatics can provide towering support.

The coastal erosion is again yet another major anthopogenically triggered disaster. The emerging coasts in general are prone for coastal erosion by the waves and the littoral currents and the later contributes to the maximum. Besides, whenever any structures are constructed like jetties or groynes, these interfere with littoral currents leading to the sand accumulation in the upstream and erosion by the deflected components of the currents in the downstream. The erosion of Mahabalipuram shrore temple and Ennore are standing testimony for such erosion. So before constructing any coastal structures protruding into the ocean, there is a need for the detailed studies on the coastal geosystems and the littoral current pattern so that their positions , orientation and length can be according designed in such a way that the deflected components of the littoral currents hit the river and creek mouths in the downstream and get dissipated without causing erosion .

CONCLUSION

Thus the coastal regions of all over the world and the Indian coasts as well face a hierarchy of challenges and the Geomatics technology possesses attention deserving virtues. Such issues, the possible case studies and the studies warranted capitalizing the vistas of Geomatics technology have been discussed in the paper.

References

Ahmed. E. (1972) Coastal geomorphology of India,Orient Longman.

Ghosh, D.B., (1976) The nature of the Narmada–Son lineament. Geological Survey of India, Miscellaneous Publication, 34, pp. 119–132.

Larson, K. M., Burgmann, R., Bilgham, R. and Fremullaer, J. T. (1999) Kinematics of the India - Eurasia collision zone from GPS measurements. Journal Geophysical research,104 (B1):pp1077-1093

Ramasamy, S.M., (1987) Morpho-Tectonic Evolution of East and West Coasts of Indian Peninsular - Geological Survey of India, Spec. Pub. No.24. pp 333- 339.

Ramasamy, SM. (1992), A Remote Sensing Study of River Deltas of Tamil Nadu. Memoirs of Geological Society of India, No.22, pp 75-89.

Ramasamy, SM., (2003) Facts and Myths about Adam's bridge. GIS@development, Vol. 7(12), pp. 43-44.

Ramasamy S. M., (2006) Remote Sensing and Active tectonics of South India. International Journal of Remote Sensing, Taylor and Francis, London, Vol.27, No.20

Ramasamy, S. M. (2006) Holocene tectonics revealed by Tamilnadu deltas,India.joural of Geological Society of India,Vol.67(5): pp 637-648

Ramasamy, SM. and Ravikumar, R. (2002) GIS Based Visualisation of Land- Ocean Interactive Phenomenon along Vedaranniyam Coast, Tamil Nadu, India. ISG Newsletter, Vol.8, pp.72 - 77.

Ramasmy, SM., Ramesh, D., Paul, M.A., Sheela Kusumgar, Yadav, M.G., Nair, A.R., Sinha U.K. and Joseph, T.B. (1998), Rapid Land Building Activity along Vedaranniyam Coast and its Possible Implications. Current Science, Vol. 75, No. (9). pp 884 - 886.

Ramasamy, S. M., Saravanavel, J. and Selvakumar, R. (2006 a) Late Holocene geomorphic Evolution of Cauvery delta, Tamil Nadu, India. Journal of Geological Society of India, Vol.67(5) pp 649-657

Ramasamy, SM., Kumanan, C.J., Saravanavel J. and Selvakumar R. (2006 b) Geosystem Responses to December 26 (2004) Tsunami And Mitigation Strategies For Cuddalore – Nagapattinam Coast, Tamil Nadu, India. Journal of Geological Society of India, Vol.68(6), pp. 967-983.

Ramasamy,SM.,Saravanavel,J.,Yadav,M.G. and Ramesh ,R.(2006c)Radiocarbon dating of some Palao drainages and their significance in Tamilnadu, India. Current science,Vol.91.No12:pp1609-1613

Sambasivarao, M.(1982)Morphology and evolution of modern Cauvery delta,Tamilnadu.Trans.Institute of Indian geographers .V.4(1):pp68-78.

Shailesh Nayak (2004)Role of remote sensing to integrated coastal zone management.Spec.Vol.ISPRS Commission. VII: pp1-12

Shailesh Nayak (2004) Role of remote sening to integrated coastal zone management.XX th conference of ISPRS

Subrahmanya, K.R., 1996, Active intraplate deformation in South India. Tectonophysics, 262, pp. 231–241.

Geomatics based vulnerability analysis of accelerated sea level rise on world's second largest Beach, Marina beach, Chennai, Tamil Nadu, India

C. J. Kumanan[1], J. Saravanavel[1], N. Nagappan[1], S. Gunasekaran[1], A. S. Rajawat[2], and Ajai[2]

[1] Centre for Remote Sensing, Bharathidasan University, Tiruchirappalli, India

[2] Space Applications Centre, ISRO, Ahmedabad, India

Email: cjkcers@hotmail.com, cersbard@yahoo.co.in

ABSTRACT

The coastal zones are highly sensitive in general where the multivariate geologic / geomorphic processes viz. tectonic, fluvial, marine and aeolian processes act in varying degrees and exposed to various natural disasters such as coastal erosion, flooding, storm surges, tsunami, etc. The dynamic of these disasters are further incremented by the improper human intervention through the various developmental activities without proper understanding of ongoing coastal dynamic processes. Global warming and its related accelerated sea level rise is one of the major long-term disasters along the low-lying coastal margin of India in addition to other coastal disasters. The recent studies carried out in India and Tamil Nadu show that the accelerated sea level rise is expected to cause threats and damages to the infrastructures, tourist spot, archaeological monuments, etc. along the soft sediment coastal regions. In this context, the present study has brought out significant information using advanced credential of emerging Geomatics technology on the response of world second largest beach, Marina beach to the projected accelerated sea level rise.

Keywords: Marina beach, Accelerated sea level rise, Impact analysis

INTRODUCTION

The global warming and climate change has expected to cause series of environmental problems over the planet Earth. That too its impacts are expected to be more along the coastal regions in the form of accelerated sea level rise (ASLR) triggered by the ice and snow melt and thermal expansion of oceanic water. The IPCC AR4 2007[1] (Intergovernmental Panel on Climate Change report Assessment Report 4) report suggests that the global mean sea level rose at an average rate of 1.7 mm per year in the 20th century, 1.8 mm per year from 1961 to 2003 and at a rate of 3.1 mm per year from 1993 to 2003 and projected upper rate of ASLR (accelerated sea level rise) as 0.59 m in 2100. The analysis of data from 258 tide gauges across the world confirms that the increasing trend in extreme sea levels world over since 1970s [2]. Since the IPCC AR4 2007 [1], various models with 20th and early part of 21st century tide gauge and satellite based

altimetry data have brought out the varied projections on accelerated sea level rise at 2100 such as 0.47 to 1.00 m [3], 0.50 to 1.40 m [4], 0.75 to 1.90 m [5] and 0.90 to 1.30 m [6]. The above models might have overestimated the future sea levels, but the realistic projection of sea level rise of 0.8m at 2100 AD may be possible with the increased ice dynamics [7].

Similarly, the impacts of the accelerated sea level rise over the coastal resources and environment have gained greater attention among the researchers and they have brought out the various national and international studies. For example, due to increase of mean sea level, accelerated erosion, and shoreline retreat due to increased wave strength as water depth increases near the shore [8,9,10], changes in coastal height in the permafrost coastal region due to isostatic rebound [11,12], the increased sea-surface temperature and changes in frequent and intensified cyclonic activity and associated storm surges in the low lying coastal region [13,14,15], changes in wave speed, refraction and direction and can alter the present pattern of coastline [16,17,18], the loss of natural protective measures such as coral reefs, mangroves, sand dunes [18,19,20], inundation in the wetlands and estuaries and threatening to historic, cultural resources and infrastructure [21,22], etc.

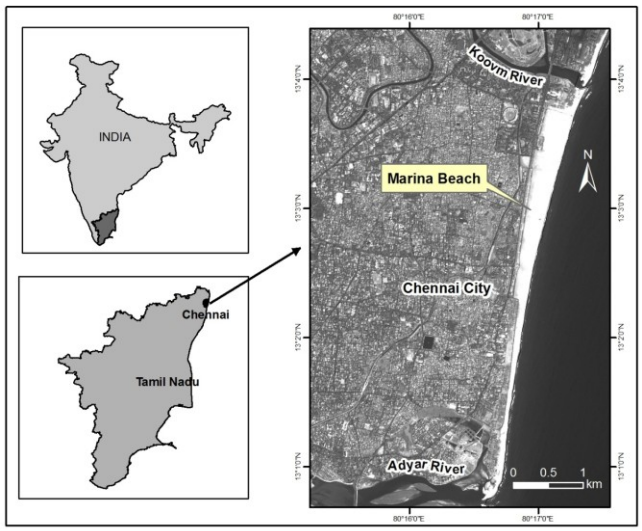

***Figure 1**: Study Area*

With the above background and utilizing the advanced credentials available with geomatics technology comprising of Remote Sensing, GIS (Geographic information System), DGPS (Differential Global Positioning System) and Photogrammetry, the present study has been taken up to analyze the response of world's second largest Marina beach to the various projected accelerated sea level rise due to global warming.

STUDY AREA

Study area extends for a length of 6km from Koovm river mouth in the north to Adyar river mouth in the south. The Marina beach having the width nearly 600 m in the north and gradually decreases to 80 m in the south near Adaiyarriver mouth (Figure 1). The Chennai harbor is located just north of the Marina beach region i.e. just north of Koovm river mouth.

DATA AND MATERIALS

For the present study, using the stereo pair Cartosat data, an ortho image with fine resolution DEM (Digital Elevation Model) was generated using the Leica photogrammetric suit to visualize the pattern of inundation due to projected accelerated sea level rise along the study area under the 3D GIS environment. To understand the off shore bathymetry, GEBCO (General Bathymetric Chart of the Oceans) bathymetry data was used.

With the aid of five multi-dated satellite dataset such as Landsat MSS (1972 & 1981), Landsat

TM (1991), Landsat ETM (2000 & 2006), long-term shoreline accretion and erosion pattern for last 34 years was analyzed.

Using the above various data and materials, the response of World's second largest Marina Beach to accelerated sea level rise at 2100 AD was analyzed.

STUDIES AND FINDINGS

Precise Analysis for identification of rate of shoreline change

To precisely estimate the rate of shoreline change, the trajectories were drawn from the common and permanent features like roadjunction, prominent building, etc. at every 100 m interval to shoreline of the multi-dated satellite data such as Landsat MSS (1972 & 1981), Landsat TM (1991), Landsat ETM (2000 & 2006).

The distance between the common features to shoreline for each year was calculated. From the

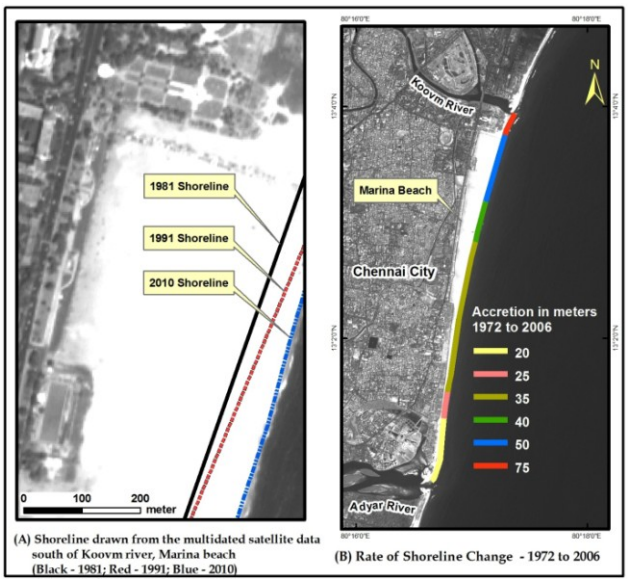

***Figure 2**: Rate of Shoreline Change deduced from multi-dated satellite data*

difference between the lengths of the trajectories of two successive periods i.e. 1991-2000, the length of erosions or accretions of the coast was brought out. Similarly, the length of erosion or accretion was brought out for the period of 1972-1981, 1981-1991, 1991-2000, 2000-2006 and so on. From the above, rate of erosion or accretion per year was worked out for every 100 m length of the coast from 1972 – 2006. The Figure 2A shows the accretion pattern of shoreline in northern Marina beach in-between 1981 and 2010 and Figure 2B shows the rate of erosion or accretion for 34 years from 1972 to 2006 derived from the multi-dated satellite data.

From the above analysis, it was observed that the Marina beach extending from the Koovm river in the north to Adyar river in the south shows the accretion pattern overall for 34 years. The rate of accretion per year was nearly 4m per year in the northern extremity of the beach just south of Chennai harbour. But towards southern part of the beach the accretion gradually reduces to 0.5m per year. The reason for the higher rate of accretion in the northern part of the beach is the northerly moving littoral currents obstructed by the groin of Chennai harbour, so the most of the sediments being brought by the northerly moving littoral currents are being dumped in the northern part of the marina beach.

Offshore profiles and their significance

The accretion coasts are generally thought as least vulnerable to coastal disasters like flooding, storm surges, tsunami, etc. But, it was observed that during the tsunami (2004), Thane cyclone (2011) and Nilam cyclone (2012), most part of the marina beach was inundated and submerged (Figure 3). To analyze the reason for the vast inundation due to tsunami and storm surges in Marina beach, the offshore profiles were drawn

along the accretional Marina coast and erosional Tiruvottiyur coast using the comprehensive DEM generated using the CartosatDEM and GEBCO bathymetry data.

The offshore profile along the marina beach shows gentle slope when compare with Tiruvottiyur offshore profile. Due to long term accretion in Marina beach area, a gentle nature of slope was developed towards the continental shelf but on the contrary, because of long term erosion along the Tiruvottiyur coast, the slope is steep towards the continental shelf (Figure 4). So, taking advantage of the gentle nature of the slope in the Marina beach, the beach was inundated and submerged by the Tsunami (2004), Thane cyclone (2011) and Nilam cyclone (2012) (Figure 3A,B,C). But at the same time, for example, in Pondicherry's erosional coast, during December 2011 Thane cyclone, there is not much of inundation by storm surges. Thus, it can be said that the accretion coasts are more prone to inundation and submergence when compare to erosional coast in the context of the accelerated sea level rise during 2100.

***Figure 3**: Inundation pattern of Tsunami (2004), Thane (2011) and Nilam (2012) in Marina and Pondicherry coast*

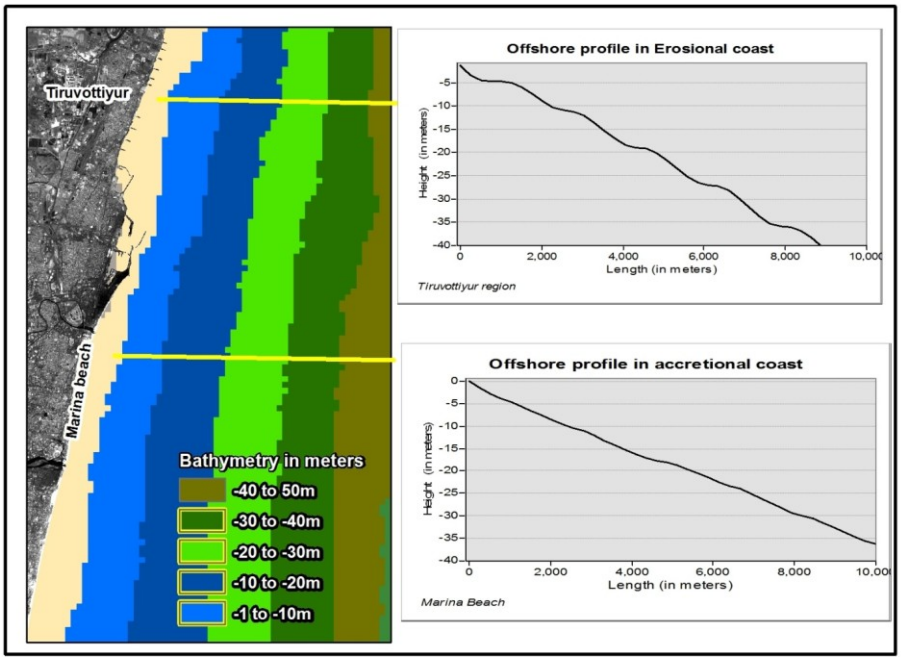

***Figure 4**: Offshore profile along the accretion Marina Beach and Erosion Tiruvottiyur coast*

Visualization of projected sea level rise at 2100 AD

The fine resolution DEM (Digital Elevation Model) generated using stereo Cartosat data was used to visualize the extend of inundation and submergence due to projected sea level rise during 2100 AD along the Marina beach. For the same, the recent projection on sea level rise at 2100 AD by the various workers were taken into consideration such as 0.26 to 0.59m [1], 0.75 to 1.40 m [4], 0.47 to 1.00m[3], 0.75 to 1.90m [5], 0.90 to 1.30m [6] and 0.80m[7]

From the above varied projection on sea level rise during 2100 AD, 0.59 m, 0.8 m, 1.40 m and 1.90m were taken as guidance and visualized using Cartosat DEM and the response of Marina beach to the above projected sea level rise from present day MSL (Mean Sea Level) was analyzed (Figure 5).

The Marina beach in this part covers an area of 4.4 sq. km. If the sea level rise to 0.59 m, 0.8 m, 1.4 m, 1.9m from the present day MSL, then respectively 1.1, 2.3, 2.8 and 3.0 sq. km area will be under the inundation and submergences (Figure 5). In this context, as per the recent study [7] most plausible accelerated sea level rise will be 0.8m at 2100 AD, it can be summarized from the above analysis that the Marina beach, in this part, may lose its 50% of the area due to inundation and submergence.

Response of Marina beach to projected sea level rise at 2100 AD

The shore line change analysis using multi-dated satellite data, the study on and off shore profile and visualization of various projected sea level rise at 2100 AD with the aid of Cartosat DEM revealed the following significant information on response of Marina beach to the projected sea level rise:

- The shoreline change analysis with the aid of multi-dated satellite data shows that the rate of accretion is high in the northern extreme part of the Marina beach. But on the contrary, the inundation and submergence due to projected sea level rise are also more in the same part of the beach (1, Figure 5). From the same, it can be concluded that the accretion coasts are more prone to inundation and submergence to the projected sea level rise. Further, this fact was very well seen in the inundation pattern of sea during the tsunami (2004), Thane cyclone (2011) and Nilam cyclone (2012). The onshore and offshore profile along the Marina beach shows the very gentle slope towards the continental shelf. Such a gentle nature of the slope would have facilitated the inundation

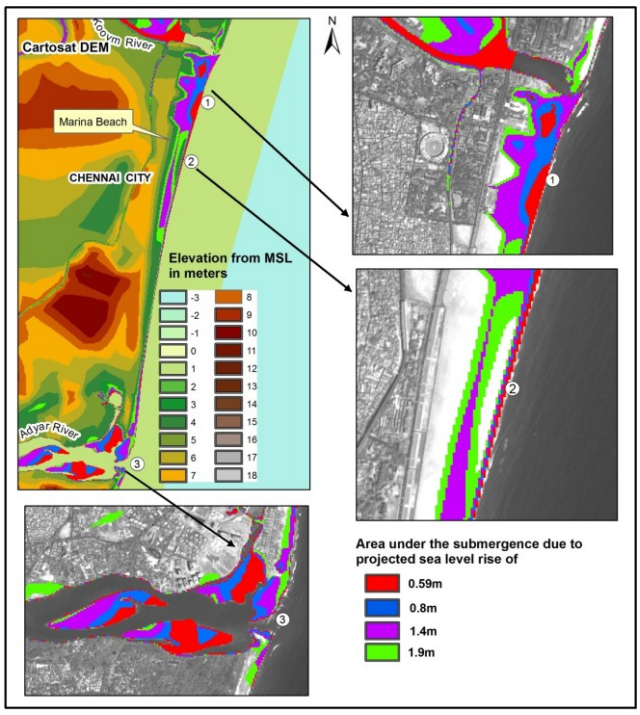

***Figure 5**: Visualization of projected sea level rise in Marina beach using Cartosat DEM*

and submergence in Marina beach region during the tsunami and storm surges. Form the above, it was inferred that the Marina beach will response to projected sea level rise in a similar way it was responding to the Thane cyclone (2011) and Nilam cyclone (2012) (Figure 3).

- The middle part of the Marina beach may be modified as barrier beach and subsequently may develop into sandy islands (2, Figure 5). Further, the barrier beach pattern along Marina beach also witnessed during the Thane cyclone (2011) and Nilam cyclone (2012) (Figure 3B,3C)

- The sand bars found in the Adyar river mouth,may be submerged to the projected sea level rise of even for 0.59m (3, Figure 5).

- The inundation of sea due to tsunami and storm surges may possibly enter into the part of Chennai city in the context of projected sea level rise during 2100 AD.

- From the above, it can be inferred that the environment and ecosystem of the Marina beach region may be modified in the context of accelerated sea level during 2100 AD

CONCLUSION

The present study using geomatics technology has brought out newer and comprehensive information on how the Marina beach will respond to projected sea level rise during 2100 AD. Further study with ALTM / LIDAR data may provide more accurate information on this issue. The above analysis has raised a question that how long the Marina Beach will retain the name as second largest beach in World?

References

1. IPCC: Climate Change 2007. The Fourth Assessment Report of theIntergovernmental Panel on Climate Change.Cambridge University Press,Cambridge, United Kingdom and New York, NY, USA (2007).
2. Menendez, M. and WoodworthP.L., Changes in extreme high water levels basedon a quasi-global tide-gauge dataset. Journal of Geophysical Research, 115, C10011(2010).
3. Horton, R., HerweijerC., RosenzweigC., LiuJ.,GornitzV., and RuaneA.C., Sealevel rise projections for current generation CGCMs based on the semi-empiricalmethod. Geophysical Research Letters, 35, L02715 (2008)
4. Rahmstorf, S., A semi-empirical approach to projecting future sea-level rise.Science, 315(5810), 368-370(2007).
5. Vermeer, M. and RahmstorfS., Global sea level linked to global temperature.Proceedings of the National Academy of Sciences, 106(51), 21527-21532 (2009).
6. Grinsted, A., MooreA.J., and JevrejevaS., Reconstructing sea level from paleoand projected temperatures 200 to 2100 AD. Climate Dynamics, 34(4), 461-472 (2010).
7. Church, J.A., GregoryJ.M., WhiteN.J., PlattenS.M., and MitrovicaJ.X., Understanding and projecting sea level change. Oceanography, 24(2),130-143 (2011).
8. Pye K, Blott SJ., Coastal processes and morphological change in the Dunwich—Sizewell area, Suffolk, UK. J Coast Res 22:453–473 (2006).
9. Nageswara Rao K., Subraelu P., Rajawat AS., Ajai, Beach erosion in Visakhapatnam: causes and remedies. East Geography 14, 1–8(2008)
10. Ranasinghe, R., and StiveM., Rising seas and

retreating coastlines. ClimaticChange, 97(3), 465-468 (2009).

11. Blewitt, G., Z. Altamimi, J. Davis, R. Gross, C.-Y.Kuo, F.G. Lemoine, A.W. Moore, R.E.Neilan, H.-P.Plag, M. Rothacher, C.K. Shum, M.G. Sideris, T. Schöne, P. Tregoning,and S. Zerbini, Geodetic observations and global reference framecontributions to understanding sea-level rise and variability. In: Understanding sea level rise and Variability [Church, J.A., P.L. Woodworth, T. Aarup, and W.S.Wilson (eds.)]. Wiley-Blackwell, Chichester, UK, pp. 256-284 (2010)
12. Mitrovica, J.X., M.E. Tamisiea, E.R. Ivins, L.L.A. Vermeersen, G.A. Milne, and K.Lambeck, Surface mass loading on a dynamic earth: complexity andcontamination in the geodetic analysis of global sea-level trends. In:Understanding Sea-Level Rise and Variability [Church, J.A., P.L. Woodworth, T.Aarup, and W.S. Wilson (eds.)].Wiley-Blackwell, Chichester, UK, pp. 285-325 (2010).
13. Wu, Y., TingM., SeagerR., HuangH.-P., and CaneM., Changes in storm tracksand energy transports in a warmer climate simulated by the GFDL CM2.1model. Climate Dynamics, 37(1-2), 53-72 (2011)
14. Zhang, K.Q.,.DouglasB.C, and LeathermanS.P., Global warming and coastalerosion.Climatic Change, 64(1-2), 41-58 (2004).
15. Unnikrishnan AS, Rup Kumar K, Fernandes SE., Sea level changes along the Indian coast: observations and projections.CurrSci 90, 362–368(2006).
16. Ranasinghe, R., McLoughlinR., ShortA., and SymondsG., The SouthernOscillation Index, wave climate, and beach rotation. Marine Geology, 204(3-4),273-287 (2004)
17. Bryan, K.R., KenchP.S., and HartD.E., Multi-decadal coastal change in NewZealand: Evidence, mechanisms and implications. New Zealand Geographer,64(2), 117-128 (2008).
18. Tamura, T., HoraguchiK., SaitoY., VanL.N., TateishiM., ThiK.O.T., NanayamaF., andWatanabeK., Monsoon-influenced variations in morphology and sedimentof a mesotidal beach on the Mekong River delta coast. Geomorphology, 116(1-2),11-23 (2010)
19. Sheppard, C., DixonD.J., GourlayM., SheppardA., and PayetR., Coral mortalityincreases wave energy reaching shores protected by reef flats: Examples fromthe Seychelles. Estuarine Coastal and Shelf Science, 64(2-3), 223-234 (2005)
20. Gravelle, G. and MimuraN., Vulnerability assessment of sea-level rise in VitiLevu, Fiji Islands. Sustainability Science, 3(2), 171-180, (2008)
21. Pendleton EA, Thieler ER, Williams SJ., Coastal vulnerability assessment of Cape Hettaras National Seashore (CAHA) to sea level rise. USGS Open File Report 2004-1064,http://pubs.usgs.gov,(2004).
22. Ramasamy. SM, Kumanan. C. J, Saravanavel. J, Rajawat. A. S. and Tamilarasan. V., Geomatics based Visualization of Predicted Sea Level Rise and its Impacts in Parts of Tamil Nadu Coast, India. Journal of Indian Society of Remote Sensing, 38(4) 640-653(2011).